THE UNIVERSITY OF CHICAGO

SEQUENTIAL ENTRY OF HEPATITIS C VIRUS INTO POLARIZED HEPATOMA ORGANOIDS

A DISSERTATION SUBMITTED TO

THE FACULTY OF THE DIVISION OF THE BIOLOGICAL SCIENCES

AND THE PRITZKER SCHOOL OF MEDICINE

IN CANDIDACY FOR THE DEGREE OF

DOCTOR OF PHILOSOPHY

COMMITTEE ON MICROBIOLOGY

BY

CHUI WA SO

CHICAGO, ILLINOIS

JUNE 2023

TABLE OF CONTENTS

LIST OF FIGURES

ACKNOWLEDGEMENTS

I would like to thank my mentor Glenn Randall and my thesis committee Jueqi Chen and Raymond Roos for their support and guidance. I would like to thank the current and former members of the lab for their companion – Rebecca Reis, Joshua Hackney, Shamila Sarwar, Jessica Oros, Vlad Nicolaescu, Natalia Povarova, Soowon Kang, Chaitanya Kurhade, Kevin Furlong, and Yasmine Baktash. I would like to acknowledge my cohort Ellen Ketter, Keven Dooley, and Emily Fogarty for joining the amazing Microbiology community together.

CHAPTER I

INTRODUCTION

Hepatitis C virus (HCV) is a hepatotropic RNA virus and a cause of hepatocellular carcinoma and cirrhosis. In this chapter, we summarize the use of three-dimensional cell culture systems in studies of HCV infection. It highlights the significance of studying entry host factors in the context of polarized hepatoma organoids. The second half of this chapter summarizes the mechanism of HCV entry, focusing on functions performed by βII-spectrin (SPTBN1), scavenger receptor class B member 1 (SR-BI), E3 ubiquitin ligase c-Cbl, epidermal growth factor receptor (EGFR), and tight junction proteins claudin-1 (CLDN1) and occludin (OCLN).

Hepatitis C virus

Hepatitis C virus (HCV) is a hepatotropic, enveloped, positive-sense RNA virus of the *Flaviviridae* family. The World Health Organization estimated that 58 million people are chronically infected with HCV. In each year around 1.5 million new infections occur. HCV can cause both acute and chronic hepatitis, ranging from a mild, weeks-long illness to a serious, life-long one. In 2019, 290,000 people died from HCV infection, primarily from hepatocellular carcinoma and cirrhosis. (WHO, 2017; WHO, 2023) Currently there is no effective vaccine against HCV. Pan-genotypic direct-acting antivirals (DAAs) have been developed based on contributions from academia, industry, and government funding agencies. The DAAs cure more than 95% of people with HCV infection, therefore reducing the risk of death from cirrhosis and hepatocellular carcinoma. However, failure and non-applicability of available DAAs hinder further improvement of anti-HCV treatment. For example, failure of DAA-based therapy is associated with viral variants having resistance-associated substitutions in NS5A, which is a major target of DAAs.

Resistance-associated substitutions have also been observed in NS3 and NS5B. Moreover, DAA combinations consisting of protease inhibitors are not applicable to people with advanced liver disease. Therefore, further research on HCV is crucial to optimize diagnosis, therapy, and the development of vaccines. In addition, discoveries related to HCV have been enriching the knowledge of positive-stranded RNA viruses, and fields of microbiology, molecular and cell biology, and immunology. (WHO, 2017; Bartenschlager et al., 2018; Li and Chung, 2019; WHO, 2023)

Other than liver, HCV replicates at a low level in other organs such as the brain. In the liver, it infects primarily hepatocytes, but also endothelial cells, Kupffer cells, stellate cells, and lymphocytes. (Miao et al., 2017) The development of the cell culture system, based on the HCV JFH-1 clone and the human-derived hepatoma Huh-7 cell line, was a breakthrough in HCV research. (Lindenbach et al., 2005; Wakita et al., 2005; Zhong et al., 2005) Since then, our knowledge of HCV infection in both basic and translational research has greatly advanced. Huh-7 cell line and its derivatives, such as Huh-7.5 and Huh-7.5.1, are widely used in studies of HCV infection.

Three-dimensional cell culture systems for studying HCV

Hepatocytes, the major target of HCV, are highly polarized. HCV infection requires extensive trafficking to distinct subcellular domains in the polarized hepatocyte. Polarized cells and three-dimensional organoids are commonly used to study liver functions and differentiation. Researchers have begun adapting these cell culture models that morphologically and physiologically resemble hepatocytes in vivo to study HCV infection. This section summarizes the use of three-dimensional cell culture systems in studies of HCV infection.

Hepatocytes, comprising 60% of the total cells of the liver (Malarkey et al., 2005; Decaens et al., 2008), are highly polarized with two distinct types of membrane domains. The apical domains of adjacent hepatocytes form a continuous bile canaliculus into which bile is secreted, while the basolateral domains are in contact with sinusoids and regulate the exchange of materials with the circulation. Tight junctional proteins play a crucial role in separating the two domains and keeping bile away from the blood circulation. In addition to membrane domains, specific cytoskeletal, endoplasmic reticulum, and Golgi apparatus networks contribute to the complex polarity of hepatocytes. (Luzzatto et al., 1981; Feracci et al., 1987; Decaens et al., 2008; Treyer and Müsch, 2013)

In cell culture-based studies of liver functions, researchers are aware of the importance of hepatocyte polarity. Various human polarized liver cell lines were generated, such as HepG2 and HepaRG. (Decaens et al., 2008) Moreover, human-derived induced pluripotent stem cells (Takebe et al., 2013), human fetal liver cells (Ng et al., 2018), and bile duct cells isolated from biopsy samples (Huch et al., 2015) were cultured in extracellular matrices, such as Matrigel and inverted colloidal crystal scaffold, to generate hepatic organoids. The organoids performed liver functions upon transplantation into mice. (Takebe et al., 2013) Lineage and polarity markers, gene expression profiling, and electron microscopy were used to assess differentiation status, polarity, and the degree of similarity between the in vivo systems and the liver. (Kawada et al., 1998; Aizaki et al., 2003; Decaens et al., 2008; Molina-Jimenez et al., 2012; Rajalakshmy et al., 2015; Kim et al., 2017; Baktash et al., 2018) Currently, researchers are exploring the use of the organoids in examining liver toxicity of drugs prior to clinical trials. (Meng et al., 2010; Lee et al., 2020)

While the use of polarized cells and organoids is not new to the field of liver research, HCV researchers are still exploring ways to generate infection models that morphologically and physiologically resemble the liver. The development of the cell culture system, based on the HCV JFH-1 clone and the human-derived hepatoma Huh-7 cell line, was a breakthrough in HCV research. (Lindenbach et al., 2005; Wakita et al., 2005; Zhong et al., 2005) Since then, our knowledge of HCV infection in both basic and translational research has greatly advanced. Huh-7 cell line and its derivatives, such as Huh-7.5 and Huh-7.5.1, are widely used in studies of HCV infection. Conventionally, the cells are cultured in two-dimensional (2D) monolayers. The poor polarity of 2D Huh-7 cells has become increasingly appreciated, especially in studies of HCV entry.

HCV entry requires two tight junctional proteins, claudin-1 (CLDN1) and occludin (OCLN). (Evans et al., 2007; Liu et al., 2009; Ploss et al., 2009) In 2D Huh-7 and 7.5 cells, tight junctional markers, ZO-1 and CLDN1, are distributed uniformly on the plasma membrane. (Coller et al., 2009; Molina-Jimenez et al., 2012; Baktash et al., 2018) As a result, the cells poorly resemble the bile canaliculus structure, the distinct separation of the apical and basolateral domains, and the retention of bile in the liver. Since CLDN1 and OCLN are known to be essential for HCV entry, they may not exhibit completely conserved functions in nonpolarized cells. (Narbus et al., 2011) Therefore, three-dimensional (3D) cell culture systems that are more physiologically relevant are required to study their roles in HCV entry.

Recently, Huh-7 and 7.5 cells were cultured in Matrigel in HCV studies. Matrigel is a solubilized protein extract from the Engelbreth-Holm-Swarm (EHS) mouse sarcoma. (Kleinman et al., 1986) Matrigel was first used to show the requirement of a basement membrane in the differentiation and polarization of human endothelial cells. (Kubota et al., 1988) Molina-Jimenez

et al. and Baktash et al. showed polarized localization of apical, basolateral, and tight junctional markers when Huh-7 and 7.5 cells were cultured in Matrigel. (Diagram in Figure 36) Moreover, the bile analog 5-chloromethyfluorescein diacetate (CMFDA) was retained at the apical domains, suggesting that the organoids formed functional bile canaliculi. Using Matrigel-cultured Huh-7.5 cells and single particle fluorescent labeling of HCV, Baktash et al. showed the movement of HCV particles from the basolateral domains to the tight junctions during entry. The data also suggested that HCV particles preferentially internalized at the tight junctions. This entry pattern had not been shown before in 2D Huh-7.5 cells, which do not have distinct apical and basolateral domains. The findings suggest that the use of 3D cell culture systems may reveal unknown mechanisms of HCV infection. (Baktash et al., 2018)

Baktash et al. further showed that epidermal growth factor receptor (EGFR) is dispensable for HCV to migrate to the tight junctions. However, it is required for HCV to recruit clathrin components for endocytosis. (Baktash et al., 2018) Moreover, Brown et al. used the organoid system to characterize the role of two transmembrane proteins, Cd302 and Cr1l, in HCV infection. They are species barriers restricting HCV replication in rodents. Expressing mCd302 or mCd302/mCr1l in Matrigel-cultured Huh-7.5 cells inhibits HCV trafficking to the tight junctions. (Brown et al., 2020) These studies suggest that Matrigel-based 3D organoid system is useful in understanding HCV infection. Certain steps of HCV entry, such as trafficking to the tight junctions, cannot be evaluated in 2D cells.

HepG2 is another human hepatoma cell line commonly used in HCV studies. Expressing CD81 and miR-122 in HepG2 cells significantly increases their susceptibility to HCV infection. (Mee et al., 2009; Narbus et al., 2011) HepG2 cells polarize partially. Mee et al. observed that 76%

of HepG2-CD81 cells developed apical domains. The apical domains formed bile canaliculus-like structures that retained CMFDA. While CLDN1 was distributed more uniformly on the plasma membrane in nonpolarized cells, it predominantly localized at the apical domains in polarized cells. However, OCLN was only detected at the apical domains in polarized cells. As the cells became more polarized over time, an inverse correlation was observed with respect to the cell culture derived HCV (HCVcc) and HCV pseudoparticle (HCVpp) infection. It suggested a possible influence of hepatocyte polarity on HCV infection, and hence the importance of polarity in HCV studies. Since HepG2 cells do not completely polarize, researchers have attempted to isolate subclones of HepG2 with an enhanced ability to polarize. (Decaens et al., 2008; Snooks et al., 2008)

Other than entry, studies using 3D cell culture systems to examine other stages of the HCV life cycle are limited. Benedicto et al. evaluated the roles of clathrin and dynamin in HCV egress and found no significant differences between 2D and Matrigel-cultured Huh-7 cells. Besides the membrane domains, the complex polarity of hepatocytes is displayed in cytoskeletal, endoplasmic reticulum, and Golgi apparatus networks. (Decaens et al., 2008) The effect of cell polarity on other stages of the HCV life cycle, including RNA replication and assembly/egress is yet to be addressed. Liu et al. generated a JFH-1 EGFP reporter virus and validated its infection in Matrigel-cultured Huh-7.5 cells. The reporter virus may be useful in live cell analysis of HCV entry and assembly/egress and antiviral screening in 3D cells.

Mebiolgel is another matrix-based cell culture system that has been used in HCV studies. In contrast to Matrigel, Mebiolgel is a synthetic polymer free of potential biological contaminants. Mebiolgel-cultured Huh-7 cells form spherical clusters and have increased expression of hepatic

differentiation markers relative to 2D cells. (Rajalakshmy et al., 2015) Using an immortalized hepatocyte cell line HuS-E/2, Aly et al. showed a significant increase in HCV replication when the cells were cultured in Mebiolgel, as compared to 2D cells. The 2D and 3D cells also showed differences in gene expression profiling. The findings highlight the significance of addressing the effect of cell culture systems on HCV infection. Further evaluation of different 3D systems is needed to compare their relevance to infection in vivo.

In addition to extracellular matrices and various cell lines, bioreactor-based approaches have been used to culture hepatocytes in HCV studies. Radial flow and hollow fiber bioreactors are used to mimic the cellular environment in vivo. In the bioreactors, cells attach to semi-permeable capillaries (Knazek et al., 1972; McSharry et al., 2011) or porous glass beads. (Kawada et al., 1998) The cells are nurtured by continuous feeding of fresh medium and removal of toxic metabolites. Aizaki et al. and Kawada et al., respectively, showed that human hepatoma cells FLC-4 and FLC-7 cultured in the radial flow bioreactor were spherical and microvilli-lined. (Kawada et al., 1998; Aizaki et al., 2003) It was in sharp contrast to 2D cells which were flattened and extended with cytoplasmic projections. Using FLC-4 cells cultured in the radial flow bioreactor, Murakami et al. propagated HCV from carriers' serum samples and showed the change in quasispecies composition. (Murakami et al., 2008) In a study of HCV production, Pihl et al. cultured Huh-7.5 cells in the hollow fiber bioreactor. Since the cells grew at a higher density in the bioreactor than in monolayers (McSharry et al., 2011), higher titers of HCV were produced. When the cells were treated with the NS5A inhibitor daclatasvir, lower infectious viral titers were observed. (Pihl et al., 2018) However, the morphology of Huh-7.5 cells in the hollow fiber bioreactor is yet to be evaluated. Thus far, both the radial flow and hollow fiber bioreactors have been mainly used in the production of HCV stocks. For other viruses, such as human

immunodeficiency virus and influenza A virus, the bioreactors have been widely used to determine the pharmacodynamics of antivirals. (Bilello et al., 1994; Drusano et al., 2002; McSharry et al., 2009) The potentials of the systems in studies of HCV life cycle and antivirals are worth exploring.

The use of another bioreactor, the rotating wall vessel, has been explored in HCV studies. While rotating, cells attached to collagen-coated beads experience less shear and turbulence than in flow bioreactors. (Gardner et al., 2016) Sainz et al. showed that Huh-7 cells formed 3D aggregates in the rotating vessel. The cells had higher expression of host factors of HCV entry, including CD81, CLDN1, and OCLN, than 2D cells. How the change in expression affects HCV infection and its relevance to infection in vivo are yet to be addressed.

To conclude, HCV infection, particularly entry, depends on the complex polarity of hepatocytes. While the use of 2D Huh-7 cells have advanced our understanding of HCV infection, the nonpolarized cells may not fully resemble the physiology of hepatocytes in vivo. Development of the optimal 3D systems is obstructed by their relevance and permissiveness to HCV infection. Polarized cell lines, such as HepG2, and matrix or bioreactor-based cell culture are promising 3D infection models. Thus far, they have been used in studies of HCV entry and egress, and exhibited processes of entry that are not observed in 2D cells. Further studies of the localization and functions of host factors in 3D cells may reveal unknown mechanisms of entry and egress. Besides membrane proteins, other cellular components, such as the endoplasmic reticulum and secretory pathway, also exhibit polarity in hepatocytes. Its effect on HCV replication and assembly is yet to be evaluated.

DiD labeling of HCV

The lab has developed single particle tracking of HCV. HCV virions are labelled with lipophilic dye DiD. DiD-HCV particles are then purified by density-gradient ultracentrifugation to enrich for highly infectious virions. (Coller et al., 2009) The lab has characterized DiD-HCV infection in 3D Huh-7.5 organoids with immunostaining of cellular markers over a time course of infection. The data suggest that DiD-HCV entry occurs in three sequential steps: 1) DiD-HCV migrates from the basolateral side to tight junctions at the internal side of 3D organoids. 2) DiD-HCV recruits clathrin endocytic machinery. 3) DiD-HCV is incorporated into early endosomes and uncoated. (Baktash et al., 2018) Using DiD-HCV, we can examine which stages of HCV entry in 3D organoids are blocked when potential host factors are depleted or targeted by inhibitors. We can then reveal the roles of the host factors in HCV entry.

The lab has published a DiD-HCV uncoating assay. Intact DiD-HCV virions colocalize with immunofluorescence signal of HCV core. After virion fusion with endosomes, DiD signal no longer colocalizes with core. Therefore, quantifying the percentage of DiD-HCV particles colocalizing with core indicates if DiD-HCV uncoating has occurred. Using the uncoating assay, the lab has shown that, most DiD-HCV virions have uncoated at 360 minutes post temperature shift in 3D organoids. (Coller et al., 2009; Baktash et al., 2018) Using this assay, we can examine if uncoating is blocked when potential host factors of HCV entry are depleted or when cells are treated with inhibitors targeting host factors or related signaling pathways.

When DiD fluorophores are at a higher concentration, the fluorescent signal is lower due to self-quenching. After the fusion of DiD-HCV particles and host membranes, DiD fluorophores diffuse away from each other. The fluorescent signal increases due to de-quenching. Therefore,

the fluorescent intensity reflects the fusion of DiD-HCV particles. (Sainz et al., 2012) By measuring the fluorescent intensity of DiD over a time course of infection, we can examine if fusion is blocked when potential host factors are depleted or targeted by inhibitors.

HCV entry

This study focuses on the mechanism of HCV entry. HCV entry is complex. It requires multiple cellular receptors and cofactors which are potential targets of antiviral therapies. Those host factors are involved in various cellular functions including cell proliferation, cholesterol uptake, membrane scaffolding, and cell-cell adhesion. Cellular functions of some of the host factors are yet to be fully understood. Studying HCV entry not only contributes to the development of antiviral therapies. It also reveals knowledge of basic cell biology of receptors and signaling pathways.

HCV entry is a complex and multi-step process. (Figure 1) A virion consists of host-derived lipids and apolipoproteins (Apos) that are acquired during assembly. (André et al., 2002; Merz et al., 2011; Catanese et al., 2013) Interactions of the lipids and Apos with attachment factors, such as low-density lipoprotein receptor (LDLR) (Owen et al., 2009) and glycosaminoglycans (GAG) (Jiang et al., 2012), facilitate initial binding of the virion to hepatocytes. After that, HCV envelope glycoprotein E2 binds to receptors cluster of differentiation 81 (CD81) (Pileri et al., 1998) and scavenger receptor BI (SR-BI) (Scarselli et al., 2002). The virion is then internalized via clathrin-mediated endocytosis (Blanchard et al., 2006; Farquharet al., 2012) and sorted into Rab5-positive early endosomes to undergo fusion (Meertens, Bertaux, and Dragic, 2006).

CD81, SR-BI, and tight junction proteins claudin-1 (CLDN1) and occludin (OCLN) are crucial host factors of HCV entry. Expressing all four proteins together renders non-permissive

cells infectable with pseudotyped HCV particles (HCVpp). CD81 and OCLN contribute to the species specificity of HCV. (Ploss et al., 2009) Studies suggest that CD81 acts prior to CLDN1, while CLDN1 acts prior to OCLN during HCV entry. (Evans et al., 2007; Sourisseau et al., 2013; Shimizu et al., 2018) While studies have shown that CLDN1 and OCLN are co-immunoprecipitated with HCV E2, so far there is no evidence of direct binding on the cell surface. (Yang et al., 2008; Liu et al., 2009) CLDN1 mutants that are expressed on the plasma membrane but not exclusively at the cell-cell contact are less efficient in rendering non-permissive cells infectable with HCVpp. (Liu et al., 2009) This suggests that the tight junctional localization of CLDN1 is crucial for its function during HCV entry. The first extracellular loop of CLND1 regulates its interaction with CD81 and HCV entry. (Evans et al., 2007; Cukierman et al., 2009; Harris et al., 2010; Davis et al., 2012) For OCLN, the second extracellular loop is required for HCV entry and contributes to the species tropism of HCV. (Ploss et al., 2009; Michta et al., 2010; Ding et al., 2017)

Hepatocyte membrane is divided into the basal (sinusoidal), lateral, and apical (canalicular) domains. On top of hepatocytes is the space of Disse, above which is the endothelial layer. Blood circulation is above the endothelial layer. Lipoproteins absorbed from the intestines is brought to the space of Disse and binds to glycosaminoglycan (GAG), facilitated by hepatocyte-secreted ApoE. HCV particles are lipoviralparticles (LVP). They consist of lipid, apolipoprotein (Apo), and cholesterol. During HCV infection, LVP binds to GAG. LVP is then hydrolyzed by lipoprotein lipases. Lipoprotein lipases regulate the conversion of high-density lipoprotein (HDL)-bound cholesterol to cholesteryl esters. The hydrolysis of LVP exposes ApoB, which interacts with low density lipoprotein receptor (LDLR). (Miao et al., 2017)

siRNA silencing of clathrin heavy chain inhibited HCVcc infection. (Blanchard et al., 2006) Dynasore, an inhibitor of dynamin, inhibited HCVpp entry or HCVcc infection. (Farquhar et al., 2012) The lab has showed that DiD-HCV entered Huh-7.5 organoids via clathrin-mediated endocytosis. (Baktash et al., 2018) These studies suggest that clathrin-mediated endocytosis regulates HCV internalization.

The field of HCV entry has identified various host factors using proteomics and knockdown screens. They include CD81, EGFR, SR-BI, CLDN1, and OCLN. (Pileri et al., 1998; Scarselli et al., 2002; Evans et al., 2007; Ploss et al., 2009; Lupberger J, et al. 2011) However, detailed roles of individual host factors are yet to be understood. The lab has optimized protocols of three-dimensional (3D) Huh-7.5 cell culture system and single particle tracking of HCV. The protocols are valuable to the study of HCV entry due to 1) The display of individual stages of HCV entry: association with early receptors, migration to tight junctions, and incorporation of virions into early endosomes and uncoating. 2) Spatial constraint of host factors, especially tight junction proteins CLDN1 and OCLN, that represents in vivo infection better than two-dimensional (2D) cell culture. We propose studies using the imaging approaches to further reveal the roles of EGFR and other host factors including CLDN1, OCLN, and newly identified host factors. In this study, we evaluated the roles of SPTBN1, SR-BI, c-Cbl, EGFR, CLDN1, and OCLN.

βII-spectrin (SPTBN1)

Using single particle tracking of HCV and immunostaining in 3D organoids, the lab showed that, after HCV encounter with early receptors CD81, EGFR, and SR-BI, HCV-receptor complex migrates to the tight junction and undergoes internalization. (Baktash et al., 2018) The mechanism of HCV migration to the tight junction is mostly unknown. Lupberger et al. reported that EGFR inhibitor erlotinib or siRNA silencing of EGFR inhibited FRET signaling between

CD81 and CLDN1 in 2D HepG2-CD81 cells. (Lupberger et al., 2011) Moreover, Zona et al. suggested that EGFR regulated the lateral diffusion of CD81 to CLDN1 for HCV entry. (Zona et al., 2013) However, it was not observed when EGFR was studied in the context of polarized hepatoma organoids. Instead, in 3D Huh-7.5 organoids, EGFR was not required for HCV migration to the tight junction. EGFR was required for HCV internalization. CD81-blocking antibody JS-81 or actin inhibitor cytochalasin D inhibited HCV accumulation at the tight junction in Huh-7.5 organoids. (Baktash et al., 2018) Moreover, CD81 binds to HCV envelope protein E2. (Pileri et al., 1998) siRNA silencing of CD81 inhibited E2 relocalization to cell-cell contact in 2D Huh-7 cells. (Brazzoli et al., 2008) Overall, the data suggest that CD81 and actin filaments regulate HCV migration to the tight junction.

We proposed a model of HCV entry in which HCV-receptor complex migrates along actin filaments to the tight junction. (Baktash et al., 2018) In this study, we aimed to find out how the HCV-receptor complex associated with actin filaments. Our collaborator Thomas Pietschmann identified a group of CD81-interacting partners using a proteomic approach. They had enhanced association with CD81 upon HCV infection. (Gerold et al., 2015) Among the top hits, we were interested in βII-spectrin (SPTBN1). Gerold et al. verified that SPTBN1 is a HCV host factor. SPTBN1 was silenced using siRNA. The cells showed a reduction in replication of luciferase reporter-encoding HCV. (Gerold et al., 2015) SPTBN1 has an actin-binding domain that interacts with actin filaments. (Machnicka et al., 2014) It is a scaffolding protein that crosslinks transmembrane proteins, lipids, and actin filaments to assemble signaling complexes. (Baines, 2009) Associating with both CD81 and actin filaments, SPTBN1 had a potential role in HCV migration to the tight junction. We proposed that SPTBN1 acted as a linkage protein bridging the

HCV-receptor complex and actin filaments. The complex migrated along actin filaments to the tight junction for internalization. The hypothesis would be tested in a later chapter.

Scavenger receptor BI (SR-BI)

Cellular functions of SR-BI

SR-BI is a scavenger receptor and belongs to the CD36 family. It consists of 509 amino acids. Its molecular weight changes from 57 kDa to 82 kDa after N-glycosylation on cysteines. 42 amino acids on the C-terminus of SR-BI are replaced by 40 amino acids in SR-BII by an alternatively spliced exon. (Rigotti, Miettinen, and Krieger, 2003) SR-BI is highly expressed in the liver. (Eyre, Drummer, and Beard, 2010; Miao et al., 2017) In normal liver tissue, SR-BI is primarily expressed in the sinusoidal endothelium and hepatocytes. It is also expressed minimally on bile ducts. In terms of the distribution on the plasma membrane, SR-BI is primarily expressed on the basolateral membrane of hepatocytes and apical membrane of some other polarized cells such as enterocytes and colangiocytes. (Rigotti, Miettinen, and Krieger, 2003)

SR-BI is the main transmembrane receptor for high density lipoproteins (HDL). (Eyre, Drummer, and Beard, 2010; Yamamoto et al., 2016) It also binds to low density lipoproteins (LDL). (Rigotti, Miettinen and Krieger, 2003) SR-BI regulates the endocytosis of cholesteryl esters. (Miao et al., 2017) It is done via the bi-directional flux of free cholesterol between cells and lipoproteins. (Eyre, Drummer, and Beard, 2010) To uptake cholesterol associated with HDL in the blood, SR-BI interacts with HDL. When the cell needs to release cholesterol into blood, it is also through the interaction between SR-BI and lipoproteins. (Yamamoto et al., 2016) Cholesterol uptake does not involve lysosomal degradation of lipoproteins. This process is referred to as selective uptake. It contrasts with the function of low density lipoprotein receptor (LDLR), which is internalized via

endocytosis and lipoproteins are degraded in lysosomes. (Rigotti, Miettinen and Krieger, 2003; Eyre, Drummer and Beard, 2010)

The C-terminus of SR-BI has 2 tyrosines (471, 490) and 7 lysines (469, 478, 479, 482, 484, 500, 508). (Calvo and Vega, 1993) The C-terminus of SR-BI interacts with the N-terminal PDZ domain of PDZK1 in 293T cells. (Eyre, Drummer and Beard, 2010)

Roles of SR-BI in HCV infection

Lipoproteins absorbed from the intestines are brought to the space of Disse in the liver and bind to glycosaminoglycan (GAG). The process is facilitated by ApoE secreted by hepatocytes. HCV particles are lipoviralparticles (LVP). They consist of lipid, apolipoprotein (Apo), and cholesterol. During HCV infection, LVP binds to GAG. LVP is then hydrolyzed by lipoprotein lipases. Lipoprotein lipases regulate the conversion of high-density HDL-bound cholesterol to cholesteryl esters. The hydrolysis of LVP exposes ApoB, which interacts with LDLR. (Miao et al., 2017) After binding to LDLR, LVP interacts with SR-BI. (Ploss and Evans, 2012; Shulla and Randall, 2012) SR-BI regulates the transfer of ApoA and ApoC1 from HDL to LVP. (Miao et al., 2017) It is proposed that the interaction sequentially changes the arrangement of lipoproteins on LVP and exposes HCV glycoproteins E1E2 to interactions with other receptors including CD81. (Ploss and Evans, 2012; Shulla and Randall, 2012; Miao et al., 2017)

Expressing CD81, SR-BI, CLDN1, and OCLN together rendered certain mouse cell lines susceptible to the infection of HCVpp, but not that of HCVcc. (Ploss et al., 2009) It suggested that those four host factors facilitated HCV entry. However, additional host factors were required for the cell lines to be permissive to HCV infection.

Studies have suggested a direct interaction between SR-BI and HCV. SR-BI binds to HCV E2. (Scarselli et al., 2002) Antibody targeting or siRNA knockdown of SR-BI inhibited binding of recombinant soluble E2 to Huh-7.5.1 cells. (Krieger et al., 2010; Lupberger et al., 2011) E2 bound to CHO cells expressing CD81 or SR-BI but not cells expressing CLDN1. (Krieger et al., 2010) Anti-SR-BI antibodies blocked viral binding to HepG2+miR-122+CD81 cells. (Sourisseau et al., 2013) In addition, anti-SR-BI antibodies inhibited HCVcc infection post-binding. (Zeisel et al., 2007; Lupberger et al., 2011) It suggests that SR-BI functions in multiple steps of HCV entry.

Treating Huh-7 cells with HDL enhanced HCVpp and HCVcc infection. (Voisset et al., 2005; Dreux et al., 2006; Zeisel et al., 2007) Treating cells with LDL, ApoA-I, or ApoA-II had no effect. (Voisset et al., 2005) HCVpp did not bind to HDL significantly as observed in sedimentation, plasmon resonance, and sensorchip assays. (Voisset et al., 2005; Dreux et al., 2006) HDL did not enhance HCVpp binding to Huh-7 cells. It suggests that HDL functions at a post-binding step to enhance HCVpp infection. Inhibitors blocking the cholesteryl ester transfer activity of SR-BI inhibited HCVpp infection with or without HDL treatment. siRNA silencing of SR-BI or deleting the region on E2 that interacted with SR-BI abolished HDL-mediated enhancement of HCVpp infection. Overall, the data suggest that the enhancement is achieved by the cholesteryl ester transfer activity of SR-BI and SR-BI – E2 interaction. (Voisset et al., 2005) Human serum or HDL inhibited the neutralization effect of anti-E2 antibodies on HCVpp. It was dependent on the cholesteryl ester transfer activity of SR-BI and SR-BI – E2 interaction. (Dreux et al., 2006)

Yamamoto et al. did a thorough study to explore how SR-BI regulated HCV infection. They knocked out SR-BI in Huh-7 cells using CRISPR/Cas9. Knockout cells of SR-BI showed a defect in HCVcc infection. siRNA knockdown of low density lipoprotein receptor (LDLR) in the

SR-BI knockout cells caused a larger defect in HCV infection than siRNA knockdown of LDLR in wildtype cells. Expressing very low density lipoprotein receptor (VLDLR) in Huh-7 cells double knocked out of SR-BI and LDLR rescued the defect in HCV infection. Expressing VLDLR in Huh-7 cells knocked out of CD81, CLDN1, or OCLN did not rescue the defect in HCV infection. It suggests that VLDLR functions similarly to SR-BI and LDLR during HCV infection. To assay viral binding, cells were incubated with HCV at 4°C for an hour. Cells were then washed three times with PBS and HCV RNA was quantified using quantitative real-time PCR. Huh-7 cells double knocked out of SR-BI and LDLR had less HCV RNA. Expressing SR-BI, LDLR, or VLDLR in Huh-7 cells double knocked out of SR-BI and LDLR increased the amount of HCV RNA. It suggested that SR-BI, LDLR, and VLDLR enhanced HCV binding. To examine the function of SR-BI in lipid uptake, cells were incubated with fluorescent labeled HDL and LDL. Huh-7 cells double knocked out of SR-BI and LDLR showed defect in the uptake of both HDL and LDL. Expressing SR-BI or LDLR rescued the phenotype. S112 and T175 of SR-BI and the lipid binding domain of LDLR were essential. The efficiency of the mutants in lipid uptake correlated to their function in supporting HCV infection. Huh-7 cells double knocked out of SR-BI and LDLR showed no defect in the infection of HCVpp produced in 293T cells, which lacked lipoprotein production. In contrast, Huh-7 cells knocked out of CD81 were not susceptible to HCVpp infection. (Yamamoto et al., 2016) It suggests that SR-BI and LDLR facilitate HCVcc infection via lipoproteins on virions.

siRNA knockdown of SR-BI did not affect cell surface expression of CLDN1 or CD81 in Huh-7.5.1 cells. (Lupberger et al., 2011) It suggested that the defect in HCV infection when SR-BI was depleted was not due to changes in other HCV host factors.

In normal liver tissue, SR-BI is primarily expressed on sinusoidal endothelium and hepatocytes and minimally on bile ducts. In hepatocytes, it is located mainly at the basolateral membrane and minimally at canalicular membrane. (Reynolds et al., 2008) In tumor tissue of HCV-associated hepatocellular carcinoma, SR-BI showed no difference in localization or expression compared to surrounding non-tumor tissues. (Reynolds et al., 2008; Sekhar et al., 2018) In normal and infected tissues, CLDN1 and SR-BI colocalized primarily at the basolateral membrane and minimally at the canalicular membrane. (Reynolds et al., 2008) These data suggest that HCV infection does not alter SR-BI expression.

c-Cbl

c-Cbl is a E3 ubiquitin ligase. Its substrates include receptor tyrosine kinases (RTKs) and downstream proteins of RTK signaling pathways. c-Cbl regulates the endocytosis and proteasomal degradation of RTKs. N-terminal tyrosine kinase binding (TKB) domain of c-Cbl recognizes phospho-tyrosines. It allows c-Cbl to interact directly with activated RTKs on the plasma membrane. RING finger domain of c-Cbl recruits ubiquitin-loaded enzymes E2s. (Pennock et al., 2008) After RTK is internalized into vesicles, it phosphorylates Hrs on the early endosome. Activated Hrs causes membrane invagination and the formation of multivesicular bodies. RTK signaling is then inactivated and RTK is degraded. (Miao et al., 2017) EGFR is one of the known substrates of c-Cbl. The interaction between c-Cbl and EGFR will be discussed in detail in the following section.

c-Cbl was identified as a HCV entry factor in a siRNA screen. siRNA knockdown of c-Cbl inhibited HCVcc and HCVpp infection by 72% and 57% respectively. By fluorescent microscopy, the lab observed colocalization of DiD-HCV and c-Cbl in infected Huh-7.5 cells. (Coller et al.,

2009) In addition, siRNA silencing of c-Cbl inhibited HCVcc infection in Lunet N hCD81 cells. (Bruening et al., 2018) Other than that, how c-Cbl is involved in HCV infection is largely unknown. In this study, we proposed to examine the functions of c-Cbl during HCV entry.

Epidermal growth factor receptor (EGFR)

EGFR is a transmembrane signaling protein and a receptor tyrosine kinase. Known EGFR ligands include epidermal growth factor (EGF), transforming growth factor alpha (TGFα), heparin-binding EGF-like growth factor (HB-EGF), betacellulin (BTC), amphiregulin (AR), epiregulin (EPI), epigen (EPG), and CCN2. The binding of the ligands to EGFR regulates a wide range of cellular functions including cell migration, proliferation, differentiation, and survival. After ligand binding, EGFR is either degraded or recycled back to the plasma membrane. Different EGFR ligands differentially induced EGFR Y1173 phosphorylation, ubiquitination, endocytosis, recycling, and degradation. (Roepstorff et al., 2009) The outcomes of EGFR activation and the fates of EGFR depend on multiple factors including: 1) Types of ligands bound; 2) Binding affinity of the ligands to EGFR; 3) Cell types; 4) Stabilities of receptor-ligand complexes in different pH values; 5) Conformation of dimerized EGFR, which causes different accessibilities to C-terminal phosphorylation sites. (Knudsen et al., 2014; Wee and Wang, 2017) The binding affinity of the ligands to EGFR does not correlate to the intensity of EGFR signaling. (Knudsen et al., 2014) Moreover, stress-induced EGFR activation has different outcome from EGF-induced EGFR activation.

Roles of EGFR in HCV entry

siRNA silencing of EGFR inhibited HCVcc infection of various genotypes. (Lupberger J, et al. 2011) EGFR inhibitor erlotinib inhibited HCVcc infection in Huh-7.5, Huh-7.5.1, and PHH

cells in a dose-dependent manner. (Lupberger J, et al. 2011; Diao et al., 2012) Erlotinib inhibited EGF-mediated phosphorylation of EGFR. The inhibitor also inhibited HCVpp entry into HepG2-CD81 or PHH cells. (Lupberger J, et al. 2011) Interestingly, erlotinib had no effect on H77 HCVpp entry into Huh-7.5 cells. (Diao et al., 2012) EGF enhanced HCVpp entry into Huh-7.5.1, HepG2-CD81, and PHH cells in a concentration-dependent manner. It was not observed when cells were treated with erlotinib or anti-EGFR antibodies. (Lupberger J, et al. 2011) EGF or TGF-α enhanced HCVcc infection in Huh-7.5 cells. (Diao et al., 2012) Similar to erlotinib, anti-EGFR antibodies inhibited HCVpp entry and HCVcc infection in PHH cells. In vivo, erlotinib inhibited HCV infection in a chimeric uPA-SCID mouse model. (Lupberger J, et al. 2011)

Erlotinib treatment or siRNA silencing of EGFR did not affect the expression or cell surface expression of SR-BI, OCLN, CLDN1, or CD81 in Huh-7.5.1 cells. Moreover, siRNA silencing of EGFR or anti-EGFR antibodies did not affect the binding of recombinant soluble E2 to Huh-7.5.1 cells. It suggests that EGFR functions at a post-binding step of HCV entry. (Lupberger J, et al. 2011) By adding erlotinib or neutralizing antibodies at different time points, Diao et al. found that EGFR phosphorylation was required after the step involving CD81 and CDLN1 but before clathrin-mediated endocytosis of HCV. (Diao et al., 2012)

siRNA silencing of CD81 or anti-E2 antibodies that blocked E2-CD81 interaction inhibited HCV-induced EGFR phosphorylation at tyrosine 1068. In contrast, anti-CLDN1 antibodies had no effect. Anti-CD81 antibodies induced EGFR phosphorylation at tyrosine 1068. (Diao et al., 2012) The data suggest that E2 binding to CD81 activates EGFR.

Erlotinib or siRNA silencing of EGFR inhibited FRET signaling between CD81 and CLDN1 in HepG2-CD81 cells. (Lupberger J, et al. 2011) Along with the study of Zona et al., the

data suggested that EGFR regulated the lateral diffusion of CD81 to CLDN1 for HCV entry. (Zona et al., 2013) However, it was not observed when EGFR was studied in the context of polarized hepatoma organoids. Instead, in 3D Huh-7.5 organoids, EGFR was not required for HCV migration to the tight junction but was required for HCV internalization. (Baktash et al., 2018)

In addition to HCV entry, erlotinib or siRNA silencing of EGFR inhibited cell-cell transmission of HCV. They also inhibited the fusion of Huh-7 or 293T cells expressing HCV glycoproteins. It suggests that EGFR also functions in other stages of infection. (Lupberger J, et al. 2011)

RAF-MEK-ERK signaling pathway

EGFR phosphorylation regulates multiple downstream signaling pathways. (Wee and Wang, 2017) We previously showed that phosphorylation of EGFR Y1148 and Y1173 were required for HCV infection. (Baktash et al., 2018) Phosphorylated Y1148 and Y1173 of EGFR interact with adaptor proteins Grb2 and SHC to activate the RAF-MEK-ERK pathway. (Batzer et al., 1994; Okabayashi et al., 1994)

The RAF-MEK-ERK pathway is one of the mitogen-activated protein kinase (MAPK) pathways. It is a three-tiered kinase cascade (Cargnello and Roux, 2011) in which activated RAF facilitates phosphorylation of MEK. Activated MEK then leads to phosphorylation of ERK. (Lavoie and Therrien, 2015) RAF has been proposed to activate substrates other than MEK. (Matallanas et al., 2011)

We previously showed that phosphorylation of EGFR Y1148 and Y1173 were required for HCV infection. (Baktash et al., 2018) HCVcc infection of Huh-7.5 cells enhanced phosphorylation of EGFR Y1068, RAF S259 and S338, and ERK T202 Y204. The activation occurred at 3 hours

but not at 1 hour post infection. The activation could be inhibited by IFI6. (Meyer et al., 2015) siRNA silencing of SHC inhibited HCV infection. (Zona et al., 2013) U0126, a MEK inhibitor, inhibited HCVcc infection in Huh-7.5.1 cells. (Mailly et al., 2015) It inhibited HCVcc infection when added at or after 3 hours post temperature shift. (Brazzoli et al., 2008) The studies suggest that the RAF-MEK-ERK pathway is required for HCV infection. In this study, we aimed to examine the functions of the RAF-MEK-ERK pathway in HCV entry.

Grb2 and SHC are adaptor proteins binding to phosphorylated EGFR. They are crucial factors relaying signal from EGFR to the RAF-MEK-ERK pathway. (Batzer et al., 1994; Okabayashi et al., 1994) Their bindings to EGFR are described below.

Upon stimulation with different ligands, EGFR shows differential interactions with Grb2. (Roepstorff et al., 2009) EGF stimulation causes the relocalization of Grb2 from the cytosol to the plasma membrane. This process requires the SH2 but not the SH3 domains of Grb2. In contrast, AG-1478, an EGFR kinase inhibitor, did not inhibit the relocalization. It suggested that EGFR phosphorylation is not required. (Yamazaki et al., 2002; Jozic et al., 2012) In immunoprecipitation assay, EGF enhanced Grb2 binding to EGFR. Less Grb2 bound to EGFR Y1068F, Y1173F, or EGFR with 63 residues from the C-terminus deleted. Deleting 126 residues from EGFR C-terminus drastically impaired Grb2 binding. EGFR Y1148F enhanced Grb2 binding. Y1068 or Y1086 containing peptides inhibited Grb2 binding to phosphorylated EGFR. Y992 or Y1173 containing peptides showed the same effect but at lower degrees. Y1148 had no effect but Y1148 and Y1173 together had a strong blocking effect. (Batzer et al., 1994) The data suggest that EGFR C-terminal tyrosines contribute to Grb2 binding at different extents.

Similar to Grb2, SHC was relocalized from the cytosol to the plasma membrane upon EGF stimulation. AG-1478 did not inhibit the relocalization. It suggested that EGFR phosphorylation is not required. (Jozic et al., 2012) SHC was co-immunoprecipitated with EGFR upon EGF stimulation. The N-terminal domain of SHC was required. A phosphotyrosine-containing peptide competed with EGFR-SHC binding. (van der Geer et al., 1995) EGF enhanced SHC binding to EGFR in immunoprecipitation assay. Less SHC bound to EGFR mutants Y1068F, Y1148F, or Y1173F. Y1148F and Y1173F double mutation drastically impaired SHC binding to EGFR. (Okabayashi et al., 1994) GST-SHC SH2 pulled down EGFR in lysate of EGF-stimulated cells but not that of unstimulated cells. (Pelicci et al., 1992) Y992 or Y1173 containing peptides inhibited SHC binding to phosphorylated EGFR. Y1068, Y1086, or Y1148 containing peptides showed the same effect but at lower degrees. (Batzer et al., 1994; Okabayashi et al., 1994) Gotoh et al. mutated EGFR Y992F or deleted 1011 residues from the C-terminus. The mutants were then expressed in NIH 3T3 cells. Upon EGF stimulation, no binding between SHC and EGFR was detected. However, Grb2, SHC, and ERK were activated. It might be due to a small amount of wildtype EGFR expressing in the cells. (Gotoh et al., 1994)

In addition to direct binding to EGFR, activated SHC provides an additional binding site for Grb2 to EGFR. (Salcini et al., 1994) Grb2 then activates the downstream signaling pathway RAF-MEK-ERK. (Wee and Wang, 2017) After endocytosis, Grb2 and SHC are still bound to internalized EGFR in endosomes. (Yamazaki et al., 2002; Mohapatra et al., 2013)

The studies above suggest that EGFR tyrosines 1068, 1086, 1148, and 1173 all contribute to Grb2 and SHC binding to EGFR, and hence the activation of the RAF-MEK-ERK pathway. The lab previously found that mutating EGFR tyrosines 1045, 1068, and 1086 did not affect HCV

infection, while mutating tyrosines 1148 and 1173 caused more than a log decrease in HCV infection. It suggests a ligand- or infection-specific requirement in activating downstream EGFR signaling pathway. In the next chapter, we would examine the roles of the RAF-MEK-ERK pathway in HCV entry.

EGFR internalization

The lab showed that shRNA silencing of EGFR inhibited HCV recruitment of clathrin light chain for internalization. (Baktash et al., 2018) It suggests that EGFR internalization by clathrin-mediated endocytosis regulates HCV entry. Therefore, in this study, we proposed to study the mechanisms of EGFR internalization in the context of HCV infection.

EGFR mutants defective in endocytosis have been reported. (Goh et al., 2010; Fortian et al., 2015) Studies have suggested that EGFR internalization is regulated by redundant mechanisms, some of which are listed below.

1) **EGFR phosphorylation**

EGFR forms asymmetric dimers in which the ligands are not involved in the dimerization interface. In dimerized EGFR, the activator kinase allosterically activates the receiver kinase. EGFR is also phosphorylated by other kinases. The C-terminal tail of EGFR ranges from Q958 to A1186. aa 958-1043 is the proximal region or the autoinhibitory domain. When those domains of both receiver and activator are deleted, EGFR is constitutively dimerized and activated. Mutant of V924R, which is in the kinase domain, renders the receptor defective in dimerization. I682Q is a receiver-impaired mutant, while V924R is an activator-impaired mutant. Deletion of aa 999-1186 causes a decrease in phosphorylation at Y845, Y974, and Y992. In contrast, deletion of aa 958-1186 does not have significant effect on the phosphorylation of Y1173. Mutation of Y1086A

causes a decrease in phosphorylation at Y845, Y974, and Y992. (Kovacs et al., 2015; Wee and Wang, 2017) Mutating the dileucine motif of EGFR inhibited EGF-mediated phosphorylation and EGF internalization. (Morrison, Chung, and Rosner, 1996)

AG-1478 is an EGFR kinase inhibitor. It competes with ATP to bind to K721 of EGFR. It inhibits EGFR phosphorylation induced by EGF (Han et al., 1996; Wang et al., 2002; Wang et al., 2005) or TGF-α (Arteaga et al., 1997). AG-1478 does not affect EGFR dimerization induced by EGF. In AG-1478 treated cells, EGF and EGFR were internalized into cytoplasmic Rab5-positive puncta without phospho-tyrosine signal. In contrast, EGFR deleted of the dimerization loop was not dimerized, phosphorylated, or internalized upon EGF stimulation. (Wang et al., 2002; Wang et al., 2005) Biparatopic nanobodies caused EGFR clustering and EGF internalization by clathrin-mediated endocytosis without causing EGFR Y1068 phosphorylation. (Heukers et al., 2013) The studies suggest that dimerization acts upstream of phosphorylation and internalization of EGFR. Phosphorylation is not required for dimerization or internalization. Kinase-independent oncogenic activity of EGFR has been suggested. On the other hand, Heukers et al. showed that EGFR dimerization was not required for EGF-mediated phosphorylation of EGFR Y1068 or ERK T202 Y204. (Heukers et al., 2013)

Honegger et al. showed that, upon EGF treatment, EGFR K721A mutant was phosphorylated at serine and threonine residues, but not tyrosine residues. K721A mutation did not affect EGF binding affinity or EGF internalization or degradation. In contrast, the mutation inhibited EGFR internalization and degradation. (Honegger et al., 1987) Felder et al. showed that EGFR K721A internalized EGF comparable to EGFR wildtype. In contrast to Honegger et al., Felder et al. observed that EGFR K721A was internalized at a similar rate as EGFR wildtype upon

EGF stimulation. However, there were more EGFR K721A found on the cell surface. EGFR K721A was also found on membranes of multivesicular bodies instead of in internal vesicles. (Felder et al., 1990) Data of both studies suggest a model in which EGFR K721A is recycled instead of being degraded.

2) EGFR ubiquitination

Levkowitz et al. studied EGFR ubiquitination regulated by c-Cbl. c-Cbl is a E3 ubiquitin ligase. In the study, EGFR was immunoprecipitated and treated with AG-1478. AG-1478 is an EGFR kinase inhibitor. (Han et al., 1996; Wang et al., 2002; Wang et al., 2005) Recombinant c-Cbl was then added for in vitro ubiquitination assay. The results showed that AG-1478 inhibited ubiquitination of EGFR in a dose-dependent manner. Kinase-defective mutant or Y1045F of EGFR were not ubiquitylated by c-Cbl. In EGF-treated cells, c-Cbl was not co-immunoprecipitated with EGFR Y1045F. In contrast, the mutation did not affect co-immunoprecipitation of EGFR and SHC. (Levkowitz et al., 1999)

Upon EGF treatment, c-Cbl is recruited to activated EGFR. Via TKB domain, c-Cbl associates directly with phosphotyrosine 1045 (pY1045) of EGFR. c-Cbl can also associate indirectly with activated EGFR. It is done via the adaptor protein Grb2. Grb2 binds to the proline region of c-Cbl via the SH3 domain of Grb2. Grb2 also binds to pY1068 or pY1086 of EGFR via the SH2 domain of Grb2. Upon stimulation with different ligands, EGFR shows differential interactions with c-Cbl and Grb2. (Roepstorff et al., 2009) The cooperative binding of c-Cbl and Grb2 to EGFR contributes to the threshold of EGFR endocytosis. (Sigismund et al., 2008; Capuani et al., 2015) After binding, c-Cbl Y371 is phosphorylated by EGFR. However, it is unclear if the phosphorylation is done directly by EGFR or by kinases activated by EGFR. Ubiquitin-loaded

enzymes E2s are then recruited to the RING finger of c-Cbl. Ubiquitin units are then ligated to EGFR. Known ubiquitination sites of EGFR are in the kinase domain. (Levkowitz et al., 1999; Pennock et al., 2008; Mohapatra et al., 2013) EGFR deleted of its C-terminus and mutated at K652R, K684R, K1037R, and K1075R bound to c-Cbl and was ubiquitylated. (Mosesson et al., 2003)

When cells were treated with a low concentration of EGF, EGFR was ubiquitylated by c-Cbl in a smaller degree. This triggered clathrin-mediated endocytosis of EGFR. EGFR was recycled to the plasma membrane. EGFR signaling was maintained. When cells were treated with a high concentration of EGF, EGFR was ubiquitylated by c-Cbl in a larger degree. EGFR internalization was independent of clathrin. EGFR was degraded and signaling was turned off. siRNA silencing of clathrin was used to inhibit clathrin-mediated endocytosis, while filipin was used to inhibit clathrin-independent endocytosis. (Sigismund et al., 2008; Capuani et al., 2015)

c-Cbl-mediated ubiquitination is not required for EGF-induced EGFR endocytosis. EGFR mutants that could not bound to c-Cbl and be ubiquitylated were still internalized. (Mohapatra et al., 2013) EGFR mutant Y1045F had nearly no c-Cbl recruitment and hence no EGFR ubiquitination. However, there was still clathrin-mediated endocytosis. (Sigismund et al., 2008; Capuani et al., 2015) Huang, Goh, and Sorkin mutated 15 lysine residues to alanine residues at the tyrosine kinase domain of EGFR. Upon EGF stimulation, the mutant was not ubiquitylated. However, it was phosphorylated and internalized. (Huang, Goh, and Sorkin, 2007) These studies suggest that ubiquitination is not required for EGFR internalization. On the other hand, c-Cbl binding and ubiquitination are not sufficient for EGFR internalization. (Pennock et al., 2008)

After internalization, EGFR is either degraded or recycled back to the plasma membrane. (Roepstorff et al., 2009) c-Cbl disassociates from EGFR before EGFR is degraded. (Pennock et al., 2008) Dominant-negative mutants of c-Cbl severely inhibited EGFR downregulation. However, EGFR was still observed in vesicles in the cytoplasm. Studies have suggested that c-Cbl acts downstream of EGFR internalization, at steps such as late endosome trafficking and degradation. (Levkowitz et al., 1999; Pennock et al., 2008; Mohapatra et al., 2013)

The above studies suggest that EGFR endocytosis is regulated by redundant mechanisms and dependent on ligand concentrations. Moreover, internalization of its ligands is not necessarily linked to internalization of EGFR. In this study, we would examine how EGFR regulates HCV internalization.

Tight junction proteins: claudin-1 (CLDN1) and occludin (OCLN)

HCV entry requires two tight junctional proteins, claudin-1 (CLDN1) and occludin (OCLN). (Evans et al., 2007; Liu et al., 2009; Ploss et al., 2009) Expressing CLDN1 and OCLN, along with CD81 and SR-BI, renders non-permissive cells infectable with HCVpp. (Ploss et al., 2009) In 2D Huh-7 and 7.5 cells, tight junctional markers, ZO-1 and CLDN1, are distributed uniformly on the plasma membrane. (Coller et al., 2009; Molina-Jimenez et al., 2012; Baktash et al., 2018) As a result, the cells poorly resemble the bile canaliculus structure, the distinct separation of the apical and basolateral domains, and the retention of bile in the liver. Since CLDN1 and OCLN are known to be essential for HCV entry, they may not exhibit completely conserved functions in nonpolarized cells. (Narbus et al., 2011) Therefore, we proposed that studying CLDN1 and OCLN in the context of 3D organoids might reveal unknown functions and mechanisms. HCV virions actively travel from the basolateral membrane to the tight junction in the first 90 minutes

after binding. (Baktash et al., 2018) It suggests that the tight junction contributes crucial functions that are absent at the basolateral membrane.

Claudin-1 (CLDN1)

Tight junction protein CLDN1 is a crucial host factor for HCV entry. (Evans et al., 2007) It is a tetraspanin protein located at the apical bile canalicular membrane. (Reynolds et al., 2008; Mailly et al., 2015) The first extracellular loop of CLND1 regulates its interaction with CD81 and HCV entry. (Evans et al., 2007; Cukierman et al., 2009; Harris et al., 2010; Davis et al., 2012). While studies have shown that CLDN1 is co-immunoprecipitated with HCV envelope glycoprotein E2, so far there is no evidence of direct binding on the cell surface. (Yang et al., 2008)

Expression and localization of CLDN1

In normal liver tissue, CLDN1 is primarily expressed on hepatocytes and bile ducts and minimally on sinusoidal endothelium. In hepatocytes, using higher concentration of anti-CLDN1 antibody, CLDN1 was detected on both the basolateral and canalicular membrane. However, when lower concentration of the antibody was used, the staining was confined to the canalicular membrane. (Reynolds et al., 2008) In human liver and human chimeric mouse model, CLDN1 colocalized with apical marker CD10. (Mailly et al., 2015)

In tumor tissue of HCV-associated hepatocellular carcinoma, CLDN1 showed an aggregated staining pattern on plasma membranes compared to surrounding non-tumor tissues. Tumor and non-tumor tissues showed similar expression levels of CLDN1. (Sekhar et al., 2018) In infected tissue, relative to normal tissue, CLDN1 had increased expression on the basolateral membrane of hepatocytes but no increase on sinusoidal endothelium or bile ducts. HCVcc infection upregulated CLDN1 expression in Huh-7.5 cells. In normal tissue, CLDN1 and CD81

showed stronger colocalization at the apical-canalicular membrane. In infected tissue, the colocalization was stronger at the basolateral membrane. In normal and infected tissues, CLDN1 and SR-BI colocalized primarily at the basolateral membrane and minimally at the canalicular membrane. (Reynolds et al., 2008)

CLDN1 colocalized with ZO-1 in Huh-7 cells. TNF-α treatment disrupted CLDN1 membrane localization and HCVpp and HCVcc infection in Huh-7.5.1 cells. (Yang et al., 2008) siRNA silencing of E-cadherin disrupted tight junction localization of CLDN1 in Huh-7.5.1 and HepG2 miR122 CD81 cells. (Li et al., 2016) HCVcc infection in Huh-7 cells downregulated CLDN1 and OCLN levels, but not CD81 level. (Liu et al., 2009) HCVpp induced CLDN1 internalization. (Farquhar et al., 2012)

Roles of CLDN1 in HCV infection

CLDN1 was identified as an entry factor in a screen that lentivirally expressed complementary DNA library of Huh-7.5 cell line in non-permissive 293T CD81+ SR-BI+ cell line. Anti-Flag antibody blocked HCVpp infection in 293T cells expressing CLDN1 with a Flag sequence inserted in the first extracellular loop. By introducing blocking antibodies against CD81 and CLDN1 respectively at various times during infection, the authors suggested that CD81 acted prior to CLDN1. (Evans et al., 2007)

siRNA silencing of CLDN1 inhibited infection of HCVpp or luciferase-expressing HCVcc in 2D Huh-7.5.1 cells. It did not alter the expression and membrane localization of ZO-1 (Liu et al., 2009) or E-cadherin (Li et al., 2016). Chimeric protein containing the two extracellular loops of CLDN1 and the C-terminal domain of OCLN rendered 293T cells susceptible to HCVpp infection. Mutating CLDN1 at I32, F148, and R158 respectively altered its tight junction

localization and lost its ability to render 293T cells susceptible to HCVpp infection. Liu et al. also identified CLDN1 mutants that localized on the plasma membrane but not exclusively at cell-cell contact. They were less efficient in rendering 293T cells susceptible to HCVpp infection. (Liu et al., 2009) It suggests that the tight junctional localization of CLDN1 is crucial for its regulation on HCV entry.

Yamamoto et al. knocked out CLDN1 in Huh-7 cells using CRISPR/Cas9. Knockout cells of CLDN1 had a significant defect in HCVcc infection. To assay viral binding, cells were incubated with HCV at 4°C for an hour. Cells were then washed three times with PBS and HCV RNA was quantified using quantitative real-time PCR. CLDN1 knockout cells had similar amount of HCV RNA as wildtype cells. (Yamamoto et al., 2016) It suggests that CLDN1 is not required for HCV binding.

CLDN1 mutated at four C-terminal residues, a phosphorylation site, and five palmitoylation sites supported HCVpp entry into HEK or H1H cell lines. In contrast, CLDN1 mutated at I32A or D38A of the first extracellular loop or CLDN1 mutated at the conserved motif did not support HCVpp entry into HEK or H1H cell lines. Two of the mutants at the conserved motif did not colocalize with ZO-1 in HEK cells. (Cukierman et al., 2009)

Interaction between CLDN1 and HCV envelope glycoproteins E1 E2

E1 and E2 respectively were coimmunoprecipitated with CLDN1 in 293T cells expressing CLDN1 and E1 or E2. Biomolecular fluorescence complementation assay (BiFC) showed close proximity of CLDN1 with E1, E2, CD81, and low density lipoprotein receptor (LDLR) respectively in 293T cells. The assay also showed close proximity of CD81 with E2 but not E1 in 293T cells. (Yang et al., 2008) Antibodies targeting CLDN1 inhibited binding of E2 or HCVcc to

Huh-7.5.1 cells. In contrast, they had no effect on binding of E1. E2 bound to CHO cells expressing CD81 or SR-BI but not those expressing CLDN1. (Krieger et al., 2010) HCVpp bound to the first extracellular loop of CLDN1 in BRL3A rat hepatocarcinoma cells. (Douam et al., 2013)

Interaction between CLDN1 and CD81

Anti-CLDN1 antibodies inhibited FRET signaling between CLDN1 and CD81. (Krieger et al., 2010) Mutating CLDN1 M32 or K48 in the first extracellular loop abolished CLDN1 interaction with CD81 or OCLN in 293T cells assessed using FRET. The mutation also inhibited HCVpp entry. (Harris et al., 2010) Moreover, Davis et al. identified residues on CLDN1 and CD81 respectively required for interaction between the two receptors via FRET and HCVpp entry. (Davis et al., 2012)

Farquhar et al. generated two antibodies against a linear epitope of CD81 (amino acids 173 to 192). The antibodies stimulated CD81internalization. siRNA silencing of CLDN1 had no effect on antibody induced-CD81 internalization. Upon CD81 antibody stimulation, intracellular CD81 and CLDN1 colocalized and trafficked to Rab5. (Farquhar et al., 2012) CLDN1-CD81 BiFC signal colocalized with EEA1. (Yang et al., 2008) These studies suggest that CLDN1 and CD81 are internalized and sorted into early endosomes. HCVcc infection enhanced internalization and intracellular colocalization of CD81 and CLDN1. (Farquhar et al., 2012)

Roles of the claudin family in HCV infection

In addition to CLDN1, other members of the claudin protein family have been studied in the context of HCV infection.

CLDN1 is expressed in Huh-7, Huh-7.5, HepG2-CD81, Hep3B, and PLC/PRF/5 cell lines and primary hepatocytes. (Zheng et al., 2007; Meertens et al., 2008) In contrast, it is expressed at low levels in HuH6, 293T, and NIH3T3 cell lines (Haid et al., 2014) and not expressed in U87, HeLa, Bel7402, and L02 cell lines. Interestingly, Bel7402 cells support HCVpp entry. When CLDN9 was silenced using shRNA, the cells no longer supported HCVpp entry. In 293T cells, expressing CLDN3, CLDN6, or CLDN9 enhanced HCVpp entry. (Zheng et al., 2007; Meertens et al., 2008) Entry was inhibited by HCV-infected patient serum, anti-CD81 antibody, or bafilomycin A1. (Meertens et al., 2008) In the case of CLDN9, V32 and V45 were essential for HCVpp entry. (Zheng et al., 2007) Expressing CLDN1 but not expressing CLDN6 or CLDN9 in H1H or NKNT3 cells supported HCVpp entry. Expressing CLDN6 or CLDN9 in Huh-7.5 cells silenced of CLDN1 by siRNA did not complement HCVcc or HCVpp infection. (Meertens et al., 2008)

HuH6, but not Huh-7.5, 293T, or NIH3T3 cell lines, express CLDN6. HuH6 or 293T cells expressing CLDN6 supported HCVpp entry of H77 or Con1 but not that of J6 or JFH1. When the first extracellular loop of CLDN6 was changed to that of CLDN1, the chimeric rendered 293T cells susceptible to HCVpp entry of J6 and JFH1. HuH6 cells supported HCVcc infection of certain isolates. siRNA silencing of CLDN6, but not that of CLDN1, inhibited HCVcc infection in HuH6 miR-122 cells. siRNA silencing of CLDN6 had no effect on HCVcc infection in Huh-7.5 cells. (Haid et al., 2014) Silencing of CLDN1 inhibited HCVcc infection in Huh-7.5 cells and HCVpp entry into primary hepatocytes. Silencing of CLDN2 inhibited HCVcc infection in Huh-7.5 cells but at a lower extent, while silencing of CLDN4 had no phenotypes. (Meertens et al., 2008)

Overall, the studies suggest redundancy of claudin proteins in HCV infection.

Occludin (OCLN)

Tight junction protein OCLN is a crucial host factor for HCV entry. (Ploss et al., 2009) It is a tetraspanin protein located at the apical bile canalicular membrane. (Miao et al., 2017) The second extracellular loop of OCLN contributes to the species tropism of HCV (Ploss et al., 2009; Michta et al., 2010; Ding et al., 2017). While studies have shown that OCLN is co-immunoprecipitated with HCV envelope glycoprotein E2, so far there is no evidence of direct binding on the cell surface. (Liu et al., 2009)

Roles of OCLN in HCV infection

OCLN was identified as an entry factor in a screen that retrovirally expressed complementary DNA library of Huh-7.5 cell line in non-permissive NIH3T3 cell line overexpressing human CD81, SR-BI, and CLDN1. siRNA silencing of OCLN in Huh-7.5 cells inhibited HCVpp and HCVcc infection. Expressing CD81, SR-BI, CLDN1, and OCLN together rendered certain mouse cell lines susceptible to HCVpp but not HCVcc infection. By expressing different combinations of human or murine CD81, SR-BI, CLDN1, and OCLN in mouse or hamster cell lines, the authors suggested that human CD81 and OCLN were the determinants of the species specificity of HCV. For OCLN, the authors further mapped the determinant to be within the second extracellular loop. (Ploss et al., 2009)

Mouse OCLN with human version of the second extracellular loop and mouse CD81 with human version of the second extracellular loop were knocked into mice. The mice supported HCV infection in a similar extent as mice adenovirally expressing human CD81 and OCLN. (Ding et al., 2017) Human or mice OCLN with mutations in the second extracellular loop was expressed in

786-O cells. The cells were then infected with HCVpp. The OCLN determinants were conserved across HCV genotypes. (Michta et al., 2010)

Shimizu et al. generated antibodies binding to either of the extracellular loops of OCLN. They inhibited HCVcc or HCVpp infection in Huh-7.5.1-8 cells. They also inhibited HCV infection in human liver chimeric mice. (Shimizu et al., 2018) Sourisseau et al. inserted flag epitope sequence into either of the extracellular loops of OCLN. The mutants were then expressed in cells silenced of OCLN using shRNA. Whether the mutants supported HCVcc or HCVpp infection or blocked by anti-Flag antibody was isolate-specific. (Sourisseau et al., 2013)

siRNA silencing of OCLN inhibited infection of HCVpp or luciferase-expressing HCVcc in 2D Huh-7.5.1 cells. (Liu et al., 2009) Yamamoto et al. knocked out of OCLN in Huh-7 cells using CRISPR/Cas9. Knockout cells of OCLN had a significant defect in HCVcc infection. To examine viral binding, cells were incubated with HCV at 4°C for an hour. Cells were then washed three times with PBS and HCV RNA was quantified using quantitative real-time PCR. OCLN knockout cells had similar amount of HCV RNA as wildtype cells. It suggests that OCLN is not required for HCV binding. (Yamamoto et al., 2016) By adding neutralizing antibodies at different times and examining HCVpp entry, studies suggested that the three entry factors functioned in this order: CD81, CLDN1, then OCLN. (Sourisseau et al., 2013; Shimizu et al., 2018)

OCLN was coimmunoprecipitated with E2 in HCVcc-infected Huh-7.5.1 cells. The authors noted that the assay might have reflected intracellular interaction of OCLN and E2. (Liu et al., 2009)

HCVcc infection in Huh-7 cells downregulated CLDN1 and OCLN levels, but not CD81 level. (Liu et al., 2009) HepG2+miR-122+CD81 cells were less polarized when OCLN was

silenced using shRNA. (Sourisseau et al., 2013) siRNA silencing of OCLN did not alter the expression and membrane localization of ZO-1 or CLDN1 in 2D Huh-7.5.1 cells. (Liu et al., 2009) siRNA silencing of E-cadherin disrupted tight junction localization of OCLN in Huh-7.5.1 and HepG2+miR-122+CD81 cells. (Li et al., 2016)

Interaction and internalization of CLDN1 and OCLN

Mutating CLDN1 M32 or K48 in the first extracellular loop abolished CLDN1 interaction with OCLN in 293T cells assayed using FRET. The mutation also inhibited HCVpp entry. (Harris et al., 2010) Chimeric protein containing the two extracellular loops of CLDN1 and the C-terminal domain of OCLN rendered 293T cells susceptible to HCVpp infection. (Liu et al., 2009)

Internalization of CLDN1 and OCLN have been reported. Cytokine treatment, bacterial toxins, or infection induce internalization of CLDN1 and OCLN and their colocalization with endosomal markers. The requirement of clathrin-mediated endocytosis, caveolar-mediated endocytosis, or macropinocytosis varied depending on the stimuli and cell types. Whether one or both of CLDN1 and OCLN internalized also varied. (Utech, Mennigen, and Bruewer, 2010; Yu and Turner, 2008)

In mouse brain microvascular endothelial cells treated with CCL2, GFP-OCLN colocalized with cholera-toxin and ceramide (caveolae-dependent, lipid raft-dependent pathway) but not with transferrin (clathrin-dependent pathway) or dextran (macropinocytosis pathway). siRNA silencing of caveolin-1 or inhibitor reduced CCL2-induced GFP-OCLN internalization. GFP-OCLN colocalized with Rab4 and EEA1 but not with LAMP2. (Stamatovic et al., 2017) E. coli toxin CNF-1 induced OCLN internalization and colocalization with caveolin-1 and EEA1 but not with LAMP1 in T84 epithelial cells. (Hopkins et al., 2003) IFN-γ-induced internalization of CLDN1

and OCLN was dependent on micropinocytosis but independent of clathrin- or caveolar-mediated endocytosis. Internalized OCLN and CLDN1 colocalized with EEA1 but not with Rab5 or LAMP1. (Bruewer et al., 2005) Chicken OCLN C-terminus could regulate the endocytosis of Fc receptor. (Matter and Balda, 1998)

Other than HCV, OCLN is also involved in group B coxsackievirus (CVB) infection. Upon CVB infection, OCLN was phosphorylated and internalized. Infection did not cause internalization of other tight junction proteins such as CLDN1, CAR, JAM-1, ZO-1, ZO-2, and ZO-3. siRNA silencing of OCLN inhibited CVB internalization. Dominant negative mutant of caveolin-1, but not that of dynamin II or Eps15, inhibited CVB-induced OCLN internalization. Upon infection, OCLN was observed in caveolin-1-positive vesicles and macropinosomes. Macropinocytosis inhibitors blocked OCLN internalization and CVB entry. The data suggest that macropinocytosis regulates CVB entry. Dominant negative mutant of Rab5 inhibited CVB and OCLN internalization. Constitutively active mutant of Rab5 caused the accumulation of OCLN and CVB in Rab5-positive vesicles. (Coyne et al., 2007)

HCV internalization is regulated by clathrin-mediated endocytosis. (Blanchard et al., 2006; Farquhar et al., 2012; Baktash et al., 2018) In this study, we proposed to examine if the internalization of CLDN1 or OCLN regulated this process.

Goal of this thesis

The multi-step process of HCV entry is regulated by various host factors including EGFR, tight junction proteins CLDN1 and OCLN, SR-BI, and c-Cbl. The precise functions of each of the entry factors are not fully understood. In this study, using single particle imaging of HCV in polarized hepatoma organoids, we revealed that EGFR performs multiple functions in HCV entry.

EGFR regulates the recruitment of clathrin endocytic proteins to HCV via a mechanism in which phosphorylation of EGFR is dispensable. EGFR phosphorylation is required for virion internalization after the assembly of the clathrin endocytic machinery. We also found that HCV entry activates the RAF-MEK-ERK pathway downstream of EGFR. The signaling pathway regulates the sorting of internalized HCV into early endosomal compartments enriched with APPL1 and EEA1. The two tight junction proteins, CLDN1 and OCLN, function at two distinct stages of HCV entry. CLDN1 is required for HCV to accumulate at the tight junction. OCLN regulates HCV internalization. This study produced further insight into the unusually complex HCV endocytic process.

CHAPTER II

MATERIALS AND METHODS

Cell culture

Huh-7.5 cells (Blight et al., 2002) were cultured in Dulbecco's modified high glucose media (DMEM; Gibco) supplemented with 10% fetal bovine serum (FBS; Gemini), 0.1 mM nonessential amino acids (NEAA; Gibco), 1% penicillin-streptomycin (Millipore Sigma), and incubated at 37°C in 5% CO2. Organoids were cultured as described (Baktash et al., 2018). Briefly, Huh-7.5 cells were trypsinized and diluted in DMEM + 10% FBS to a final concentration of 1 x 105 cells/mL. Equal volumes of diluted cells and Matrigel (Growth factor reduced, phenol red-free; Corning) were mixed and seeded onto cover glasses (ThermoFisher) or glass dishes (Ibidi). Cells were cultured for 6-8 days.

SHC knockout cell lines

Huh-7.5 cells were transfected with MISSION CRISPR gRNA (ID: HSPD0000038097, vector: LV05, gRNA sequence 5'- TGT TTG AAG CGC AAC TCG A, Millipore Sigma) using Lipofectamine 2000 Transfection Reagent (Invitrogen). Transfected cells were selected using puromycin (3 µg/mL, Gibco). Cell clones were then isolated and analyzed for protein expression via immunoblot. Transduced cells were selected using puromycin (3 µg/mL, Gibco).

CLDN1 knockout and complemented cell lines

Huh-7.5 cells were transfected with MISSION CRISPR gRNA (ID: HSPD0000052528, vector: LV05, gRNA sequence 5'-ATA CAC TTC ATG CCA ACG G, Millipore Sigma) using Lipofectamine 2000 Transfection Reagent (Invitrogen). Transfected cells were selected using puromycin (3 µg/mL, Gibco). Cell clones were then isolated and analyzed for protein expression

via immunoblot. To create CLDN1 expressing construct, CLDN1 ORF (template: OHu20823D, GenScript) was amplified using: forward primer (5'- GGA TCT ATT TCC GGT GAA TTC ATG GCC AAC GCG GGG CTG) and reverse primer (5'- ATC CGC GGC CGC TCT AGA TCA CAC ACG TAG TCT TTC CCG CTG GAA GG). pLVX vector was digested with EcoRI and XbaI. Amplified fragments were then inserted into digested pLVX with In-Fusion HD Cloning Plus (Takara) per the manufacturer's instructions.

OCLN knockout and complemented cell lines

OCLN'CR and Venus-OCLN expressing complemented cell lines were gifts of Matthew Evans, Icahn School of Medicine at Mount Sinai. To create OCLN expressing construct, OCLN ORF (template: OHu28110D, GenScript) was amplified using: forward primer (5'-GGA TCT ATT TCC GGT GAA TTC ATG TCA TCC AGG CCT CTT) and reverse primer (5'-ATC CGC GGC CGC TCT AGA CTA TGT TTT CTG TCT ATC ATA GTC TCC). pLVX vector was digested with EcoRI and XbaI. Amplified fragments were then inserted into digested pLVX with In-Fusion HD Cloning Plus (Takara) per the manufacturer's instructions. To create constructs expressing OCLN mutants, Q5 Site-Directed Mutagenesis Kit (NEB) was used per the manufacturer's instructions with pLVX OCLN as template and primer sets: 1) SS1 forward: 5'-AGT ACG ATA ATA GTG AGT GCT ATC C; reverse: 5'-TAA GAA GTA TCT TCT TGT TCT GG; 2) SS2 forward: 5'-AGA ACG AAG CAA GTG AAG GGA TC; reverse: 5'-ATT GAA TTC ATC AGC AGC AGC CA; 3) ΔEC2 forward: 5'-GTG GAT CCC CAG GAG GCC; reverse: 5'-TGG GTT CAC TCC CAT TAT ATA GAC AAT TG.

SR-BI knockout and complemented cell lines

SR-BI'CR cell line was a gift of Matthew Evans, Icahn School of Medicine at Mount Sinai. Constructs expressing SR-BI wildtype and mutants Y471F, Y490F, and K479R were created by Anisha Madhav and Yasmine Baktash. They were expressed in a retroviral vector pLHCX. To improve expression, the ORFs were cloned into a lentiviral vector pLVX. The ORFs was amplified using: forward primer (5'-GGA TCT ATT TCC GGT GAA TTC ATG GGC TGC TCC GCC AAA G) and reverse primer (5'-ATC CGC GGC CGC TCT AGA CTA CAG TTT TGC TTC CTG CAG CAC AG). pLVX vector was digested with EcoRI and XbaI. Amplified fragments were then inserted into digested pLVX with In-Fusion HD Cloning Plus (Takara) per the manufacturer's instructions.

To create constructs expressing SR-BI double mutant Y471F Y490F, Q5 Site-Directed Mutagenesis Kit (NEB) was used per the manufacturer's instructions with pLVX SR-BI Y490F as template and forward primer (5'- GAG AAA TGC TTT TTA TTT TGG AGT AGT AGT AAA AAG) and reverse primer (5'- TTG GCT CCG GAT TTG GCA).

c-Cbl knockout cell line

To create two c-Cbl CRISPR/Cas9 gRNA constructs, lentiCRISPRv2 vector was digested with BsmBI. Oligo sets were phosphorylated and annealed with T4 PNK (NEB) per the manufacturer's instructions. They were then ligated into digested lentiCRISPRv2 with T4 ligase (NEB) per the manufacturer's instructions. Oligo sets: 1) Forward: 5'- TTC GGG CGG TCT CAT TGG GCT CAT GAA GGA CGC CTT; reverse: 5'- ATG AGA CCG CCC GAA CCC GAG CCC CCG GA; 2) Forward: 5'- GCC GGG TAC TGT TGA CAA GAA GAT GGT GGA GAA GTG C; reverse: 5'- TCA ACA GTA CCC GGC GGG TGG GGG CTG AGG. The two gRNA

constructs were respectively transfected into 293T cells using Lipofectamine 2000 Transfection Reagent (Invitrogen). Supernatants were harvested 48 hr after transfection and filtered through a 0.45-micron filter. Huh-7.5 cells were added the two supernatants combined and 8 µg/mL polybrene (Millipore Sigma), spun for 500xg for 1.5 hr at room temperature, and incubated for 4 hr. Transduced cells were selected using puromycin (3 µg/mL, Gibco). Cell clones were then isolated and analyzed for protein expression via immunoblot.

SPTBN1 knockdown cell line

293T cells were transfected with SPTBN1 shRNA (ID: TRCN0000116826, target sequence 5'- CCA AGT GAG AAG GAA ATC AAA, Millipore Sigma) using Lipofectamine 2000 Transfection Reagent (Invitrogen). Supernatant was harvested 48 hr after transfection and filtered through a 0.45-micron filter. Huh-7.5 cells were added the supernatant and 8 µg/mL polybrene (Millipore Sigma), spun for 500xg for 1.5 hr at room temperature, and incubated for 4 hr. Transduced cells were selected using puromycin (3 µg/mL, Gibco) and analyzed for protein expression via immunoblot.

Cell viability assay

Cell viability was determined using CellTiter-Glo Luminescent Cell Viability Assay (Promega) per the manufacturer's instructions.

Pseudoparticle production and transduction

293T cells were transfected with each of the expression constructs using 2nd Gen Packaging Mix & Lentifectin Combo Pack (abm) per the manufacturer's instructions. Supernatants were harvested 48 hr after transfection and filtered through a 0.45-micron filter. Huh-7.5 cells were

added the supernatants and 8 µg/mL polybrene (Millipore Sigma), spun for 500xg for 1.5 hr at room temperature, and incubated for 4 hr.

Transient expression of GFP-Rab5 wildtype or Q79L

pTRIP-GFP-Rab5A expression construct was created by Kelly Coller. (Coller et al., 2009) To create a construct expressing GFP-Rab5A mutant Q79L, Q5 Site-Directed Mutagenesis Kit (NEB) was used per the manufacturer's instructions with pTRIP-GFP-Rab5A as template and forward primer (5'- ACA GCT GGT CTA GAA CGA TAC) and reverse primer (5'- ATC CCA TAT TTC AAA CTT TAC).

293T cells were transfected with each of the expression constructs using 2nd Gen Packaging Mix & Lentifectin Combo Pack (abm) per the manufacturer's instructions. Supernatants were harvested 48 hr after transfection and filtered through a 0.45-micron filter. Huh-7.5 cells were added the supernatants and 8 µg/mL polybrene (Millipore Sigma), spun for 500xg for 1.5 hr at room temperature, and incubated for 4 hr. Transduced cells were infected for HCV replication analysis two days after transduction. Transduced cells were lysed for Western blot analysis three days after transduction.

Highly Infectious Virus Preparation

HCV stocks were generated as described (Mateu et al., 2008; Coller et al., 2009; Baktash et al., 2018). Briefly, Huh-7.5 cells were electroporated with HCV genotype 2a RNA (infectious clone pJFHxJ6-CNS2C3). Viral supernatants were collected daily for up to 8 days after electroporation, filtered through a 0.22-micron filter, then stored at 4°C. Viral titers were determined by limiting dilution and immunohistochemical staining with a NS5A antibody (9E10) (gift of Charles Rice, Rockefeller University) as described (Randall et al., 2006). HCV stocks were

concentrated using polyethylene glycol 8000 (PEG; ThermoFisher) as described (Blight et al., 2002; Coller et al., 2009; Baktash et al., 2018). Briefly, viral supernatant was incubated at 4°C overnight with PEG (final concentration 8% (w/v)). Virus was then centrifuged (8000xg, 20 min, 4°C) and pellet was resuspended in 10 mL of the original supernatant. Resuspended sample was centrifuged again (8000xg, 10 min, 4°C) and pellet was resuspended in 1 mL DMEM. 1 mL of concentrated virus was incubated with 5 µl of lipophilic dye DiD (Invitrogen) for 90 min with shaking at 4°C. Labeled virus was loaded onto a 10%–50% (w/v) OptiPrep iodixanol gradient (Millipore Sigma) in sterile water and centrifuged for 32 x 106 revolutions (30,000 RPMs, 18 hr, 4°C). 0.5 mL fractions were isolated from the gradient. Each fraction was analyzed for HCV RNA levels by Trizol-LS extraction followed by quantitative real-time PCR and infectious virus. Fractions with the best specific infectivity were added to Amicon Ultra 100k filters (Millipore Sigma) and centrifuged (14000xg, 30 min, 4°C). Filters were then inverted in a new tube and centrifuged (1000xg, 2 min, 4°C).

Western Blot Analysis

All cells were lysed in 1% NP40 buffer (150 mM NaCl, 50 mM Tris-HCl pH 8, 10% glycerol, 2 mM EDTA) supplemented with 1 mM cOmplete Mini protease inhibitors (Roche) and 1 mM sodium orthovanadate (ThermoFisher). Proteins were separated on a 4-20% SDS-PAGE gel (BioRad) and transferred to polyvinylidene difluoride (PVDF) membrane. Membrane was incubated in 5% BSA and 0.1% Tween-20 in PBS for 1 hr, incubated overnight at 4°C with primary antibodies (1:10000 anti-β-actin, Santa Cruz #sc-47778; 1:1000 anti-phospho-SHC (Tyr239/240), Cell Signaling #2434; Phospho-p44/42 ERK (Thr202/Tyr204), Cell Signaling #4370; 1:1000 anti-EGFR, Cell Signaling #2232; 1:1000 anti-SHC, BD Transduction #610878;1:500 anti-Rab5, Santa

Cruz #sc-46692; 1:2000 anti-GFP tag, Proteintech #50430-2-AP; 1:500 anti-CLDN1, Invitrogen #37-4900; 1:350 anti-OCLN, Invitrogen #33-1500; 1:1000 anti-SR-BI, Novus Biologicals #NB400-101, #NB400-104; 1:1000 anti-c-Cbl, Cell Signaling #2747; 1:700 anti-phospho-Thr/Tyr, Cell Signaling #9381), then incubated for 1 hr at room temperature with horseradish peroxidase-conjugated secondary antibodies (1:10000 anti-rabbit, Cell Signaling #7074; 1:10000 anti-mouse, Cell Signaling #7076). Membrane was added SuperSignal West Pico PLUS Chemiluminescent or West Femto Maximum Sensitivity substrate (ThermoFisher) and exposed to CL-XPosure film (ThermoFisher).

Immunofluorescence assays

As described (Baktash et al., 2018). Briefly, Huh-7.5 cells were mixed with Matrigel (total volume 75 µl/cover glass), seeded onto cover glasses in 24-well plates, and cultured for 7 days. If indicated, cells were treated with 5 µM sorafenib or AG-1478 or 30 µM ezetimibe (Millipore Sigma) in DMEM + 10% FBS 2 hr prior to infection. Cells were pre-chilled on ice for 15 min, infected with DiD-labeled HCV diluted in DMEM + 10% FBS, incubated on ice for 1 hr, then incubated in 37°C incubator (time of temperature shift: t = 0). Cells were fixed in 4% paraformaldehyde (PFA) (20 min), permeabilized with 0.5% Triton x-100 in PBS (10 min), then rinsed with 0.1 M Glycine in PBS (3 times, 10 min each). Cells were incubated for 2 hr at 37°C in blocking solution (0.1% BSA, 0.2% Triton x-100, 0.005% Tween-20, and 20% goat serum in PBS). Cells were incubated overnight at 4°C with primary antibodies (1:450 anti-ZO-1, Invitrogen #18-7430; 1:100 anti-CLDN1, Santa Cruz #sc-81796; 1:200 anti-clathrin LC, Santa Cruz #sc-12735; 1:100 anti-AP-2µ1, Santa Cruz #sc-49150; 1:75 anti-dynamin I/II, Santa Cruz #sc-390160; 1:75 anti-Rab5, Santa Cruz #sc-46692; 1:75 anti-APPL1, Santa Cruz #sc-271909; 1:600 anti-EEA1,

Abcam #ab2900; 1:100 anti-SNX15, Santa Cruz #sc-393430; 1:250 anti-SPTBN1, Santa Cruz #sc-136074; 1:500 anti-NPC1L1, Santa Cruz #sc-166802; 1:75 anti-phospho-EGFR Y1045, Cell Signaling #2237) After overnight incubation, the Matrigel was placed for 10 min at room temperature. Cells were washed (3 times, 20 min each) with wash buffer (0.1% BSA, 0.2% Triton x-100, and 0.005% Tween-20 in PBS). Cells were incubated for 1 hr at room temperature with 1:1000 Alexa Fluor-conjugated secondary antibody (488 or 594, Invitrogen) in blocking solution, then washed (3 times, 20 min each) with wash buffer. Cover glasses were mounted with ProLong Gold Antifade Mountant with DAPI (Invitrogen).

Entry bypass assay

Huh-7.5 cells were electroporated with HCV RNA as described above and then cultured with DMEM + 10% FBS. 24 h post electroporation, medium was replaced with 5 μM sorafenib or AG-1478 (Millipore Sigma) in DMEM + 10% FBS. 48 h post electroporation, viral supernatants were collected, filtered through a 0.22-micron filter, then stored at 4°C. Viral titers were determined as described above.

HCV RNA Quantitation

RNA was extracted using NucleoSpin 96-well kit for RNA purification (Macherey-Nagel). RNA copy number was determined using quantitative real-time PCR as described (Randall et al., 2007). Copy numbers of HCV and 18S RNA were determined via comparison to concentration standards. HCV RNA was normalized to 18S RNA of the same sample, then to the normalized DMSO or Huh-7.5 control for relative HCV RNA levels.

Confocal Microscopy Analysis

As described (Baktash et al., 2018). Briefly, imaging was performed using Slidebook software and Olympus DSU Spinning Disc Confocal with a 100X NA 1.45 oil-immersion TIRFM objective (intensification: 2, auxiliary: 255). Filter sets used were: DsRed (DiD-HCV), GFP (Alexa Fluor 488), and 405 (DAPI). Z stacks of the organoids were imaged with a step size of 0.5 µm. Images were analyzed with ImageJ (NIH). DiD puncta were evaluated for their colocalization with indicated antibodies. Exposure time and thresholds were standardized for each experiment set. 'n=' value was the total number of DiD puncta quantified per treatment.

Statistical Analysis

Data were shown as mean ± standard deviation or mean ± standard error of the mean as indicated in the figure legends. Statistical significance was determined using two-tailed Student's t test. p values larger than or equal to 0.05 were displayed as ns.

Immunoprecipitation of EGFR

Unpolarized Huh-7.5 cells were treated with 5 µM AG-1478 (Millipore Sigma) in DMEM + 0% FBS for 2 hr. 40 ng/mL recombinant human EGF (Gibco) was added if indicated. Cells were incubated for 15 min before lysis. Lysates were incubated overnight at 4°C with 2 µg/mL anti-EGFR antibody (Invitrogen, #MA5-13269). Per sample 100 µl Dynabeads™ M-280 Sheep Anti-Mouse IgG (Invitrogen) was washed four times with PBS and then incubated with the antibody-bound lysates overnight at 4°C. Beads were washed four times with 1% NP40 buffer (described above) supplemented with 1 mM cOmplete Mini protease inhibitors (Roche) and 1 mM sodium orthovanadate (ThermoFisher). After the final wash, beads were boiled for 5 min at 95°C in 4X

sample buffer (250 mM Tris-HCl pH 6.8, 8% (w/v) SDS powder, 40% glycerol, 20% B-mercaptoethanol, bromophenol blue).

Immunoprecipitation of SR-BI

Unpolarized Huh-7.5 wildtype or EGFR CRISPR'ed cells were serum starved in Opti-MEM (Gibco) for 3 hr. Cells were stimulated with 20 μg/mL high density lipoprotein (Millipore Sigma), incubated on ice for 1 hr, then incubated in 37°C incubator for 10 min before lysis. Per sample 100 μl Dynabeads™ M-280 Sheep Anti-Rabbit IgG (Invitrogen) was washed four times with PBS and then incubated with 1:600 anti-SR-BI antibody (Novus Biologicals, #NB400-104) overnight at 4°C. Beads were washed four times with PBS and then incubated with lysates overnight at 4°C. Beads were then washed four times with 1% NP40 buffer (described above) supplemented with 1 mM cOmplete Mini protease inhibitors (Roche) and 1 mM sodium orthovanadate (ThermoFisher). After the final wash, beads were boiled for 5 min at 95°C in 4X sample buffer (250 mM Tris-HCl pH 6.8, 8% (w/v) SDS powder, 40% glycerol, 20% B-mercaptoethanol, bromophenol blue).

CHAPTER III

EPIDERMAL GROWTH FACTOR RECEPTOR PERFORMS MULTIPLE FUNCTIONS DURING HCV ENTRY

Abstract

Epidermal growth factor receptor (EGFR) is crucial for hepatitis C virus (HCV) entry. Using single particle imaging of HCV infection of polarized hepatoma organoids, we observed that EGFR performs multiple functions in HCV entry, both phosphorylation-dependent and -independent. EGFR is required for the recruitment of clathrin endocytic proteins in a phosphorylation-independent manner. EGFR phosphorylation is required for virion internalization after the assembly of the clathrin endocytic machinery. HCV entry also activates the RAF-MEK-ERK signaling pathway downstream of EGFR phosphorylation. This signaling pathway regulates the sorting and maturation of internalized HCV into APPL1- and EEA1-associated early endosomes, which form the site of virion uncoating.

Introduction

Roles of EGFR in HCV entry

The lab previously performed single particle imaging of HCV in Matrigel-embedded Huh-7.5 organoids. The lab revealed two sequential events in HCV entry: (1) HCV virions migrate from the basolateral membrane to the tight junction; (2) HCV virions are internalized via clathrin-mediated endocytosis at the tight junction. (Baktash et al., 2018) These two distinct steps of HCV entry were not previously revealed in two-dimensional monolayer cell culture, due to its poor resemblance of hepatocyte polarity.

The RAF-MEK-ERK signaling pathway downstream of EGFR is activated during HCV infection. (Mailly et al., 2015; Meyer et al., 2015) However, whether the activation occurs during HCV entry has not been tested. Inhibitors targeting the pathway reduced HCV entry at a post-binding step. (Brazzoli et al., 2008; Zona et al., 2013) The mechanism behind remains unknown.

To study the roles of EGFR during HCV entry in polarized organoids, the lab previously silenced EGFR using shRNA (shEGFR). The lab then examined the colocalization of DiD-HCV and ZO-1 at 0, 90, and 360 minutes post temperature shift in 3D organoids. At 90 minutes, 80-100% of DiD-HCV particles colocalized with ZO-1 for wildtype, shEGFR, and complemented cells. The results suggested that silencing EGFR did not affect DiD-HCV migration to the tight junction. EGFR is not required for HCV migration to the tight junction. (Baktash et al., 2018) The result was different from what has been observed in unpolarized hepatocytes. (Zona et al., 2013) It further highlights the discrepancy contributed by cell polarity and the importance of studying HCV entry in polarized cells. At 360 minutes post temperature shift, less than 40% of DiD-HCV particles colocalized with ZO-1 for wildtype and complemented cells. However, for shEGFR cells, the percentage of colocalization remained high, similar to the level at 90 minutes. It suggested that DiD-HCV accumulated at the tight junction instead of being internalized into the cells. The findings suggested that EGFR is not required for HCV migration to the tight junction but is required for HCV internalization. (Baktash et al., 2018)

The lab previously showed that HCV is internalized by clathrin-mediated endocytosis. DiD-HCV also co-migrated with Rab5. (Coller et al., 2009) To further define the roles of EGFR in HCV internalization, the lab examined the colocalization of DiD-HCV and clathrin light chain (LC) at 0 and 120 minutes post temperature shift in 3D organoids. At 120 minutes, 40-50% of

DiD-HCV particles colocalized with clathrin LC for wildtype cells. However, for shEGFR cells, less than 20% of DiD-HCV particles colocalized with clathrin LC. It was the same level as the control cells at 0 minute. The results suggested that EGFR is required for recruiting clathrin endocytic machinery for HCV internalization. (Baktash et al., 2018)

The C-terminus of EGFR consists of tyrosine and serine residues. Phosphorylation of the residues has been characterized to activate STAT, AKT, ERK, and PKC pathways respectively. (Molina and Adjei, 2006) The lab showed that EGFR was phosphorylated at Y1045, Y1148, and Y1173 upon HCV infection of 3D Huh-7.5 organoids from 90 to 150 minutes post temperature shift. The kinetics mirror the kinetics of DiD-HCV internalization in the imaging assay. It suggests a role of EGFR phosphorylation in HCV internalization.

To further study the role of the three phosphorylation sites of EGFR, the lab expressed mutants Y1045A, Y1148A, and Y1173A respectively in shEGFR cells. Both Y1148A and Y1173A mutants were defective in HCV RNA replication assayed by qRT-PCR. (Baktash et al., 2018) To study their phenotypes in HCV entry, the lab examined the colocalization of DiD-HCV and ZO-1 in 3D organoids. Interestingly, for the two mutants, DiD-HCV did not accumulate at the tight junction at 360 minutes post temperature shift. The results suggested that DiD-HCV internalization was not affected. It contrasted with the phenotype of shEGFR cells as mentioned above.

When DiD fluorophores are at a higher concentration, the fluorescent signal is lower due to self-quenching. After the fusion of DiD-HCV particles and host membranes, DiD fluorophores diffuse away from each other. The fluorescent signal increases due to de-quenching. Therefore, the fluorescent intensity reflects the fusion of DiD-HCV particles. (Sainz et al., 2012) The lab

measured the fluorescent intensity of DiD-HCV at 90 and 360 minutes post temperature shift. In Huh-7.5 organoids, the fluorescent intensity was higher at 360 minutes relative to 90 minutes. It suggested that, at 360 minutes, DiD-HCV particles had fused with host membranes. In contrast, in organoids of EGFR Y1148A and Y1173A mutants, the fluorescent intensity did not increase from 90 to 360 minutes. It suggested that the mutants were defective in HCV fusion. EGFR Y1148 and Y1173 are required at a step after internalization but before fusion of HCV.

Based on the findings, we proposed that EGFR had two distinct roles in HCV entry. 1) One was phosphorylation dependent. We proposed that HCV activated EGFR phosphorylation. Phosphorylated EGFR then activated signaling pathways to regulate HCV entry. 2) Another role was phosphorylation independent. We proposed that EGFR regulated HCV internalization in which EGFR phosphorylation was dispensable.

Studying EGFR using genetic approaches

At the beginning of this study, I attempted to study the roles of EGFR in HCV entry using genetic approaches. CRISPR/Cas9 was used to knock out EGFR in the Huh-7.5 cell line (EGFR'CR). Several EGFR gRNAs were used individually and in combination. Bulk populations of EGFR'CR were generated. Clones were then isolated and analyzed for EGFR expression by Western bolt and immunofluorescent imaging. EGFR was significantly knocked down but not eliminated. EGFR'CR cells were unhealthy and grew slowly. It suggested that knocking down EGFR was cytotoxic. It hindered the generation of polarized organoids for DiD-HCV infection assay. EGFR'CR cells showed only a slight defect in HCV RNA replication assayed by qRT-PCR. It suggested that a low amount of EGFR was sufficient for HCV infection.

To study the role of EGFR phosphorylation, I expressed mutants Y1148A and Y1173A in EGFR'CR and shEGFR cells respectively. EGFR expression was examined using Western bolt and HCV infection was examined using qRT-PCR. Across multiple trials of the experiments, the results were not consistent. It might be due to cytotoxicity of the knockdown. Alternatively, cells expressing wildtype EGFR might have outgrown cells knocked down of EGFR or expressing EGFR mutants. It made the results of the experiments inconclusive.

Because of the failed attempts using genetic approaches, EGFR inhibitors were used instead to study the role of EGFR in HCV entry.

Studying EGFR using inhibitors

To study the roles of EGFR in HCV entry, we used two well-characterized pharmacological inhibitors that distinctly and specifically target respective EGFR functions: (1) AG-1478 and (2) sorafenib.

(1) AG-1478

AG-1478 is an EGFR kinase inhibitor. It competes with ATP to bind to K721 of EGFR. It induces reversible EGFR dimer with no kinase activity. It inhibits EGFR phosphorylation induced by EGF (Figure 2) (Han et al., 1996; Wang et al., 2002; Wang et al., 2005) or TGF-α (Arteaga et al., 1997). It is more potent in inhibiting EGF-mediated phosphorylation of EGFR mutant deleted of the extracellular domain than that of wildtype EGFR. (Han et al., 1996) In AG-1478 treated cells, EGF and EGFR were internalized into cytoplasmic Rab5-positive puncta without phospho-tyrosine signal. (Wang et al., 2002; Wang et al., 2005) It suggests that AG-1478 does not affect the internalization of EGF or EGFR. AG-1478 has also been shown to inhibit EGF-mediated

phosphorylation of ERK Y204 and Akt S473. The inhibition is reversible by washing. (Eguchi et al., 1998; Wang et al., 2002)

Arteaga et al. showed that AG-1478 induced reversible EGFR dimerization in a dose-dependent manner without inducing phosphorylation of EGFR tyrosines. Wildtype EGFR and two kinase-defective mutants (D813A and K721R) were respectively expressed in cells. D813 is the catalytic base in phosphoryl transfer, while K721 is in the ATP-binding domain. AG-1478 induced dimerization of wildtype or D813A, but not K721R EGFR. ATP analog FSBA, which covalently binds to K721, inhibited AG-1478-induced EGFR dimerization. A tyrosine-containing substrate did not affect AG-1478-induced EGFR dimerization. It suggests that AG-1478 does not cause EGFR dimerization by interacting with its tyrosine sites. (Arteaga et al., 1997)

(2) Sorafenib

The lab previously showed that phosphorylation of EGFR Y1148 and Y1173 were required for HCV infection. (Baktash et al., 2018) Phosphorylated Y1148 and Y1173 interact with adaptor proteins Grb2 and SHC. Activated SHC provides an additional binding site for Grb2. Grb2 then activates the downstream signaling pathway RAF-MEK-ERK. (Batzer et al., 1994; Okabayashi et al., 1994; Salcini et al., 1994) siRNA silencing of SHC inhibited HCV infection. (Zona et al., 2013) It suggests that the RAF-MEK-ERK pathway regulates HCV infection.

To investigate if the RAF-MEK-ERK pathway was required for HCV entry, we used a RAF inhibitor sorafenib. The crystal structure of B-RAF kinase domain in complex with sorafenib has been solved. Sorafenib occupied the ATP binding pocket and catalytic motifs. Residues of B-RAF that contacted sorafenib are conserved in RAF. It suggests that sorafenib occupies the ATP binding pocket and catalytic motifs of RAF. (Wan et al., 2004) Wilhelm et al. reported the IC_{50} of

sorafenib on the RAF-MEK-ERK pathway and receptor tyrosine kinases measured by biochemical assays. Sorafenib significantly inhibited the kinase activity of RAF but not that of EGFR, MEK-1, or ERK-1. (Wilhelm et al., 2004) Sorafenib is an FDA-approved compound for renal cell carcinoma and hepatocellular carcinoma.

As a RAF inhibitor, sorafenib inhibits the activation of the RAF-MEK-ERK pathway. Sorafenib inhibited phosphorylation of ERK T202 Y204 and MEK S217 S221, but not that of PKB S473. Sorafenib inhibited VEGF-mediated phosphorylation of VEGFR Y1054 Y1059 and PDGF-mediated phosphorylation of PDGFR Y857. Moreover, it inhibited phosphorylation of ERK T202 Y204 in human tumor xenografts. (Adnane et al., 2006) Sorafenib enhanced phosphorylation of MEK S217 S221 from 0.01 to 0.3 μM but inhibited it from 1 to 30 μM. (Poulikakos et al., 2010) Sorafenib has no effect on the activation of the PI3K-AKT pathway, which is another downstream signaling pathway mediated by EGFR. (Adnane et al., 2006)

Using the two inhibitors, we revealed that EGFR performed multiple functions during HCV entry into polarized hepatoma organoids. EGFR regulated HCV recruitment of clathrin endocytic proteins. In this process, EGFR phosphorylation was dispensable. EGFR phosphorylation was required for HCV dissociation from the tight junction. HCV entry activated the RAF-MEK-ERK pathway downstream of EGFR. The signaling pathway regulated the recruitment of early endosomal proteins APPL1 and EEA1 to internalized HCV.

Results

EGFR phosphorylation regulates HCV internalization after the assembly of the clathrin endocytic machinery

We previously showed that EGFR was phosphorylated at Y1148 and Y1173 upon HCV infection of Huh-7.5 organoids. The kinetics mirrored the kinetics of HCV internalization observed in the imaging assay. We also showed that phosphorylation of Y1148 and Y1173 were required for HCV infection. (Baktash et al., 2018) It suggests a role of EGFR phosphorylation in HCV internalization.

To further investigate the function of EGFR phosphorylation in HCV entry, we used an EGFR kinase inhibitor AG-1478. AG-1478 competes with ATP to bind to K721 of EGFR. It induces reversible EGFR dimer with no kinase activity. It inhibits EGFR phosphorylation induced by EGF (Figure 2) (Han et al., 1996; Wang et al., 2002; Wang et al., 2005) or TGF-α (Arteaga et al., 1997). AG-1478 inhibited HCV RNA replication in Huh-7.5 cells upon HCV infection in a dose-dependent manner. (Figure 3) The inhibitor did not cause a major decrease in cellular viability. (Figure 3) We asked if AG-1478 inhibition of HCV replication observed in our experiment was due to a defect in viral entry. We bypassed entry by electroporating HCV RNA into Huh-7.5 cells. AG-1478 had no effect on infectious virus production. (Figure 4) It suggests that AG-1478 inhibits HCV entry.

We next asked how EGFR phosphorylation contributed to HCV entry. We examined the effect of AG-1478 on DiD-HCV colocalization with tight junction proteins ZO-1 and CLDN1 respectively. In DMSO- or AG-1478-treated organoids, DiD-HCV colocalization with the tight junction markers peaked at 90 min post temperature shift. (Figure 5) It indicates that AG-1478 had

no effect on DiD-HCV migration to the tight junction. It is consistent with our previous study showing that EGFR is not required for HCV migration to the tight junction. (Baktash et al., 2018) At 360 min post temperature shift, DiD-HCV colocalization with the tight junction markers was significantly higher in AG-1478-treated organoids than in DMSO-treated organoids, indicating that AG-1478 inhibited DiD-HCV dissociation from the tight junction. (Figure 5) We previously showed that DiD-HCV entered Huh-7.5 organoids via clathrin-mediated endocytosis. (Baktash et al., 2018) We asked if AG-1478 inhibited endocytosis of DiD-HCV. We infected DMSO- or AG-1478-treated organoids with DiD-HCV and probed for clathrin light chain (LC), AP-2µ1, and dynamin, respectively. AG-1478 had no significant effect on DiD-HCV colocalization with the three endocytic proteins over the time course of infection. (Figures 6-8) We previously showed that shRNA silencing of EGFR inhibited DiD-HCV colocalization with clathrin LC. (Baktash et al., 2018) The results in these two studies suggest that during HCV entry, EGFR regulates recruitment and assembly of clathrin components via a mechanism in which EGFR phosphorylation is dispensable. EGFR activation/phosphorylation is required after the assembly of the clathrin endocytic machinery, but prior to the disassociation of virions from the tight junction.

EGFR-mediated RAF-MEK-ERK pathway regulates the sorting of HCV into APPL1- and EEA1-associated early endosomes

The lab previously showed that phosphorylation of EGFR Y1148 and Y1173 were required for HCV infection. (Baktash et al., 2018) Phosphorylated Y1148 and Y1173 interact with adaptor proteins Grb2 and SHC. Activated SHC provides an additional binding site for Grb2. Grb2 then activates the downstream signaling pathway RAF-MEK-ERK. (Batzer et al., 1994; Okabayashi et

al., 1994; Salcini et al., 1994) siRNA silencing of SHC inhibited HCV infection. (Zona et al., 2013) It suggests that the RAF-MEK-ERK pathway regulates HCV infection.

We examined if the RAF-MEK-ERK pathway was activated upon HCV entry. We infected Huh-7.5 organoids and lysed them at 120 min post temperature shift. (Figure 9) Phosphorylation of SHC at Y239/240 and ERK at T202/Y204 were enhanced in infected organoids relative to uninfected or mock infected organoids. (Figure 9) AG-1478 treatment inhibited HCV-mediated phosphorylation of both ERK and SHC. (Figure 9A) It suggests that HCV entry activates the pathway via EGFR phosphorylation.

We used CRISPR/Cas9 to knock out SHC in the Huh-7.5 cell line (SHC'CR). (Figure 10A) HCV RNA replication was significantly reduced in SHC'CR cells upon HCV infection. (Figure 10B) It suggests that HCV infection requires SHC.

To investigate if the RAF-MEK-ERK pathway was required for HCV entry, we used a RAF inhibitor sorafenib. Sorafenib occupies the ATP binding pocket and catalytic motifs of RAF. (Wan et al., 2004) It significantly inhibits the kinase activity of RAF but not that of EGFR, MEK-1, or ERK-1. (Wilhelm et al., 2004) Sorafenib inhibited HCV RNA replication. (Figure 11) (Zona et al., 2013) It did not cause a major decrease in cellular viability. (Figure 11) When entry was bypassed via electroporation of HCV RNA, sorafenib had no effect on infectious virus production. (Figure 4) It demonstrates that the antiviral effect was due to inhibition of HCV entry but not that of later stages of the viral life cycle. In EGFR-regulated RAF-MEK-ERK pathway, RAF functions downstream of SHC and upstream of ERK. As expected, sorafenib treatment inhibited HCV-mediated phosphorylation of ERK but not that of SHC. (Figure 9B) It demonstrates the selectivity of this inhibitor in examining the RAF-MEK-ERK pathway in HCV infection.

We next asked the effect of sorafenib on HCV entry. We examined the effect of sorafenib on DiD-HCV colocalization with tight junction markers ZO-1 and CLDN1 respectively. In DMSO- or sorafenib-treated organoids, the colocalization peaked at 90 min and then decreased at 360 min post temperature shift. (Figure 12) This indicates that most DiD-HCV particles had undergone internalization, suggesting that HCV internalization is independent of the activation of the RAF-MEK-ERK pathway.

After endocytosis, HCV is sorted into early endosomes to undergo fusion. (Meertens, Bertaux, and Dragic, 2006) We previously showed that internalized DiD-HCV was trafficked to the early endosomes. (Baktash et al., 2018) We asked if the RAF-MEK-ERK pathway regulated this process. We examined the effect of sorafenib on DiD-HCV colocalization with early endosomal proteins: Rab5, APPL1, and EEA1, respectively. APPL1 and EEA1 are effectors that interact with Rab5. (Simonsen et al., 1998; Miaczynska et al., 2004; Zhu et al., 2007) Rab5 is present in both clathrin-coated vesicles and early endosomes (Chavrier et al., 1990; Bucci et al., 1992; Rubino et al., 2000; van der Beek et al., 2022), while APPL1 and EEA1 are Rab5 effector proteins that label two distinct pools of early endosomes (Simonsen et al., 1998; Miaczynska et al., 2004; Zhu et al., 2007; van der Beek et al., 2022). During endocytosis, cargoes from clathrin-coated vesicles are sequentially sorted into Rab5- and APPL1-positive endocytic organelles then into EEA1-positive early endosomes. (Mu et al., 1995; Rubino et al., 2000; Miaczynska et al., 2004; Zoncu et al., 2009)

In DMSO-treated organoids, DiD-HCV colocalization with Rab5 and APPL1 peaked at 120 min post temperature shift, while colocalization with EEA1 peaked at 150 min. (Figures 13-15) The dynamics is consistent with previous studies showing sequential colocalization of

internalized cargoes with Rab5 and APPL1, then EEA1. (Mu et al., 1995; Rubino et al., 2000; Miaczynska et al., 2004) Sorafenib had no effect on DiD-HCV colocalization with Rab5. (Figure 13) In contrast, sorafenib significantly reduced DiD-HCV colocalization with APPL1 and EEA1. (Figures 14 and 15) It suggests that the RAF-MEK-ERK pathway regulates DiD-HCV sorting into APPL1- and EEA1-associated endosomes.

As mentioned above, AG-1478 inhibits EGFR phosphorylation. Sorafenib inhibits the RAF-MEK-ERK pathway which is one of the signaling pathways regulated by EGFR phosphorylation. Therefore, we expected that, same as sorafenib, AG-1478 inhibited DiD-HCV sorting into early endosomes. To test that, we infected DMSO- or AG-1478-treated organoids with DiD-HCV. We then examined DiD-HCV colocalization with Rab5 and EEA1, respectively. As expected, AG-1478 significantly reduced DiD-HCV colocalization with EEA1. (Figure 16) While we showed above that AG-1478 inhibited DiD-HCV dissociation from the tight junction, it had no effect on DiD-HCV colocalization with Rab5. (Figure 17)

We also examined DiD-HCV colocalization with APPL1 in DMSO- or AG-1478-treated organoids. Four independent trials were performed. (Figure 18A) Results of the trials varied. When results of the four trials were combined, AG-1478-treated organoids did not show a significant defect in DiD-HCV colocalization with APPL1. (Figure 18B)

Expressing GFP-Rab5 inhibits HCV infection

We showed above that when the RAF-MEK-ERK pathway was inhibited, internalized HCV associated with Rab5 (Figure 13) but failed to associate with APPL1 or EEA1 (Figures 14 and 15). APPL1 and EEA1 are recruited to early endosomes via interaction with the active form of Rab5 (Rab5-GTP). (Simonsen et al., 1998; Miaczynska et al., 2004; Zhu et al., 2007; Haas et

al., 2005; Jozic et al., 2012) Overexpression of Rab5 enhanced the colocalization of APPL1 and EEA1. (Zoncu et al., 2009) We proposed that the RAF-MEK-ERK pathway facilitated Rab5 activation and hence the interaction of APPL1 and EEA1 with HCV-containing vesicles. If that was the case, a constitutively active mutant of Rab5 (Q79L) (Stenmark et al., 1994) might rescue the inhibition of HCV entry by sorafenib. To test that, we transiently expressed GFP-Rab5 wildtype or Q79L mutant in Huh-7.5 cells. (Figure 19A) We then treated the cells with sorafenib. (Figure 19B) Expressing either GFP-Rab5 wildtype or Q79L mutant significantly inhibited HCV RNA replication upon infection. The defect in HCV infection was more prominent upon sorafenib treatment.

Discussion

Hepatitis C virus (HCV) entry is a multi-step process involving various host factors. The requirement of a broad range of host factors suggests that each performs distinct functions. In our previous studies, we developed single particle imaging of HCV in three-dimensional polarized hepatoma organoids. It has revealed the sequential steps of entry and the functions of entry factors in cell culture that physiologically resembles the polarity of hepatocytes in vivo. (Baktash et al., 2018) In this study, we performed the assay to study epidermal growth factor receptor (EGFR).

Despite extensive studies of EGFR, the complex regulations and wide-ranging functions of the receptor are far from fully understood. We have demonstrated that EGFR regulation on HCV entry does not solely depend on phosphorylation. shRNA silencing of EGFR inhibited HCV recruitment of clathrin light chain for internalization. (Baktash et al., 2018) When EGFR phosphorylation was blocked by AG-1478 (Figure 2), DiD-HCV colocalized with clathrin light

chain, AP-2µ1, and dynamin. (Figures 6-8) It suggests that, during HCV entry, EGFR recruits endocytic proteins independent of phosphorylation.

Various mechanisms have been proposed to regulate clathrin-mediated endocytosis of EGFR, such as ubiquitination (Waterman et al., 2002; Pennock and Wang, 2008) and AP-2 binding sites (Chang et al., 1993; Sorkin et al., 1996). EGFR is ubiquitylated by E3 ligase c-Cbl via interaction with phosphorylated Y1045 of EGFR. (Levkowitz et al., 1999) Y1045 is not required for HCV infection. (Baktash et al., 2018) Moreover, AG-1478 inhibits phosphorylation and hence ubiquitination of EGFR. (Levkowitz et al., 1999) Therefore, our data suggests that EGFR ubiquitination is not required for HCV recruitment of clathrin. (Figure 6) AP-2 binding sites and/or other unknown mechanisms may be responsible. Moreover, ubiquitination and AP-2 binding sites of EGFR are redundant for EGF endocytosis. (Goh et al., 2010) HCV may utilize multiple functions of EGFR to recruit clathrin.

Despite efficient recruitment of the clathrin endocytic machinery, HCV failed to dissociate from the tight junction and undergo internalization when EGFR phosphorylation was blocked by AG-1478. (Figures 5-8) EGFR phosphorylation is not required for EGF internalization. (Honegger et al., 1987; Felder et al., 1990) AG-1478 does not affect the internalization of EGF or EGFR. (Wang et al., 2002; Wang et al., 2005) Our data suggests that the internalization of HCV does not fully resemble that of EGF. HCV requires EGFR phosphorylation-dependent functions for efficient internalization. It is independent of the activation of the RAF-MEK-ERK signaling pathway. (Figure 12)

When EGFR phosphorylation was blocked by AG-1478, most DiD-HCV particles accumulated at the tight junction (Figure 5) and colocalized with Rab5 (Figure 17). Studies have

shown that Rab5 can be found on the plasma membrane and clathrin-coated vesicles in addition to early endosomes. Immunofluorescent staining of Rab5 showed localization on both the plasma membrane and cytoplasmic vesicles. (Chavrier et al., 1990) Rab5, together with clathrin heavy chain and adaptors, were detected in clathrin-coated vesicles purified via density gradient. (Bucci et al., 1992) GTP-bound Rab5 was required on both clathrin-coated vesicles and early endosomal membrane for fusion to occur in vitro. In contrast, EEA1 did not bind to purified clathrin-coated vesicles in vitro. (Rubino et al., 2000) By coupling immunofluorescent microscopy to electron microscopy, van der Beek et al. showed that 70% of Rab5 were found in vesicles and tubules, while 20% were in early endosomes. More than 80% of APPL1 were in vesicles, while the remaining were in early endosomes. Around 35% of EEA1 were in early endosomes, while only 5% of them were in vesicles. (van der Beek et al., 2022)

In the AG-1478-treated organoids, it is possible that DiD-HCV particles stayed on the cell surface and colocalized with Rab5 on the plasma membrane and/or attached to clathrin endocytic proteins. Significantly fewer DiD-HCV colocalized with EEA1. (Figure 16) For the recruitment of APPL1, four trials showed variable results. (Figure 18) AG-1478, relative to sorafenib, showed a slighter effect on HCV infection. (Figures 3 and 11) The moderate phenotype of DiD-HCV/APPL1 colocalization in AG-1478-treated organoids might be due to a lower efficiency of the inhibitor. Collectively, our data suggest that EGFR phosphorylation is required for HCV internalization and sorting into the early endosomes. It functions at a step downstream of the recruitment of clathrin endocytic proteins.

Time-lapse TIRF microscopy showed the transformation of clathrin light chain-enriched vesicles to APPL1-positive organelles and the subsequent transformation of APPL1-positive

organelles to EEA1-positive early endosomes. Time-lapse TIRF microscopy also showed the sorting of EGF into APPL1-positive organelles. When dominant negative mutant of dynamin K44A was overexpressed to block the scission of clathrin-coated vesicles, APPL1-positive organelles were significantly depleted. (Zoncu et al., 2009) Phosphorylated EGFR is preferentially sorted to endosomes then lysosomes for degradation, rather than recycling back to the plasma membrane. (Honegger et al., 1987; Felder et al., 1990) Our finding suggests that HCV hijacks this EGFR function in cargo endocytic sorting.

We showed that HCV activates the EGFR-mediated RAF-MEK-ERK signaling pathway for sorting into early endosomes after endocytosis (Figures 9, 14, and 15). Knocking out SHC of the pathway caused a reduction in HCV infection. (Figure 10) When RAF was inhibited by sorafenib, DiD-HCV was internalized (Figure 12) and colocalized with early endosomal protein Rab5 (Figure 13). However, DiD-HCV failed to colocalize with APPL1 or EEA1. (Figures 14 and 15) Both are effectors of Rab5 and preferentially interact with the active form of Rab5 (Rab5-GTP). (Simonsen et al., 1998; Miaczynska et al., 2004; Zhu et al., 2007; Haas et al., 2005; Jozic et al., 2012) The interaction regulates the localization of APPL1 on membranes (Miaczynska et al., 2004) and the maturation and formation of EEA1-positive endosomes (Haas et al., 2005). EGFR-natural ligand EGF activates Rab5 via EGFR phosphorylation. (Jozic et al., 2012) Therefore, we propose that HCV-activated RAF-MEK-ERK pathway facilitates Rab5 activation and hence fusion or maturation of HCV-containing vesicles to early endosomes. RAF or proteins downstream of RAF in the pathway are potential regulators of Rab5.

We found that expressing wildtype or a constitutively active mutant of Rab5 (Q79L) (Stenmark et al., 1994) inhibited HCV infection. (Figure 19) It has been reported that expressing

Rab5 wildtype or Q79L mutant caused the enlargement of early endosomes. (Stenmark et al., 1994) It also enhanced internalization of EGFR and OCLN. The phenotype in EGFR internalization was more pronounced when expressing the Q79L mutant relative to expressing wildtype Rab5. (Dinneen and Ceresa, 2004; Coyne et al., 2007) The changes in cell morphology and endocytosis of EGFR and OCLN, two crucial HCV entry factors, might have inhibited HCV entry and replication.

AG-1478 has been shown to inhibit the replication of subgenomic HCV replicons of genotype 1b but not that of 2a expressed in Huh-7 cells. (Dorobantu et al., 2016) In our study, we observed that AG-1478 inhibited HCV replication in Huh-7.5 cells upon infection with cell culture derived HCV. (Figure 3) Importantly, when HCV endocytosis was bypassed via electroporation of HCV RNA, AG-1478 had no effect on infectious virus production. (Figure 4) It suggests that that the antiviral effect of AG-1478 was due to an inhibition of HCV entry but not that of later stages of the viral life cycle.

CHAPTER IV

HCV UTILIZES TIGHT JUNCTION PROTEINS CLAUDIN-1 AND OCCLUDIN AT SEQUENTIAL STEPS OF ENTRY

Abstract

Tight junction proteins claudin-1 (CLDN1) and occludin (OCLN) are required for hepatitis C virus (HCV) entry. Using single particle imaging of HCV in polarized hepatoma organoids, we reveal the functions of CLDN1 and OCLN respectively during HCV entry into organoids. CLDN1 is required for HCV accumulation at the tight junction. OCLN regulates HCV internalization.

Introduction

Tight junction proteins CLDN1 and OCLN are crucial host factors for HCV entry. (Evans et al., 2007; Ploss et al., 2009) They are tetraspanin proteins located at the apical bile canalicular membrane of hepatocytes. (Reynolds et al., 2008; Mailly et al., 2015; Miao et al., 2017) The first extracellular loop of CLND1 regulates its interaction with CD81 and HCV entry. (Evans et al., 2007; Cukierman et al., 2009; Harris et al., 2010; Davis et al., 2012) For OCLN, the second extracellular loop contributes to the species tropism of HCV. (Ploss et al., 2009; Michta et al., 2010; Ding et al., 2017) While studies have shown that CLDN1 and OCLN are co-immunoprecipitated with HCV envelope glycoprotein E2, so far there is no evidence of direct binding on the cell surface. (Yang et al., 2008; Liu et al., 2009)

In this study, we characterized cells knocked out of CLDN1 and OCLN respectively using CRISPR/Cas9. We revealed the functions of CLDN1 and OCLN during HCV entry in polarized hepatoma organoids. CLDN1 regulates HCV accumulation at the internal membrane. OCLN

regulates HCV internalization. Our findings reveal a complex regulation of HCV entry by the tight junction proteins.

Results

CLDN1 regulates HCV accumulation at the tight junction

The roles of tight junction proteins CLDN1 and OCLN in HCV entry had not been studied in the context of hepatoma organoids, which displayed better polarity than monolayer cell cultures. In this study, we used CRISPR/Cas9 to knock out CLDN1 in the Huh-7.5 cell line (CLDN1'CR). The CLDN1'CR cell line was then virally transduced to express CLDN1 (CLDN1'CR + CLDN1). (Figure 20A) HCV RNA replication was significantly reduced in CLDN1'CR cells upon HCV infection. The defect was rescued in CLDN1'CR + CLDN1 cells. (Figure 20B)

We then investigated the function of CLDN1 in HCV entry. We infected Huh-7.5 or CLDN1'CR organoids with DiD-HCV and examined DiD-HCV/ZO-1 colocalization. In CLDN1'CR organoids, the colocalization was lower than that in Huh-7.5 organoids at 90 min post temperature shift. (Figure 21) Significantly fewer DiD-HCV particles accumulated at the internal membranes of CLDN1'CR organoids (less than 20%) than that of Huh-7.5 organoids (60%) at 90 min post temperature shift (Figure 21). The data indicates that CLDN1 is required for DiD-HCV accumulation at the tight junction.

OCLN regulates HCV internalization

The lab received a Huh-7.5 cell line knocked out of OCLN using CRISPR/Cas9 (OCLN'CR) from Matthew Evans. The OCLN'CR cell line were virally transduced to express OCLN (OCLN'CR + OCLN) (Figure 22A) or Venus-OCLN (Figure 22B). HCV RNA replication

was significantly reduced in OCLN'CR cells upon HCV infection. The defect was rescued in complemented cells. (Figures 22C and D)

We then investigated the function of OCLN in HCV entry. We infected Huh-7.5, OCLN'CR, or OCLN'CR + OCLN organoids with DiD-HCV and examined DiD-HCV/ZO-1 colocalization. In all the organoids, the colocalization peaked at 90 min post temperature shift. It indicates that OCLN is not required for DiD-HCV migration to the tight junction. (Figure 23) At 360 min post temperature shift, DiD-HCV/ZO-1 colocalization decreased in Huh-7.5 or OCLN'CR + OCLN organoids. It indicates that most DiD-HCV particles had undergone internalization. In contrast, in OCLN'CR organoids, the colocalization remained high. It indicates that DiD-HCV failed to internalize. (Figure 23)

We previously showed that DiD-HCV entered Huh-7.5 organoids via clathrin-mediated endocytosis. (Baktash et al., 2018) We asked if OCLN was required for endocytosis of DiD-HCV. We infected Huh-7.5 or OCLN'CR organoids with DiD-HCV and probed for clathrin light chain (LC), AP-2µ1, and dynamin, respectively. In OCLN'CR organoids, DiD-HCV colocalized with clathrin LC and dynamin over a time course indistinguishably from Huh-7.5 organoids. (Figures 24 and 25) For AP-2µ1, in Huh-7.5 or OCLN'CR + OCLN organoids, DiD-HCV/AP-2µ1 colocalization peaked at 120 min and decreased gradually from 120 min to 360 min post temperature shift. In OCLN'CR organoids, the kinetics of AP-2µ1 localization with DiD-HCV was significantly delayed. The level of DiD-HCV/AP-2µ1 colocalization in OCLN'CR organoids at 360 min was comparable to the level in Huh-7.5 organoids at 120 min. (Figure 26)

We next asked what motifs of OCLN were required for its function in HCV entry. Human but not mouse OCLN supports HCV infection, and the species determinant lies within the second extracellular loop of OCLN. (Ploss et al., 2009; Michta et al., 2010; Ding et al., 2017) We asked if that region was required for DiD-HCV entry. We virally transduced the OCLN'CR cell line to express OCLN deleted in the second extracellular loop (OCLN'CR + OCLN ΔEC2). (Figure 22A) The mutation did not alter the tight junction localization of OCLN (Figure 27A) or ZO-1 (Figure 27B). Like OCLN'CR organoids, ΔEC2 organoids showed a delayed localization of AP-2μ1 with DiD-HCV. (Figure 26)

AP-2 is an adaptor complex in which the μ2 subunit (AP-2μ1) directly binds to tyrosine-based sorting signal motifs of endocytic cargoes (YXXΦ; Φ: a bulky hydrophobic residue L/I/M/V/F). (Ohno et al., 1995) Fredriksson et al. suggests that OCLN interacts with AP-2. (Fredriksson et al., 2015) Moreover, OCLN has two potential YXXΦ motifs: YLSV (aa 172-175) and YNRL (aa 481-484). (Fletcher and Rappoport, 2014) However, their functions in endocytosis of OCLN have not been studied. We asked if the motifs were required for HCV infection. For each of the motifs, we mutagenized the tyrosine to phenylalanine and the Φ to hydrophilic threonine. We virally transduced the OCLN'CR cell line to express OCLN mutated at one (SS1 and SS2) or both (SS1&2) of the motifs. (Figure 22A) All mutants rescued the defect in HCV RNA replication of the OCLN'CR cell line. (Figure 28) It suggests that the motifs are not required for HCV infection. Expression levels of wildtype and some of the mutants were higher than the endogenous level of OCLN in Huh-7.5 cells. The expression level of ΔEC2 was comparable to that of SS2 or SS1&2, which completely rescued the OCLN'CR cells. (Figure 22A) Therefore, the defect of ΔEC2 in HCV replication and internalization was not due to the expression level.

OCLN is not required for HCV-mediated activation of the RAF-MEK-ERK pathway

In the previous chapter, we showed that HCV activates the EGFR-mediated RAF-MEK-ERK signaling pathway for sorting into early endosomes. We examined if OCLN was required for the activation. We infected Huh-7.5 or OCLN'CR organoids with DiD-HCV and probed for EGFR phosphorylated at tyrosine residue 1045. (Figure 29A) There was no significant difference in DiD-HCV/phospho-EGFR colocalization between Huh-7.5 and OCLN'CR organoids. Moreover, we infected Huh-7.5 or OCLN'CR organoids and lysed them at 120 min post temperature shift. HCV infection induced ERK phosphorylation at T202/Y204 in OCLN'CR organoids. (Figure 29B) The results indicate that OCLN is not required for HCV-mediated activation of the pathway. EGF treatment did not rescue the defect in HCV infection of OCLN'CR cells. (Figure 29C) It suggests that OCLN and EGFR acts independently during HCV entry.

NPC1L1 regulates HCV dissociation from early endosomes

YXXΦ motifs of OCLN were not required for HCV infection. (Figure 28) Therefore, we proposed that other host factors regulate the recruitment of AP-2 to HCV for endocytosis. NPC1L1, a regulator of cholesterol internalization, consists of two YXXΦ motifs and interacts with AP-2µ1. (Altmann et al., 2004; Ge et al., 2008; Betters and Yu, 2010) NPC1L1 is a HCV entry factor. (Sainz et al., 2012) We then investigated the functions of NPC1L1 in HCV entry. We infected Huh-7.5 or OCLN'CR organoids with DiD-HCV and probed for NPC1L1. (Figure 30) DiD-HCV/NPC1L1 colocalization peaked at 120-150 min post temperature shift. It showed a similar kinetics as DiD-HCV recruitment of AP-2µ1. (Figure 26) OCLN'CR organoids did not show a significant difference in DiD-HCV/NPC1L1 colocalization. (Figure 30) It suggests that NPC1L1 interaction with HCV does not require OCLN.

To further characterize the roles of NPC1L1, we treated Huh-7.5 organoids with ezetimibe which is an inhibitor of NPC1L1 internalization and HCV infection. (Sainz et al., 2012) We then infected the organoids with DiD-HCV and examined DiD-HCV/EEA1 colocalization. (Figure 31) DMSO- and ezetimibe-treated organoids showed a similar level of DiD-HCV/EEA1 colocalization at 120 min post temperature shift. It suggests that ezetimibe has no effect on DiD-HCV sorting into early endosomes. At 360 min post temperature shift, DiD-HCV/EEA1 colocalization in DMSO-treated organoids dropped. It indicated that most virions were dissociated from the early endosomes. In contrast, in ezetimibe-treated organoids, the level of colocalization increased from 120 to 360 min post temperature shift. (Figure 31) It suggests that NPC1L1 is required for HCV to dissociate from the early endosomes.

Discussion

The lab previously revealed two sequential events during HCV entry in polarized hepatoma organoids: (1) HCV virions migrate from the basolateral membrane to the tight junction; (2) Virions are internalized via clathrin-mediated endocytosis at the tight junction. (Baktash et al., 2018) In this study, we found that tight junction proteins, claudin-1 (CLDN1) and occludin (OCLN) act at spatiotemporally distinct events of HCV entry.

For CLDN1, we found that it is required for HCV accumulation at the internal membrane. (Figure 21) It is interesting because, in polarized hepatoma organoids, CLDN1 does not have direct contact with basolateral virions. Knocking out CLDN1 did not affect the polarization of organoids, or the integrity of the tight junction as shown in our images. (Figure 21) Li et al. showed that siRNA silencing of CLDN1 did not affect the expression or tight junction localization of E-cadherin, an adhesion protein. Therefore, the defect in HCV entry was not due to a significant

change in organoid structure. CLDN1 interacts with tetraspanin CD81 and the interaction is required for HCV entry. (Harris et al., 2010; Davis et al., 2012; Yang et al., 2008; Krieger et al., 2010) CD81 regulates HCV trafficking to the tight junction in polarized hepatoma organoids. (Baktash et al., 2018) Moreover, HCV infection induces the internalization and intracellular colocalization of CLDN1 and CD81. (Farquhar et al., 2012) We propose that, after HCV virions attach to the basolateral membrane of hepatocytes, CLDN1-CD81 interaction serves as an anchor to tether migrating HCV virions to the tight junction. In the absence of CLDN1, migrating virions resurface at the basolateral membrane. Alternatively, CLDN1 may regulate signaling events that promote CD81-driven migration to the tight junction without direct physical interaction of the two host proteins. At the tight junction, CD81 may interact with CLDN1 for internalization of the virions. Our data is consistent with published studies showing that CLDN1 acts prior to OCLN during HCV entry. (Sourisseau et al., 2013; Shimizu et al., 2018)

Virions actively travel from the basolateral membrane to the tight junction in the first 90 minutes after binding. It suggests that the tight junction contributes crucial functions that are absent at the basolateral membrane. Indeed, we found that OCLN is required for HCV internalization. (Figure 23) It was proposed that OCLN interacts with AP-2 via the tyrosine-based sorting signal motifs in the cytosolic tail of OCLN for internalization. (Fletcher and Rappoport, 2014; Fredriksson et al., 2015) We showed that the sorting signal motifs of OCLN are not required for HCV endocytosis. (Figure 28) Moreover, despite the slower kinetics, HCV colocalized with AP-2 in the absence of OCLN. (Figure 26) Our finding suggests that OCLN is not required for the recruitment of AP-2 to HCV. Without OCLN, HCV colocalized with clathrin and dynamin. (Figures 24 and 25) Uninternalized HCV were retained at the tight junction (Figure 23) and

accumulated AP-2 (Figure 26). OCLN may act at the stabilization of clathrin-coated pits for successful endocytosis. (Ehrlich et al., 2004)

NPC1L1 has two potential YXXΦ motifs: YQRL aa721-724 and YAPF aa836-839. (Altmann et al., 2004; Betters and Yu, 2010) NPC1L1 interacts with AP-2µ1 and regulates cholesterol internalization in a clathrin/AP-2µ1-dependent manner. AP-2µ1 and clathrin heavy chain were co-immunoprecipitated with NPC1L1. siRNA silencing of AP-2µ1 or clathrin heavy chain inhibited the internalization of NPC1L1 and cholesterol. (Ge et al., 2008) Ezetimibe, an inhibitor of NPC1L1 internalization, inhibited HCVcc infection in Huh-7 cells when added before or during virus inoculation. Ezetimibe inhibited HCVcc infection when added up to 5 hours post temperature shift. To study the effect of ezetimibe on HCV fusion, Sainz et al. performed DiD-HCV dequenching assay. HCV virions are labelled with lipophilic dye DiD. When DiD fluorophores are at a higher concentration, the fluorescent signal is lower due to self-quenching. After the fusion of DiD-HCV particles and host membranes, DiD fluorophores diffuse away from each other. The fluorescent signal increases due to de-quenching. Therefore, the fluorescent intensity reflects the fusion of DiD-HCV particles. Sainz et al. showed that ezetimibe or anti-NPC1L1 antibodies inhibited DiD-HCV dequenching. (Sainz et al., 2012) The study suggested that NPC1L1 is required for HCV entry at a post-binding and pre-fusion step. In this study, we showed that NPC1L1 regulates HCV dissociation from the early endosomes. (Figure 31) Further study of NPC1L1 is needed to understand its functions during HCV entry. NPC1L1 can be knocked out in Huh-7.5 cells using CRISPR/Cas9. Single particle tracking of HCV in polarized organoids can then be performed to examine at what stages of HCV entry is NPC1L1 involved.

Studies have shown that OCLN is internalized upon stimulations such as group B coxsackievirus infection (Coyne et al., 2007), chemokine CCL2 (Stamatovic et al., 2012), and Escherichia coli toxin CNF-1 (Hopkins et al, 2003). Depending on the stimuli and the cell types, OCLN internalization depends on clathrin- or caveolar-mediated endocytosis or micropinocytosis. (Utech et al., 2010; Yu and Turner, 2008) Our findings provide further understanding of OCLN internalization by clathrin-mediated endocytosis and how pathogens hijack this cellular function for entry.

CHAPTER V

HCV UTILIZES SPTBN1, SR-BI, and C-CBL DURING ENTRY

Abstract

βII-spectrin (SPTBN1), scavenger receptor class B member 1 (SR-BI), and E3 ubiquitin ligase c-Cbl are host cofactors of HCV entry. The detailed functions of each are largely unknown. We hypothesized that these entry cofactors may be involved in HCV virions migrating from the basolateral membrane to the tight junction for internalization. This chapter largely presents negative data that did not support our hypothesis; however, is still valuable information to inform future studies. It is known that CD81 engagement recruits the actin binding protein SPTBN1 to the virus-receptor complex and that HCV migration is in association with actin. We hypothesized that SPTNB1 may provide the critical link between CD81 and the actin cytoskeleton. We generated a cell line that was genetically silenced of SPTBN1 and was defective in HCV infection. Another student characterized the cell line and found that HCV migration to the tight junction and internalization were unaffected by SPTNB1 silencing. We previously found that SR-BI enhanced tight junction migration. We hypothesized that c-Cbl may ubiquitylate SR-BI to facilitate an early aspect of HCV entry. To test that hypothesis, we studied the interaction between SR-BI and c-Cbl using immunofluorescent staining and immunoprecipitation; however, we did not obtain data supportive of an interaction. We then tried a genetic approach focusing on mutating two tyrosines, which are putative phosphorylation sites required for E3 ligase binding. We found that mutating the two tyrosine residues in the C-terminus of SR-BI did not affect HCV infection. Knocking out c-Cbl inhibited HCV infection but had no effect on virion migration to the tight junction and internalization. Thus, neither SPTNB1, c-Cbl, nor SR-BI tyrosine phosphorylation are required for

HCV migration to the tight junction, although SPTNB1 and c-Cbl are required for efficient HCV entry.

Introduction

SR-BI is the main receptor for high density lipoproteins (HDL) and regulates the endocytosis of cholesteryl esters. (Eyre, Drummer, and Beard, 2010; Yamamoto et al., 2016; Miao et al., 2017) Expressing SR-BI, along with CD81, CLDN1, and OCLN, renders mouse cell lines susceptible to HCVpp infection. (Ploss et al., 2009) SR-BI binds to HCV envelope glycoprotein E2. (Scarselli et al., 2002) Studies suggest that SR-BI is involved in binding and post-binding steps of HCV entry. (Krieger et al., 2010; Lupberger et al., 2011; Sourisseau et al., 2013; Yamamoto et al., 2016) HDL, a natural ligand of SR-BI, enhances HCV infection. It is dependent on the cholesteryl ester transfer activity of SR-BI and SR-BI – E2 interaction. (Voisset et al., 2005; Dreux et al., 2006; Zeisel et al., 2007) Domains of SR-BI involved in lipid uptake are required for HCV infection. Expressing very low density lipoprotein receptor (VLDLR) rescued the defect in HCV entry of SR-BI-deficient cells. It suggests that SR-BI and VLDLR share common functions during HCV entry. (Yamamoto et al., 2016)

The lab received a Huh-7.5 cell line knocked out of SR-BI using CRISPR/Cas9 (SR-BI'CR) from Matthew Evans. To study the roles of SR-BI during HCV entry, the lab infected Huh-7.5 or SR-BI'CR organoids with DiD-HCV and examined DiD-HCV/ZO-1 colocalization. At 90 minutes, 90% of DiD-HCV particles colocalized with ZO-1 in Huh-7.5 organoids. In contrast, lower colocalization (40-50%) was observed in SR-BI'CR organoids. The result suggests that SR-BI enhances HCV migration to the tight junction. In this study, we proposed to further characterize the functions of SR-BI during HCV entry.

c-Cbl is a HCV entry factor. (Coller et al., 2009) Its functions during HCV infection are largely unknown. It is an E3 ubiquitin ligase that regulates the endocytosis of receptor tyrosine kinases (RTKs). (Pennock et al., 2008) In the case of epidermal growth factor receptor (EGFR), c-Cbl binds to phosphotyrosines of EGFR. The interaction facilitates EGFR ubiquitination which regulates internalization and degradation of the receptor. (Levkowitz et al., 1999; Pennock et al., 2008; Sigismund et al., 2008; Mohapatra et al., 2013; Capuani et al., 2015)

The C-terminus of SR-BI contains 2 tyrosine residues and 7 lysine residues that are susceptible to modification. (Calvo and Vega, 1993) We hypothesized that SR-BI was a substrate of c-Cbl. We proposed that HDL enhanced phosphorylation of SR-BI C-terminal tyrosine residues. After that, the phosphotyrosines recruited c-Cbl which ligated ubiquitin to the lysine residues of SR-BI. The ubiquitination activated downstream signaling that regulated the migration and internalization of HCV. To test the hypothesis, we studied the interaction between SR-BI and c-Cbl using immunofluorescent staining and immunoprecipitation. We found that mutating the tyrosine residues on the C-terminus of SR-BI did not affect HCV infection. Knocking out c-Cbl inhibited HCV infection but had no effect on virion migration to the tight junction and internalization.

βII-spectrin (SPTBN1) is a recently identified HCV host factor that interacts with CD81 during HCV infection. (Gerold et al., 2015) CD81 is known to directly bind HCV envelope protein E2 (Pileri et al., 1998) and is required for HCV migration to the tight junction in polarized hepatoma organoids (Baktash et al., 2018). SPTBN1 consists of an actin-binding domain that interacts with actin filaments. (Machnicka et al., 2014) We proposed that, by interacting with both CD81 and actin filaments, SPTBN1 regulated HCV migration to the tight junction. To test that,

we studied SPTBN1 association with CD81 in 3D organoids. We generated a cell line that was genetically silenced of SPTBN1 and defective in HCV infection. It is useful for further characterization of the roles of SPTBN1 during HCV entry.

Results

Interaction between SR-BI and c-Cbl

We proposed that SR-BI and c-Cbl interacted with each other during HCV infection. To test that, we attempted to visualize SR-BI and c-Cbl in Huh-7.5 cells using immunofluorescence microscopy. However, when the two proteins were stained simultaneously, only the signal of SR-BI was observed. Alternative antibodies of both proteins were tested. Sequential staining was also tested. The cells were incubated with the primary antibodies targeting one of the proteins, washed, and then incubated with the primary antibodies targeting the other protein. After that, the cells were washed and incubated with secondary antibodies. In all trials, the results were the same that only the signal of SR-BI was observed.

Next, we attempted to study SR-BI – c-Cbl interaction using immunoprecipitation. Huh-7.5 cells were treated with HDL for 1 hour before lysis. SR-BI was then immunoprecipitated. (Figure 32) Western blot showed successful precipitation of SR-BI. The blot was probed with antibodies targeting c-Cbl. A protein of 25-35 kDa was co-immunoprecipitated with SR-BI and detected by the c-Cbl antibodies. The protein amount was enhanced in HDL-treated cells. The identity of this 25-35 kDa protein remains a mystery since the molecular weight of c-Cbl is 120 kDa.

We hypothesized that SR-BI was phosphorylated at the C-terminal tyrosine residues upon HDL stimulation to promote receptor internalization. To test that, we probed the blot with

antibodies targeting phospho-tyrosine/threonine. (Figure 32) We did not observe bands corresponding to the size of SR-BI or c-Cbl. Instead, a protein of 130 kDa was co-immunoprecipitated with SR-BI and stained with anti-phospho-tyrosine/threonine antibodies. The band intensity was enhanced in HDL-treated Huh-7.5 cells relative to untreated cells. It suggested that the 130 kDa protein interacted with SR-BI and was phosphorylated upon HDL stimulation.

EGFR is a known substrate of c-Cbl. (Levkowitz et al., 1999) If SR-BI is another substrate of c-Cbl, a SR-BI – c-Cbl interaction might be enhanced in the absence of EGFR. Therefore, the same experiment was done in a Huh-7.5 cell line knocked out of EGFR using CRISPR/Cas9 (EGFR'CR). (Figure 32) The cell line was a gift from Matthew Evans. The basal level of phosphorylation of the 130 kDa protein in untreated EGFR'CR cells was higher, comparable to the level in HDL-treated wildtype Huh-7.5 cells. The level was not enhanced upon HDL treatment in EGFR'CR cells. Similarly, for the protein of 25-35 kDa detected by the c-Cbl antibodies, the amount co-immunoprecipitated with SR-BI was enhanced upon HDL treatment.

Tyrosine and lysine residues of SR-BI in HCV infection

We then used a genetic approach to study the role of SR-BI phosphorylation during HCV infection. A former lab member, Anisha Madhav, expressed SR-BI wildtype and SR-BI mutated at the tyrosine and lysine residues in the C-terminus in Huh-7.5 cells. Tyrosine residues were substituted by phenylalanine residues while lysine residues were substituted by arginine residues. HCV RNA replication upon HCV infection was then examined. Expressing wildtype SR-BI enhanced HCV infection, which is consistent with published literature. Expressing SR-BI Y490F also enhanced HCV infection to a level similar to wildtype SR-BI. In contrast, expressing SR-BI Y471F, K469R, K482 484R, K500 508R, SR-BI mutated at 7 C-terminal lysine residues, or SR-

BI deleted of the C-terminus did not show an increase in HCV infection. Expressing SR-BI K6R or K478 479R enhanced HCV infection, but at levels lower than that of wildtype SR-BI. It suggests that the tyrosine residues and lysine residues are involved in HCV infection.

The above experiment was done by expressing SR-BI in wildtype Huh-7.5 cells. Endogenous expression of wildtype SR-BI and overexpression of SR-BI might have interfered with the functions of SR-BI during HCV infection. The lab received a Huh-7.5 cell line knocked out of SR-BI using CRISPR/Cas9 (SR-BI'CR) from Matthew Evans. To further verify the requirement of the tyrosine and lysine residues of SR-BI in HCV infection, the above experiment was repeated in the SR-BI'CR cells.

Previously, SR-BI wildtype and mutants were expressed in the retroviral vector pLHCX. The expression levels were unsatisfying and hence hindered further characterization. To improve expression, we cloned the genes into the lentiviral vector pLVX by In-Fusion cloning. The plasmids were then transfected into HEK 293T cells to generate pseudoparticles. After that, SR-BI'CR cells were transduced to express the SR-BI mutants Y471F, Y490F, and K479R. (Figure 33)

To examine HCV infection, Huh-7.5, SR-BI'CR, and complemented cells were seeded onto 96-well plates, infected with HCV for 48 hours, and then analyzed for relative HCV RNA levels using quantitative real-time PCR. All mutants rescued the defect in HCV RNA replication of the SR-BI'CR cell line. (Figures 33A and C) It suggests that Y471, Y490, and K479 are not required for HCV infection. In another trial, SR-BI'CR cells expressing SR-BI Y471F or Y490F were generated. In these clones, the expression of the SR-BI mutants was higher. A higher expression level of SR-BI Y471F or Y490F correlated with a higher level of HCV RNA replication.

(Figure 33B) It is consistent with published literature showing that the level of HCV infection correlates with the expression level of SR-BI. (Yamamoto et al., 2016)

To eliminate the possibility that Y471 and Y490 functioned redundantly, we expressed SR-BI double mutant Y471F Y490F in SR-BI'CR cells. We then infected the cells with HCV for 48 hours. Similar to the single mutants, the double mutant rescued the defect in HCV RNA replication of the SR-BI'CR cells. (Figure 33D) Overall, the results suggest that SR-BI Y471, Y490, and K479 are not required for HCV infection.

c-Cbl is not required for HCV migration to the tight junction and internalization

The lab has showed that SR-BI is required for HCV migration to the tight junction in polarized organoids. We proposed that c-Cbl ligated ubiquitin to phosphorylated SR-BI. The ubiquitination activated downstream signaling that regulated the migration and internalization of HCV. To test that, we examined if knocking out c-Cbl phenocopied SR-BI'CR cells. We used CRISPR/Cas9 to knock out c-Cbl in the Huh-7.5 cell line (c-Cbl'CR). (Figure 34A) HCV RNA replication was significantly reduced in c-Cbl'CR cells upon HCV infection. (Figure 34B)

We then investigated the functions of c-Cbl in HCV entry. We infected Huh-7.5 or c-Cbl'CR organoids with DiD-HCV and examined DiD-HCV/ZO-1 colocalization. In Huh-7.5 or c-Cbl'CR organoids, the colocalization peaked at 90 min and decreased at 360 min post temperature shift. (Figure 34C) It suggests that c-Cbl is not required for DiD-HCV migration to the tight junction and internalization.

HCV associates with SPTBN1 during entry

Gerold et al. showed that HCV infection enhanced CD81-SPTBN1 interaction. (Gerold et al., 2015) We hypothesized that CD81-SPTBN1 interaction regulated HCV migration to the tight junction in polarized organoids. To test that, we treated Huh-7.5 organoids with CD81-blocking antibody JS-81. The antibody inhibits HCV migration to the tight junction. (Baktash et al., 2018) We then examined the colocalization of DiD-HCV and SPTBN1. (Figure 35) At 90 min post temperature shift, JS-81-treated organoids showed a slightly lower, but not statistically significant, level of DiD-HCV/SPTBN1 colocalization. It suggests that the CD81-blocking antibody does not affect HCV association with SPTBN1. Moreover, migration to the tight junction is not required for HCV association with SPTBN1. Our data do support the conclusion that SPTBN1 associates with the HCV-receptor complex.

To study the functions of SPTBN1 during HCV entry, we silenced SPTBN1 using shRNA in Huh-7.5 cells (shSPTBN1). (Figure 36A) shSPTBN1 cells were defective in HCV RNA replication assayed by qRT-PCR. (Figure 36B) Another student characterized the cell line and found that HCV migration to the tight junction and internalization were unaffected by SPTNB1 silencing. (Rebecca Reis, data not shown)

Discussion

To test if SR-BI and c-Cbl interacted with each other, we attempted to visualize SR-BI and c-Cbl in Huh-7.5 cells using immunofluorescence microscopy. However, co-staining of the two host factors was not successful. It may be due to incompatibility of the antibodies. Epitope-tagged SR-BI or c-Cbl can be tested in the future. A previous lab study showed that SR-BI and c-Cbl were co-immunoprecipitated in uninfected and HCV-infected Huh-7.5 cells. It suggests interaction of

the two proteins in both uninfected and infected states. The current study did not reproduce the result even though the same protocol was used. (Figure 32) It might be due to the cell lysis conditions during protein preparation. Since SR-BI is a transmembrane protein, cell lysis might disrupt its interaction with c-Cbl. Different lysis conditions are worth testing.

We showed that tyrosine residues Y471 and Y490 and lysine residue K479 in the C-terminus of SR-BI are not required for HCV infection. (Figure 33) Among the seven lysine residues, only one of them was tested in the SR-BI knockout background. It is worth testing all the lysine residues in the future. Furthermore, studies suggested that low density lipoprotein receptor (LDLR) and very low density lipoprotein receptor (VLDLR) complements the functions of SR-BI in HCV infection. (Yamamoto et al., 2016) The redundancy may have led to the discrepancies in the results of the experiments expressing the SR-BI mutants in wildtype and SR-BI-deficient cells respectively. Moreover, examining the functional domains shared by the two receptors may shine a light on the roles of SR-BI during HCV entry.

Our data suggested that c-Cbl is not required for HCV migration to the tight junction. (Figure 34) This is different from the phenotype of knocking out SR-BI, which is crucial for the migration. These differing phenotypes suggest that SR-BI and c-Cbl do not function cooperatively at this stage of HCV entry. Alternatively, c-Cbl may act at later stages, such as HCV endocytosis and trafficking to the early endosomes. As mentioned in Chapter III, our findings suggest that c-Cbl is not required for EGFR-mediated endocytosis of HCV. c-Cbl may act on other unknown host factors. The c-Cbl knockout Huh-7.5 cell line generated in this study is a useful tool for further characterization. DiD-HCV particle tracking in polarized organoids will tell us what step of HCV entry is regulated by c-Cbl.

We showed that SPTBN1 colocalizes with HCV particles during their migration to the tight junction. (Figure 35) We also generated a cell line silenced of SPTBN1. (Figure 36) Another student characterized the cell line and found that HCV migration to the tight junction and internalization were unaffected by SPTNB1 silencing. (Rebecca Reis, data not shown) In future studies, we will use organoids of the cell line in single particle imaging assay to define the role of SPTBN1 during HCV entry. We will examine the mechanism of SPTBN1-CD81 association during HCV infection. SPTBN1 has been shown to associate with αII-spectrin (SPTAN1). A spectrin tetramer is formed by head-to-head association of two αβ dimers. (Bignone et al., 2007; Baines, 2009) Interestingly, SPTAN1 was also identified in the Pietschmann lab's proteomic screening. Their data showed that SPTAN1 had reduced association with CD81 upon HCV infection. (Gerold et al., 2015) It suggests that SPTBN1 alone, instead of spectrin tetramer, associates with CD81 upon HCV infection. We propose that CD81-SPTBN1 association upon HCV infection does not require SPTAN1 and the formation of spectrin tetramers. To test that, we will manipulate SPTBN1 using genetic approaches. Domains of SPTBN1 have been relatively well characterized. We are interested in the oligomerization site, which allows lateral association of SPTAN1 and SPTBN1. (Machnicka et al., 2014) We will make mutant cell line of the oligomerization site in SPTBN1-depleted background. We will then repeat the co-IP assay using the mutant. If our hypothesis holds true, we expect that mutation at the oligomerization site will not affect CD81-SPTBN1 association upon HCV infection. Reduced CD81-SPTAN1 association suggests a mechanism in which SPTAN1 dissociates from spectrin tetramers, allowing SPTBN1 to interact with CD81 upon HCV infection. An in vitro study showed that phosphorylation of SPTBN1 T2159 inhibited its interaction with SPTAN1 and hence dimerization. (Bignone et al.,

2007) We will test if SPTBN1 T2159 is phosphorylated in Huh-7.5 3D organoids during HCV entry.

CHAPTER VI

CONCLUSION

Hepatitis C virus (HCV) is a hepatotropic RNA virus. 58 million people are infected with HCV. In 2019, 290,000 people died from HCV infection, primarily from hepatocellular carcinoma and cirrhosis. (WHO, 2017; WHO, 2023) HCV entry into hepatocytes is highly complex with sequential steps and various host factors. Entry host factors and processes are potential therapeutic targets. However, precise functions of most of the host factors are not known. Moreover, studies of entry using polarized cell culture that physiologically resembles hepatocytes in vivo are limited. (So and Randall, 2021) In this study, we evaluated the roles of entry factors in polarized hepatoma organoids, focusing on epidermal growth factor receptor (EGFR), tight junction proteins claudin-1 (CLDN1) and occludin (OCLN), scavenger receptor class B member 1 (SR-BI), E3 ubiquitin ligase c-Cbl, and βII-spectrin (SPTBN1). We revealed that EGFR performs multiple functions to regulate HCV internalization and sorting into endosomes. The process involves EGFR phosphorylation and downstream RAF-MEK-ERK signaling pathway. We also showed that CLDN1 and OCLN, despite being both at the tight junction, function at two distinct stages of HCV entry. CLDN1 regulates lateral migration of virions while OCLN regulates internalization. Our findings provide insights into the mechanism of HCV entry and therapeutic strategies.

Conventional two-dimensional (2D) Huh-7.5 cell culture system represents poorly the in vivo polarized structure of hepatocytes and spatial constraint of the host factors, especially CLDN1 and OCLN. (Coller et al., 2009; Molina-Jimenez et al., 2012; Baktash et al., 2018) To tackle that limitation, the lab has developed an imaging approach to visualize single HCV particle entry into polarized three-dimensional (3D) Huh-7.5 organoids. Using this approach, the lab has revealed the sequential steps of HCV entry: association of HCV virions with early receptors, migration of

virions to tight junctions, and internalization of HCV restricted at the tight junction. (Baktash et al., 2018) This entry pattern had not been shown before in 2D Huh-7.5 cells, which do not have distinct apical and basolateral domains. Certain steps of HCV entry, such as trafficking to the tight junction, cannot be evaluated in 2D cells. The use of 3D cell culture systems reveals unknown functions of HCV entry.

In this study, we characterized several crucial host factors of HCV entry. Our findings contribute to a better understanding of the complex entry mechanism of HCV.

HCV migration to the tight junction

This study and previous studies performed by the lab showed that CD81, SR-BI, CLDN1, and actin filaments are all required for HCV accumulation at the tight junction. (Baktash et al., 2018)

In this study, we found that CLDN1 is required for HCV accumulation at the internal membrane. It is interesting because, in polarized hepatoma organoids, CLDN1 does not have direct contact with basolateral virions. The first extracellular loop of CLDN1 interacts with CD81. Importantly, the interaction is required for HCV entry. (Evans et al., 2007; Yang et al., 2008; Cukierman et al., 2009; Harris et al., 2010; Krieger et al., 2010; Davis et al., 2012) CD81 regulates HCV trafficking to the tight junction in polarized hepatoma organoids. (Baktash et al., 2018) Moreover, HCV infection induces the internalization and intracellular colocalization of CLDN1 and CD81. Internalized CD81 and CLDN1 colocalize and are sorted into Rab5-positive early endosomes. (Farquhar et al., 2012) We propose that, after HCV virions attach to the basolateral membrane of hepatocytes, CLDN1-CD81 interaction serves as an anchor to tether migrating HCV virions to the tight junction. In the absence of CLDN1, migrating virions resurface at the

basolateral membrane. Alternatively, CLDN1 may regulate signaling events that promote CD81-driven migration to the tight junction without direct physical interaction of the two host proteins. At the tight junction, CD81 may interact with CLDN1 for internalization of the virions. Our data is consistent with published studies showing that CLDN1 acts prior to EGFR and OCLN during HCV entry. (Diao et al., 2012; Sourisseau et al., 2013; Shimizu et al., 2018)

The lab has previously shown that HCV migrates along actin filaments to the tight junction. (Baktash et al., 2018) One major question remains regarding the mechanism: how is the HCV-receptor complex linked to the actin filaments? In this study, we were interested in a potential candidate: βII-spectrin (SPTBN1). Our collaborator Thomas Pietschmann has identified SPTBN1 to have enhanced association with CD81 upon HCV infection. (Gerold et al., 2015) SPTBN1 is a scaffolding protein with an actin-binding domain. (Baines, 2009; Machnicka et al., 2014) Our preliminary data show that knocking down SPTBN1 inhibits HCV infection. SPTBN1 colocalizes with HCV particles during their migration to the tight junction. However, SPTBN1 is not required for HCV migration to the tight junction. (Rebecca Reis, data not shown) Regarding the mechanism of SPTBN1-CD81 interaction, SPTBN1 has been shown to associate with αII-spectrin (SPTAN1). A spectrin tetramer is formed by head-to-head association of two αβ dimers. (Bignone et al., 2007; Baines, 2009) Interestingly, HCV infection reduces SPTAN1 association with CD81. (Gerold et al., 2015) It suggests that SPTBN1 alone, instead of spectrin tetramer, associates with CD81 upon HCV infection. Reduced CD81-SPTAN1 association suggests a mechanism in which SPTAN1 dissociates from spectrin tetramers, allowing SPTBN1 to interact with CD81 upon HCV infection.

In the process of HCV migration to the tight junction, another potential host factor is IFITM1. It is required for HCV entry but not HCV binding. IFITM1 interacts with CD81, CLDN1,

OCLN, and ZO-1. It also enhances CD81 interactions with OCLN and ZO-1. (Wilkins et al., 2013) Its interactions with tight junction proteins and crucial HCV migration factors suggest that IFITM1 may function as an additional regulator of HCV migration to the tight junction.

The lab has showed that SR-BI is required for HCV migration to the tight junction. SR-BI regulates HCV entry via lipid uptake and interaction with HCV envelope protein E2. (Scarselli et al., 2002; Voisset et al., 2005; Dreux et al., 2006; Zeisel et al., 2007; Yamamoto et al., 2016) It acts at binding and post-binding steps of HCV entry. (Krieger et al., 2010; Lupberger et al., 2011; Sourisseau et al., 2013; Yamamoto et al., 2016) In this study, we showed that two tyrosine residues in the C-terminus of SR-BI are not required for HCV infection. Among the seven lysine residues, only one of them was tested in the SR-BI knockout background. It is worth testing all the lysine residues in the future. Furthermore, very low density lipoprotein receptor (VLDLR) complements the functions of SR-BI in HCV infection. It suggests that SR-BI functions similarly to VLDLR during HCV infection. (Yamamoto et al., 2016) Examining the functional domains shared by the two receptors may shine a light on the roles of SR-BI during HCV entry.

Our data in this study suggest that SR-BI and c-Cbl do not function cooperatively at this stage of HCV entry. Alternatively, c-Cbl may act at later stages, such as HCV endocytosis and sorting into the early endosomes. EGFR is a well characterized substrate of c-Cbl. c-Cbl interacts with EGFR via phosphorylated Y1045 of the receptor. (Levkowitz et al., 1999) However, Y1045 is not required for HCV infection. (Baktash et al., 2018) Moreover, AG-1478 inhibits phosphorylation and hence ubiquitination of EGFR (Levkowitz et al., 1999), but has no effect on HCV recruitment of clathrin. Overall, the data suggest that c-Cbl may not be required for EGFR-mediated endocytosis of HCV. c-Cbl, as a E3 ubiquitin ligase, may act on other unknown entry

factors. The c-Cbl knockout Huh-7.5 cell line generated in this study is a useful tool for further characterization. DiD-HCV particle tracking in polarized organoids will tell us how c-Cbl regulates HCV entry.

HCV internalization

Our study reveals that HCV internalization is regulated by both EGFR and OCLN. During clathrin-mediated endocytosis of HCV, EGFR regulates the recruitment of clathrin in an EGFR phosphorylation-independent manner. HCV is then internalized in a process that requires both EGFR phosphorylation and OCLN.

Factors regulating EGFR endocytosis, including phosphorylation, ubiquitination, and AP-2 binding, are redundant. Moreover, the mechanism varies with different types and concentrations of ligands. (Huang, Goh, and Sorkin, 2007; Sigismund et al., 2008; Roepstorff et al., 2009; Goh et al., 2010; Capuani et al., 2015; Fortian et al., 2015) It makes the mechanism of EGFR internalization difficult to dissect. In this study, we show that when EGFR phosphorylation is inhibited, HCV recruits endocytic proteins but still fails to undergo internalization. It suggests that EGFR phosphorylation regulates a step downstream of the recruitment of endocytic proteins. For EGF internalization, EGFR phosphorylation is not required. Instead, it regulates the degradation of internalized receptor. (Honegger et al., 1987; Felder et al., 1990; Yamazaki et al., 2002) Our findings suggest that the internalization of HCV does not fully resemble that of EGF. HCV requires EGFR phosphorylation-dependent functions for efficient internalization.

The selection of endocytic cargoes into vesicles is regulated by AP-2, an adaptor complex in which the μ2 subunit (AP-2μ1) directly binds to tyrosine-based sorting signal motifs of cargoes (YXXΦ; Φ: a bulky hydrophobic residue L/I/M/V/F). (Ohno et al., 1995) We showed that the

sorting signal motifs of OCLN are not required for HCV endocytosis. Moreover, despite the slower kinetics, HCV colocalized with AP-2 in the absence of OCLN. In contrast, the recruitment or disassociation of clathrin light chain or dynamin to/from HCV is not affected. This suggests that OCLN regulates HCV endocytosis, possibly acting at the stabilization of clathrin-coated vesicles. (Ehrlich et al., 2004) We propose that, without OCLN, clathrin and dynamin colocalize with DiD temporarily without forming a stable coat structure. It inhibits the efficient association of AP-2 to the pit. Uninternalized HCV is retained at the tight junction and accumulates AP-2.

Our finding suggests that other entry factors regulate the recruitment of AP-2 to HCV. AP-2 binding sites have been identified on EGFR. (Chang et al., 1993; Sorkin et al., 1996) Ubiquitination and AP-2 binding sites of EGFR are redundant for EGF endocytosis. (Goh et al., 2010) Fortian et al. mutated AP-2 binding sites and 21 lysine residues of EGFR. The mutant was phosphorylated upon EGF stimulation. The mutant failed to internalize EGF only when cells were treated with EGFR kinase inhibitor PD158780 or siRNA targeting Grb2. (Fortian et al., 2015) It is interesting that clathrin-mediated endocytosis of EGFR is not sufficient for HCV entry. OCLN at the tight junction is also required for HCV internalization. It suggests that endocytosis of HCV does not fully resemble that of EGF.

siRNA silencing of AAK or GAK, regulators of AP-2 phosphorylation (Olusanya et al., 2001; Ricotta et al., 2002), inhibited HCV pseudoparticle (HCVpp) entry or cell culture derived HCV (HCVcc) infection in Huh-7.5 cells. It had no effect on HCV binding or HCV replication when HCV entry was bypassed by electroporation. The silencing also inhibited EGF-enhanced HCVpp entry or HCVcc infection. It inhibited EGF-stimulated EGFR colocalization with endosomal marker EEA1. Fewer Dil-HCV particles colocalized with Rab5-GFP an hour post

temperature shift. (Neveu et al., 2015) GAK inhibitor reduced HCVpp entry and HCVcc infection but had no effect on HCV replication. The inhibitor reduced AP-2µ1 phosphorylation in Huh-7.5 cells treated with PP2A inhibitor calyculin A. (Kovackova et al., 2015) siRNA or shRNA silencing of AP-2µ1, but not that of AP-1µ1, AP-1µ2, or AP-4µ1, inhibited HCVpp entry and HCVcc infection. Expressing wildtype AP-2µ1 or NUMB enhanced HCVpp entry and HCVcc infection in Huh-7.5 cells. Expressing wildtype AP-2µ1 enhanced HCVpp entry in cells silenced of AAK or GAK. siRNA silencing of NUMB inhibited HCVpp entry or HCVcc infection in Huh-7.5 cells. (Neveu et al., 2015) Overall, the data suggest that AP-2µ1 regulates HCV entry.

In addition to entry, AP-2µ1 has been shown to regulate HCV assembly. AP-2µ1 bound to HCV core in in vitro assay and protein-fragment complementation assay. Core and AP-2µ1 were co-immunoprecipitated in HCVcc-infected Huh-7.5 cells. AP-2µ1 mutant T156A was expressed in Huh-7.5 cells. The cells were then electroporated with HCV RNA. The mutant did not affect HCV replication but reduced the infectivity of intra- and extra-cellular virions. siRNA silencing of AAK or GAK reduced core-AP-2µ1 binding and infectivity of intra- and extra-cellular virions. The silencing had no effect on HCV replication in Huh-7.5 cells electroporated with HCV RNA. (Neveu et al., 2012) GAK inhibitor reduced HCVcc infection, HCV assembly, and infectious virus production. It had no effect on HCV replication. The inhibitor reduced AP-2µ1 phosphorylation in Huh-7.5 cells treated with PP2A inhibitor calyculin A. (Kovackova et al., 2015) The data suggest that AP-2µ1 regulates HCV assembly in addition to entry.

During HCV infection, CD81 is internalized. However, it does not have a YXXØ motif. (Farquhar et al., 2012) CD81 interacts with HCV glycoprotein E2 (Pileri et al., 1998), EGFR (Park et al., 2009; Bruening et al., 2018), and CLDN1 (Evans et al., 2007; Yang et al., 2008; Cukierman

et al., 2009; Harris et al., 2010; Krieger et al., 2010; Davis et al., 2012; Farquhar et al., 2012). Whether CD81 actively regulates HCV endocytosis or is internalized along with E2, EGFR, or CLDN1 is worth studying.

HCV sorting into early endosomes

After endocytosis, HCV virions are sorted into Rab5-positive endocytic organelles to undergo fusion. (Meertens, Bertaux, and Dragic, 2006) Based on our findings of the phosphorylation-dependent role of EGFR, we suggest a model in which HCV activates the RAF-MEK-ERK pathway downstream of EGFR. The pathway facilitates Rab5 activation and hence the maturation/fusion of HCV-Rab5-positive vesicles to APPL1-positive and subsequently EEA1-positive early endosomes. APPL1 and EEA1 are both effectors of Rab5 and preferentially interact with the active form of Rab5 (Rab5-GTP). (Simonsen et al., 1998; Miaczynska et al., 2004; Zhu et al., 2007; Haas et al., 2005; Jozic et al., 2012)

APPL1 preferentially bound to Rab5-GTP but not Rab5-GDP in vitro. (Miaczynska et al., 2004) APPL1 was co-immunoprecipitated with Rab5. Non-hydrolysable GTP analog, relative to GDP, enhanced APPL1 interaction with Rab5. (Zhu et al., 2007) In an immunofluorescent assay, APPL1 colocalized with Rab5, while it had low level of colocalization with EEA1 or caveolin-1. APPL1 was membrane-bound in immunofluorescent and electron microscopy assays. APPL1 mutants impaired in Rab5 binding did not localize to membranes. (Miaczynska et al., 2004) It suggests that the interaction between APPL1 and Rab5-GTP regulates the localization of APPL1 on membranes.

EEA1 colocalized with Rab5 (Mu et al., 1995) and preferentially bound to GTP-bound form of Rab5. (Simonsen et al., 1998) Rab5-GTP was co-immunoprecipitated with EEA1. (Jozic

et al., 2012) In yeast two-hybrid assay, EEA1 preferentially interacted with GTP-locked Rab5 mutant Q79L than with wildtype or GDP-locked Rab5 mutant S34N. Expressing GTPase-activating protein RabGAP-5 caused a loss of EEA1 punctate staining. siRNA silencing of RabGAP-5 led to more intense EEA1 staining. (Haas et al., 2005) It suggests that the interaction between EEA1 and Rab5-GTP regulates the formation of EEA1-positive early endosomes.

EGF activates Rab5 via EGFR phosphorylation. EGFR kinase inhibitor AG-1478 or EGFR mutant K721M inhibited EGF-mediated increase of Rab5-GTP. AG-1478 inhibited vesicle fusion in in vitro fusion assay. (Jozic et al., 2012) Rab5 regulates endosome acidification and hence viral-endosome fusion of HCV. (Miao et al., 2017) Therefore, we propose that HCV-activated RAF-MEK-ERK pathway facilitates Rab5 activation and hence the recruitment of APPL1 and EEA1 to HCV-containing vesicles.

RIN1 is a potential regulator of Rab5 during this process. RIN1 functions as a guanine nucleotide exchange factor of Rab5. Upon EGF stimulation, RIN1 relocalized from the soluble fraction to the membrane fraction. It was inhibited by AG-1478. (Jozic et al., 2012) RIN1 was co-immunoprecipitated with EGFR, but not with EGFR mutants Y992F or Y1173F. (Barbieri et al., 2003) It suggests that RIN1 interacts with phosphorylated Y1173 of EGFR, which is crucial for HCV infection (Baktash et al., 2018) and activation of the RAF-MEK-ERK pathway. Studies suggest that RIN1 regulates the negative feedback of EGF-mediated ERK activation. (Tall et al., 2001; Balaji et al., 2012)

CLDN1 and CD81, two HCV entry factors, have been reported to relate to EGFR and the RAF-MEK-ERK pathway. Co-immunoprecipitation and proteomic study showed that EGFR interacted with CD81. (Bruening et al., 2018; Park et al., 2009) CD81 interacted with HCV

glycoprotein E2 (Pileri et al., 1998) and the interaction led to EGFR phosphorylation. (Diao et al., 2012) Treating Huh-7 cells with anti-CD81 antibodies or E2 with anti-E2 antibodies induced ERK phosphorylation. (Brazzoli et al., 2008) An anti-CLDN1 antibody inhibited ERK phosphorylation in chronically infected Huh-7.5.1 cells. It did not affect EGF-induced phosphorylation of EGFR or ERK. (Mailly et al., 2015) Expressing CLDN1 in Chang cells enhanced ERK phosphorylation via c-Abl and epithelial mesenchymal transition. It also enhanced interaction between RAF and RAS in co-immunoprecipitation. (Suh et al., 2013) Whether CLDN1 and CD81 coordinate with EGFR to regulates the RAF-MEK-ERK pathway for HCV entry is worth exploring.

HCV is not the only virus whose infection involves the RAF-MEK-ERK pathway. Influenza A virus infection in MDCK cells enhanced ERK activation at 5 minutes and 8 hours post infection. U0126, a MEK inhibitor, inhibited the export of viral ribonucleoprotein complexes during IAV infection. (Pleschka et al., 2001) Coxsackievirus B3 (CVB) infection in HeLa cells enhanced ERK phosphorylation at 10 minutes and 7 hours post infection. UV irradiation of the virus inhibited the phosphorylation at 7 hours post infection. U0126 inhibited CVB infection. (Luo et al., 2002) Dominant negative mutant of Rab5 inhibited CVB internalization, while constitutively active mutant of Rab5 caused CVB accumulation in Rab5-positive vesicles. (Coyne et al., 2007) For mouse hepatitis virus, U0126 inhibited infection but not internalization. (Cai, Liu, and Zhang, 2007) We show that the RAF-MEK-ERK pathway regulates HCV sorting into early endosomes after internalization. These studies suggest a broad range of functions of the pathway hijacked by viruses to facilitate infection.

AKT pathway, another EGFR-mediated signaling pathway, has been reported to be involved in HCV infection. HCV infection enhanced the phosphorylation of AKT at T308 and

S473 30 minutes to 8 hours post infection. HCVpp infection was sufficient for the activation. UV treatment of HCV did not affect the activation. AKT was activated by antibodies targeting CD81 or CLDN1, but not by antibodies targeting SR-BI or OCLN or E2-blocking antibodies. (Liu et al., 2012)

Overall, our findings support the model that EGFR has three distinct roles in HCV entry. (1) One is phosphorylation independent. EGFR regulates HCV recruitment of clathrin for endocytosis. EGFR phosphorylation is dispensable. (2, 3) The other two roles are phosphorylation dependent. (2) EGFR phosphorylation regulates virion internalization after the assembly of the clathrin endocytic machinery. This is independent of the RAF-MEK-ERK pathway. (3) EGFR phosphorylation activates the RAF-MEK-ERK pathway to regulate HCV sorting into early endosomes. Our study provides a better understanding of the multi-step entry of HCV precisely regulated by EGFR, the RAF-MEK-ERK signaling pathway, and the tight junction proteins. Further studies using single particle imaging of HCV and polarized hepatoma cell culture will advance our knowledge of HCV infection and cellular protein functions.

Sequential events of HCV entry into polarized hepatoma organoids

Here, we propose a further refined model of HCV entry into polarized hepatoma organoids (Figure 37). There are sequential events: (1) HCV virions engage CD81, then SR-B1 in a complex containing EGFR and SPTNB1. The virus-receptor complex then migrates from the basolateral membrane to the tight junction via actin. (Baktash et al., 2018) (2) In a process that requires CLDN1, HCV virions accumulate at the tight junction. (3) Once at the tight junction, HCV virions recruit the clathrin endocytic machinery in an EGFR phosphorylation-independent manner. (4) OCLN is dispensable for the recruitment of the clathrin endocytic proteins but is required for

subsequent internalization. (5) HCV is internalized in an EGFR phosphorylation-dependent manner. (6) HCV activates the RAF-MEK-ERK signaling pathway downstream of EGFR phosphorylation. This pathway regulates the sorting and maturation of internalized HCV into APPL1- and EEA1-associated early endosomes for subsequent virion fusion and uncoating. Future studies will investigate the mechanism behind the requirement of CLDN1 for HCV accumulation at the tight junction and that of EGFR and OCLN for HCV internalization. Future studies using single particle imaging of HCV and polarized hepatoma cell culture will further advance our knowledge of HCV infection and host cellular processes.

APPENDIX

FIGURES

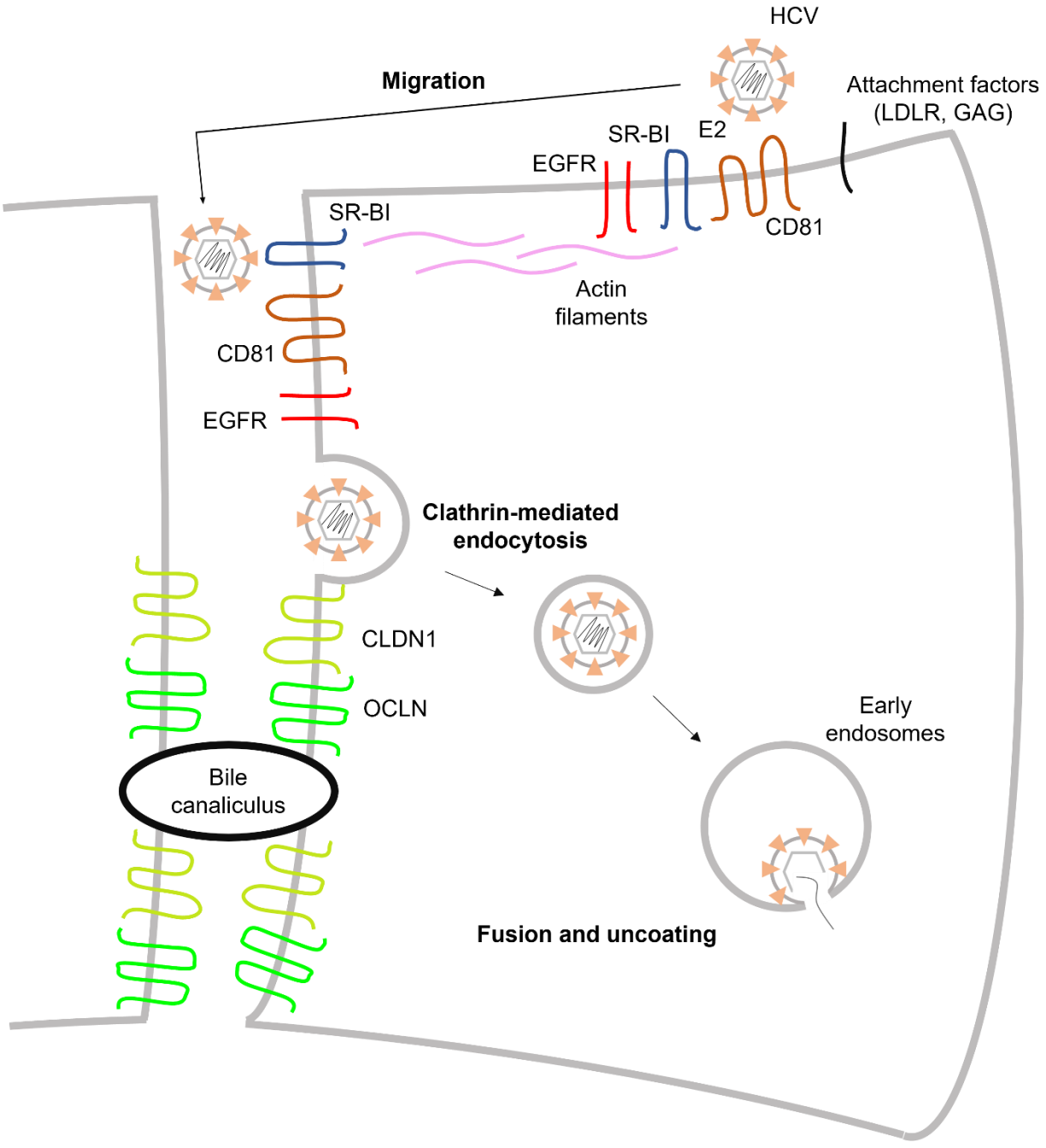

Figure 1. Model of HCV entry.

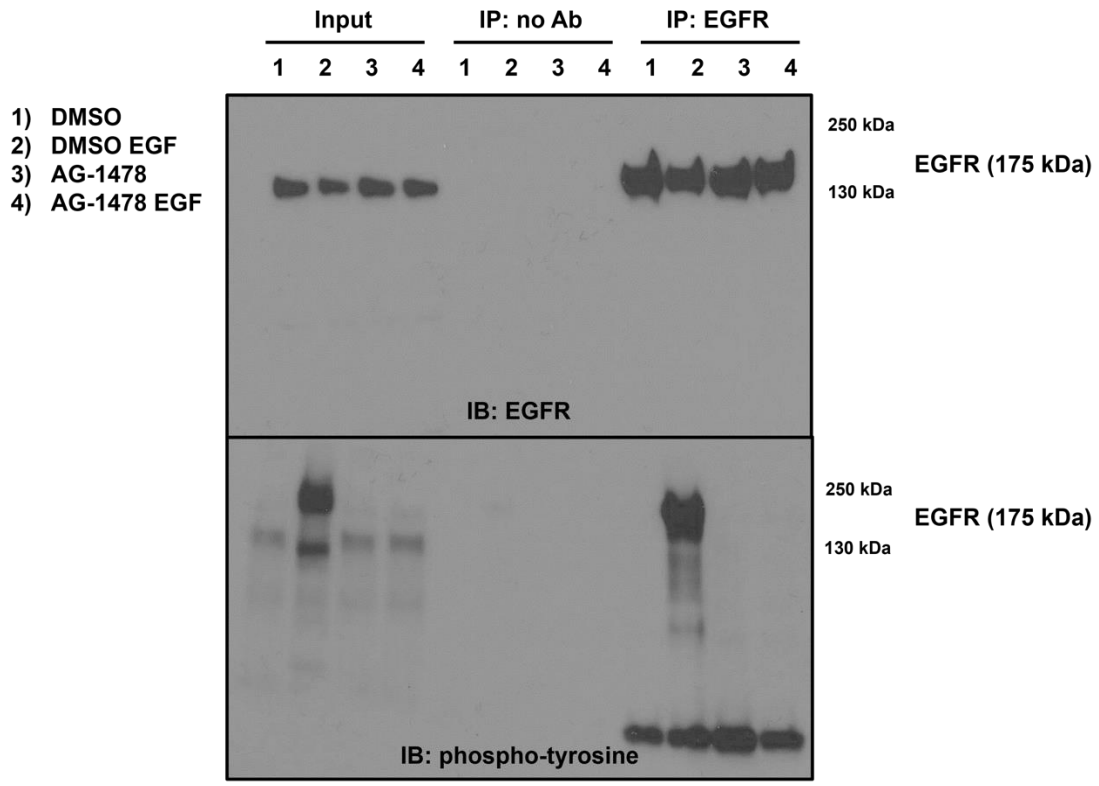

Figure 2. AG-1478 blocks EGF-induced EGFR phosphorylation. Huh-7.5 cells were serum starved, incubated with DMSO or 5 μM AG-1478 for 2h, stimulated with 40 ng/mL EGF with DMSO or AG-1478 for 15 min and lysed. EGFR was immunoprecipitated from the lysate samples and immunoblotted for the indicated proteins.

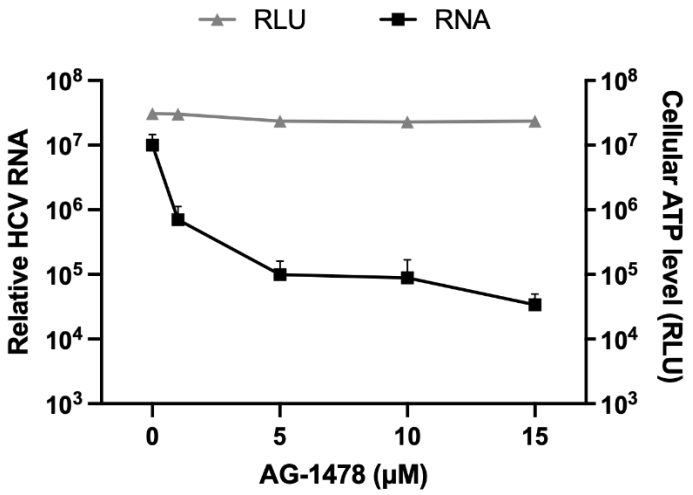

Figure 3. Inhibition of EGFR phosphorylation blocks HCV infection. Huh-7.5 cells were seeded onto 96-well plates, incubated with AG-1478 for 2h, infected with HCV with AG-1478 for 22hr, and then analyzed for relative HCV RNA levels. To examine cell viability, Huh-7.5 cells were seeded onto 96-well plates, incubated with AG-1478 for 24h, and then analyzed for cellular ATP levels. Mean +/- SD.

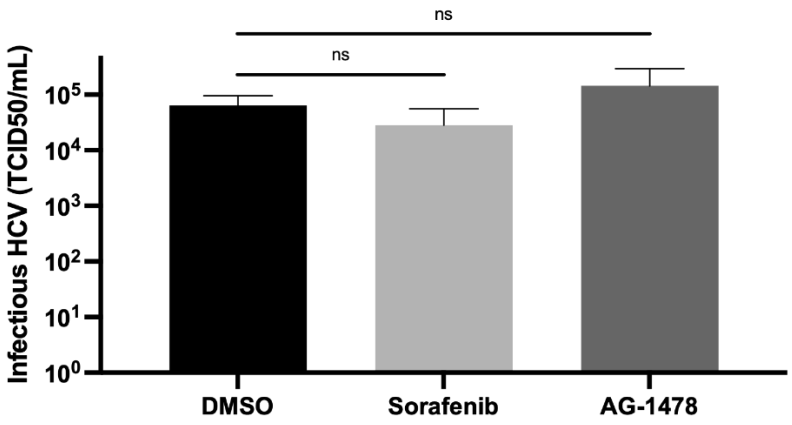

Figure 4. Sorafenib or AG-1478 does not affect HCV infectious virus production. Huh-7.5 cells were electroporated with HCV RNA. 24 h post electroporation, medium was replaced with 5 μM sorafenib or AG-1478 in medium. 48 h post electroporation, viral supernatants were collected, and infectious viral titers were determined.

A

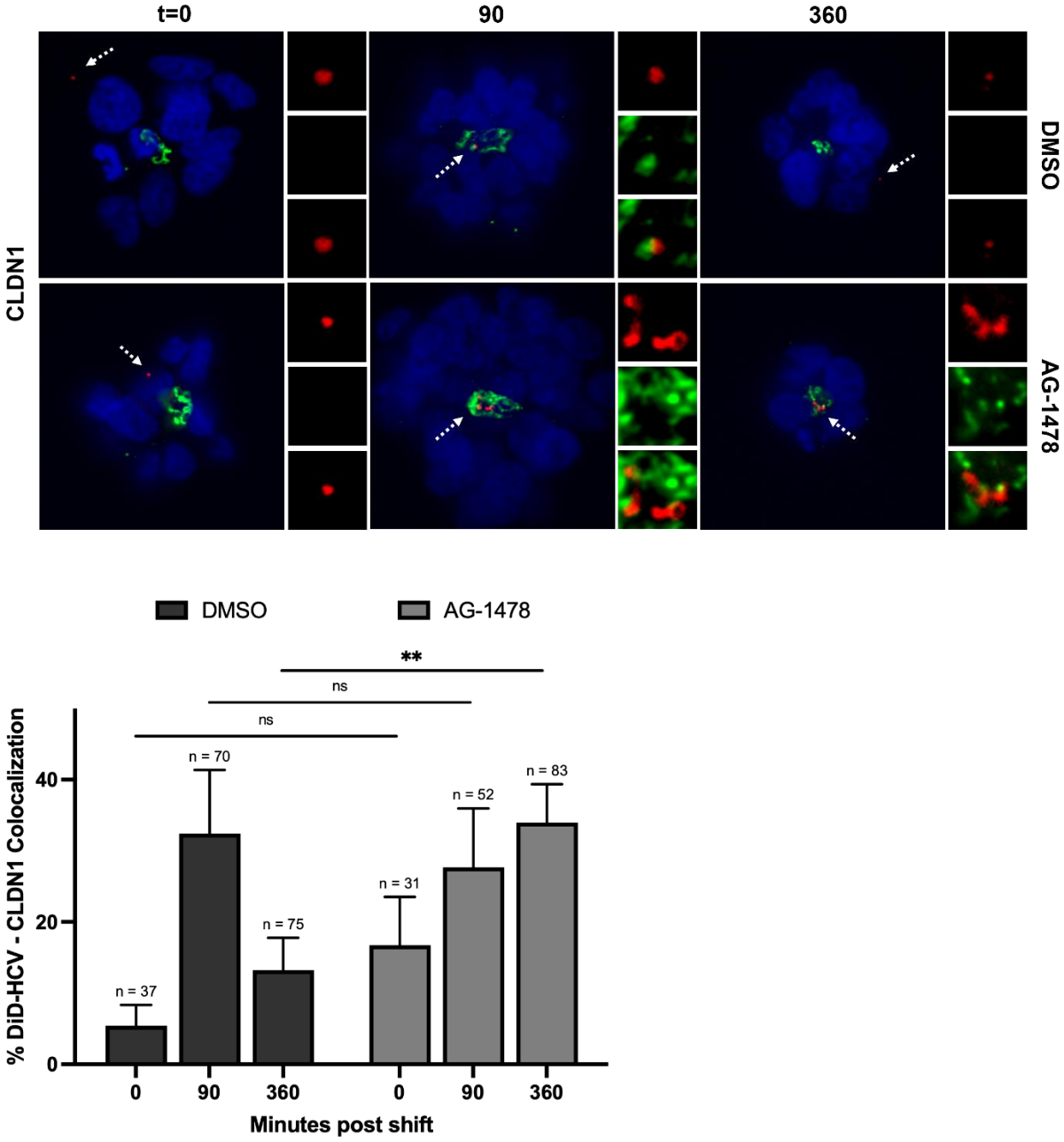

Figure 5. Inhibition of EGFR phosphorylation blocks DiD-HCV dissociation from the tight junction. Huh-7.5 organoids were incubated with DMSO or 5 μM AG-1478 for 2h, infected with DiD-HCV (red) with DMSO or AG-1478 for 1h at 4°C, shifted to 37°C for the indicated times, fixed, and probed for CLDN1 (A) (green) or ZO-1 (B). n=total DiD signal. Mean +/- SEM. **p < 0.01.

B

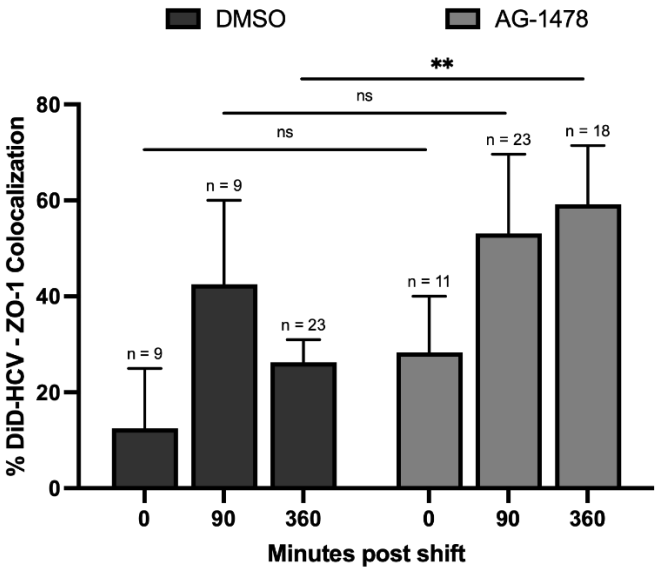

Figure 5, continued.

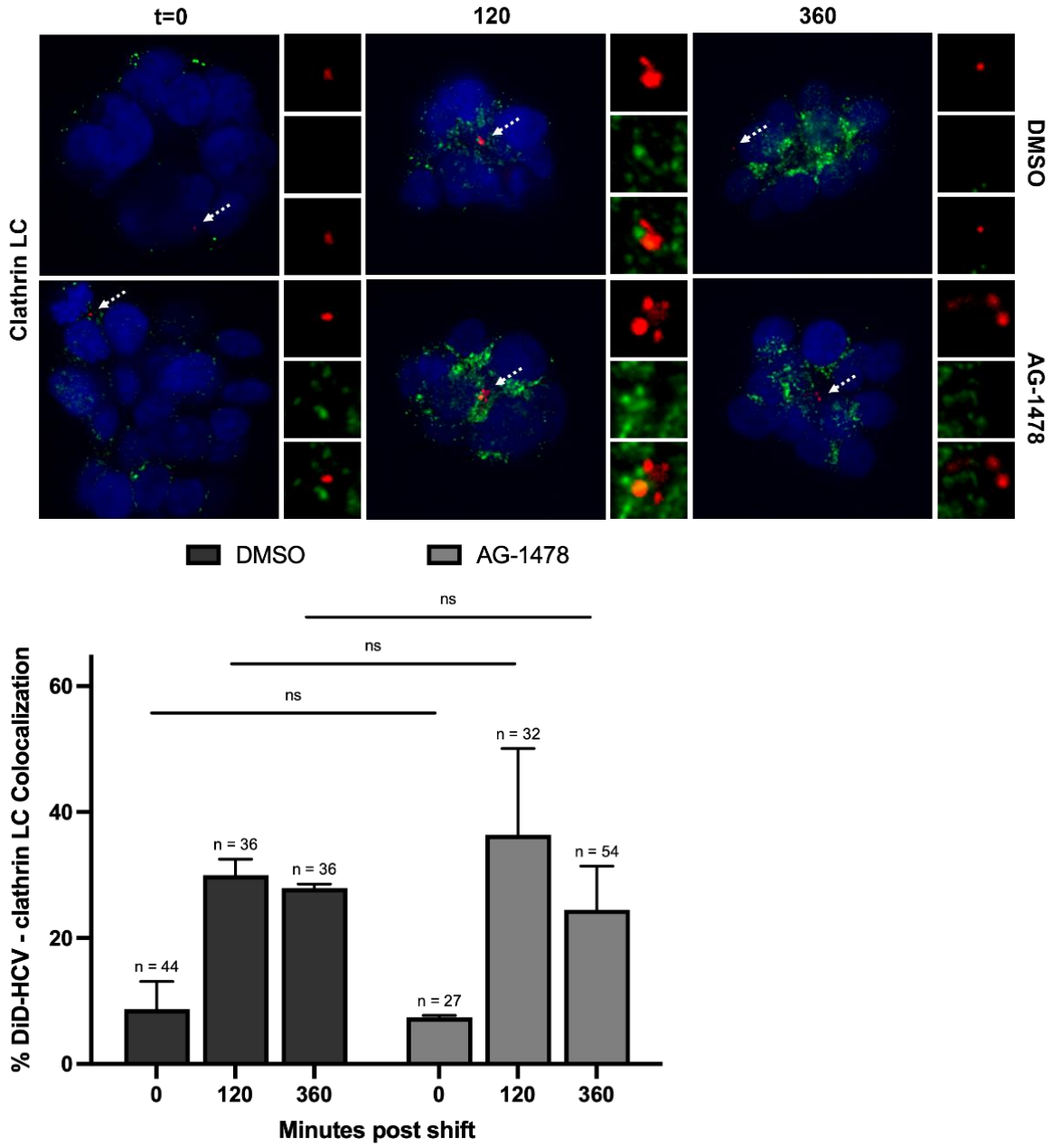

Figure 6. AG-1478 does not affect DiD-HCV recruitment of clathrin light chain. Huh-7.5 organoids were incubated with DMSO or 5 μM AG-1478 for 2h, infected with DiD-HCV (red) with DMSO or AG-1478 for 1h at 4°C, shifted to 37°C for the indicated times, fixed, and probed for clathrin light chain (clathrin LC) (green). n=total DiD signal. Mean +/- SEM.

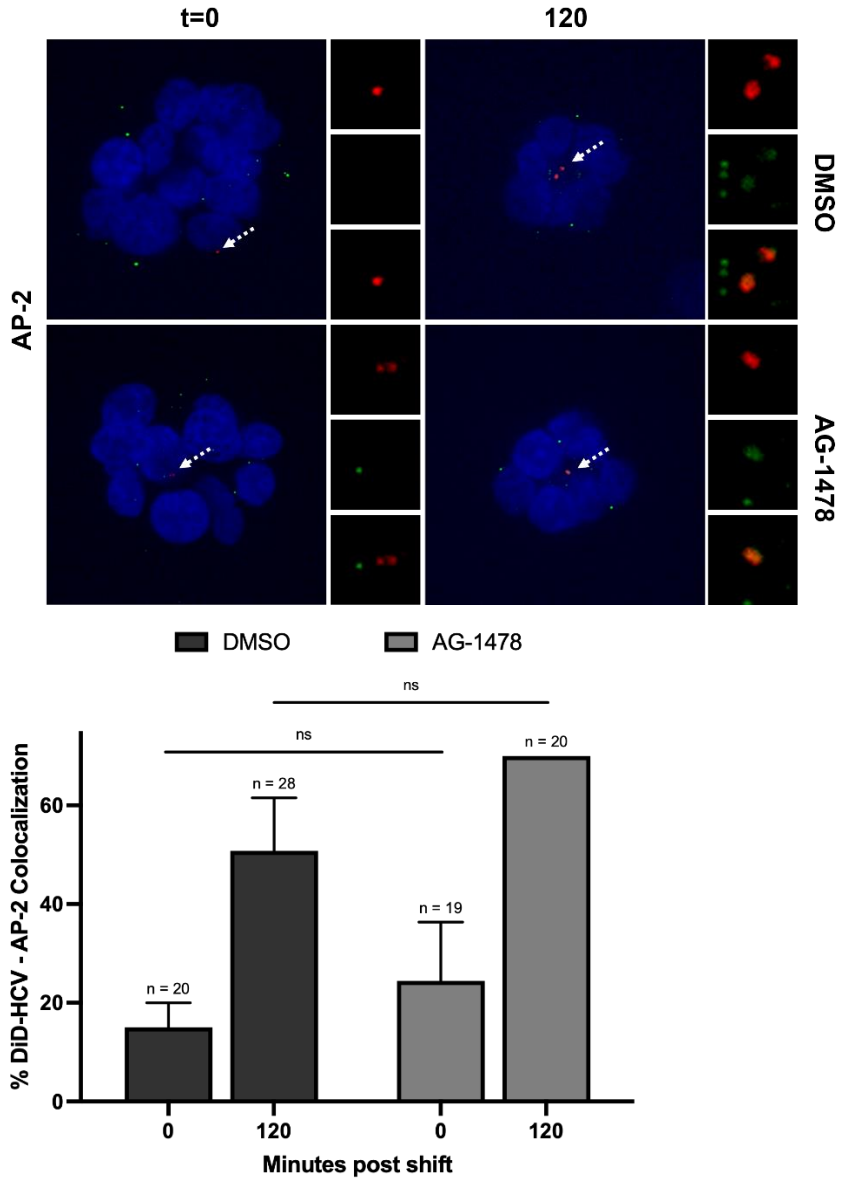

Figure 7. AG-1478 does not affect DiD-HCV recruitment of AP-2. Huh-7.5 organoids were incubated with DMSO or 5 μM AG-1478 for 2h, infected with DiD-HCV (red) with DMSO or AG-1478 for 1h at 4°C, shifted to 37°C for the indicated times, fixed, and probed for AP-2 (green). n=total DiD signal. Mean +/- SEM.

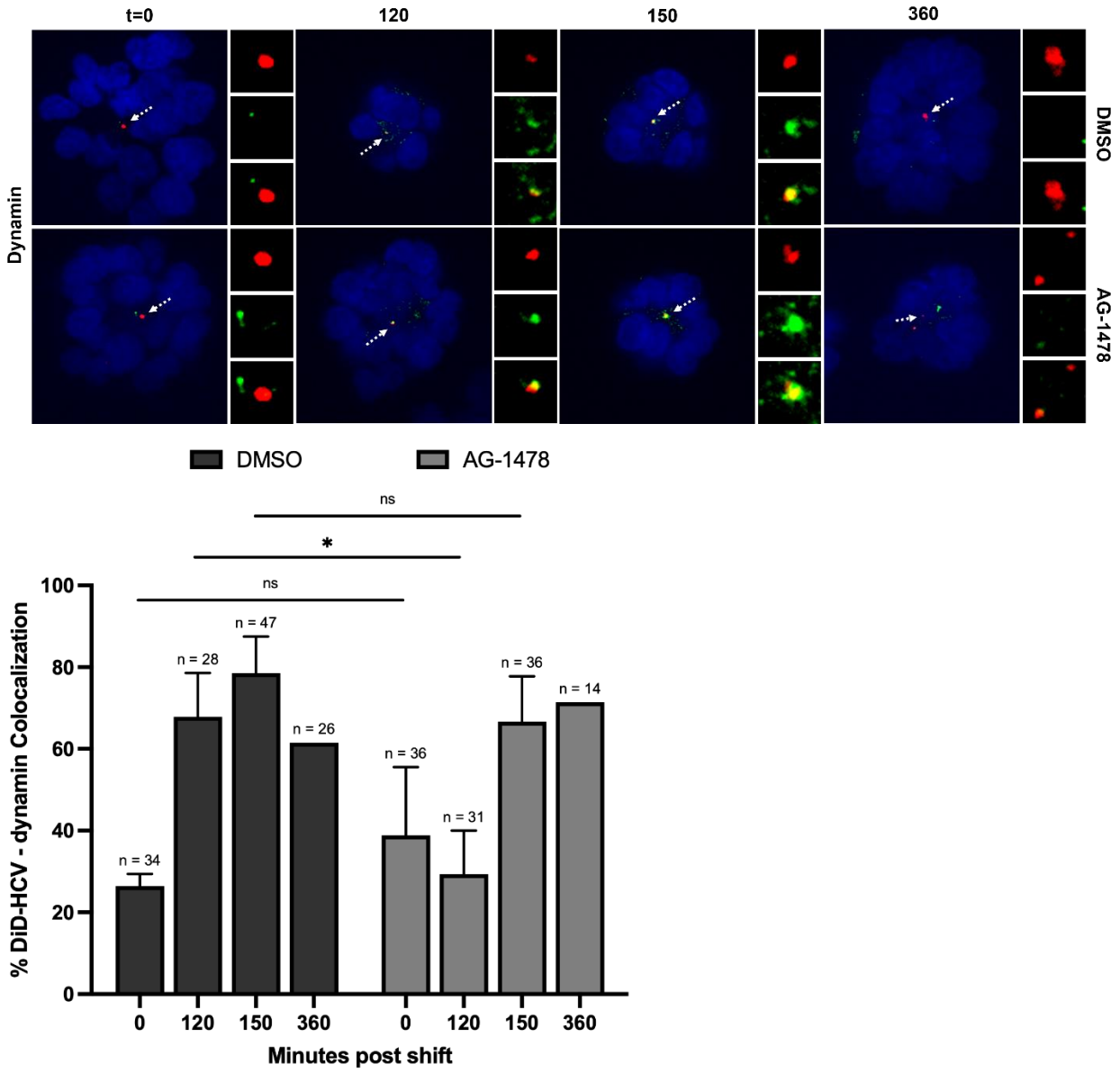

Figure 8. AG-1478 does not affect DiD-HCV recruitment of dynamin. Huh-7.5 organoids were incubated with DMSO or 5 μM AG-1478 for 2h, infected with DiD-HCV (red) with DMSO or AG-1478 for 1h at 4°C, shifted to 37°C for the indicated times, fixed, and probed for dynamin (green). n=total DiD signal. Mean +/- SEM. *$p < 0.05$.

A

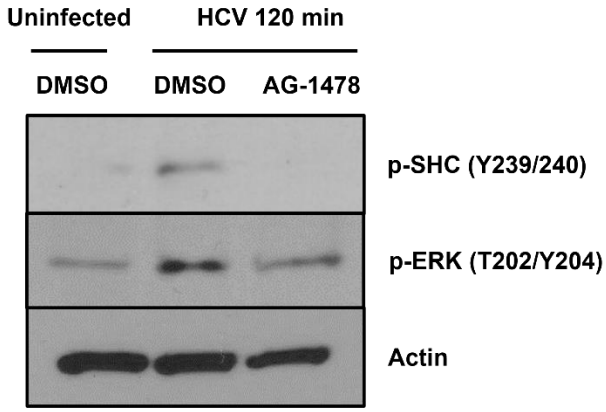

B

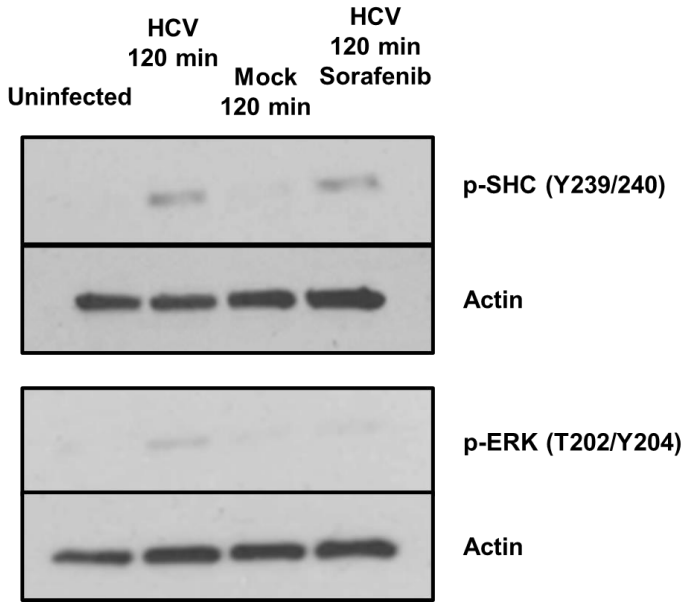

Figure 9. HCV infection activates the RAF-MEK-ERK pathway via EGFR phosphorylation. Huh-7.5 organoids were serum starved, incubated with 5 μM **(A)** AG-1478 or **(B)** sorafenib for 2h if indicated, infected with concentrated HCV with 5 μM **(A)** AG-1478 or **(B)** sorafenib (if indicated) for 1h at 4°C, shifted to 37°C, processed with Matrigel cell recovery solution, and lysed at 120 min post temperature shift. Lysate samples were immunoblotted for the indicated proteins.

A

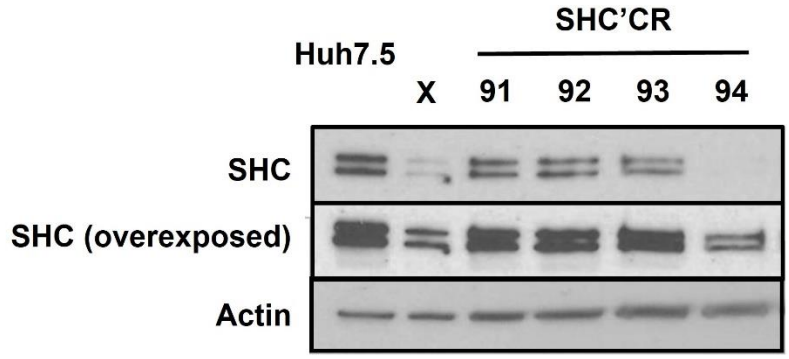

B

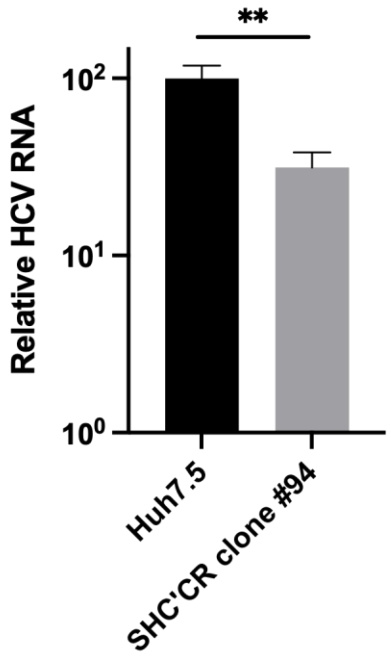

Figure 10. SHC is required for HCV infection. (A) Western blot of Huh-7.5 wildtype and SHC CRISPR'ed cells. **(B)** Huh-7.5 wildtype or SHC CRISPR'ed cells were seeded onto 96-well plates, infected with HCV for 48hr, and then analyzed for relative HCV RNA levels. Mean +/- SD. **p < 0.01.

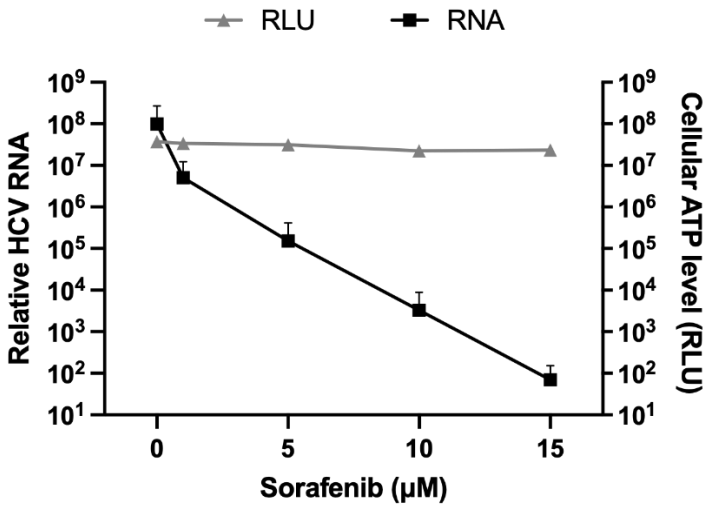

Figure 11. Inhibition of the RAF-MEK-ERK pathway blocks HCV infection. Huh-7.5 cells were seeded onto 96-well plates, incubated with sorafenib for 2h, infected with HCV with sorafenib for 22hr, and then analyzed for relative HCV RNA levels. To examine cell viability, Huh-7.5 cells were seeded onto 96-well plates, incubated with sorafenib for 24h, and then analyzed for cellular ATP levels. Mean +/- SD.

A

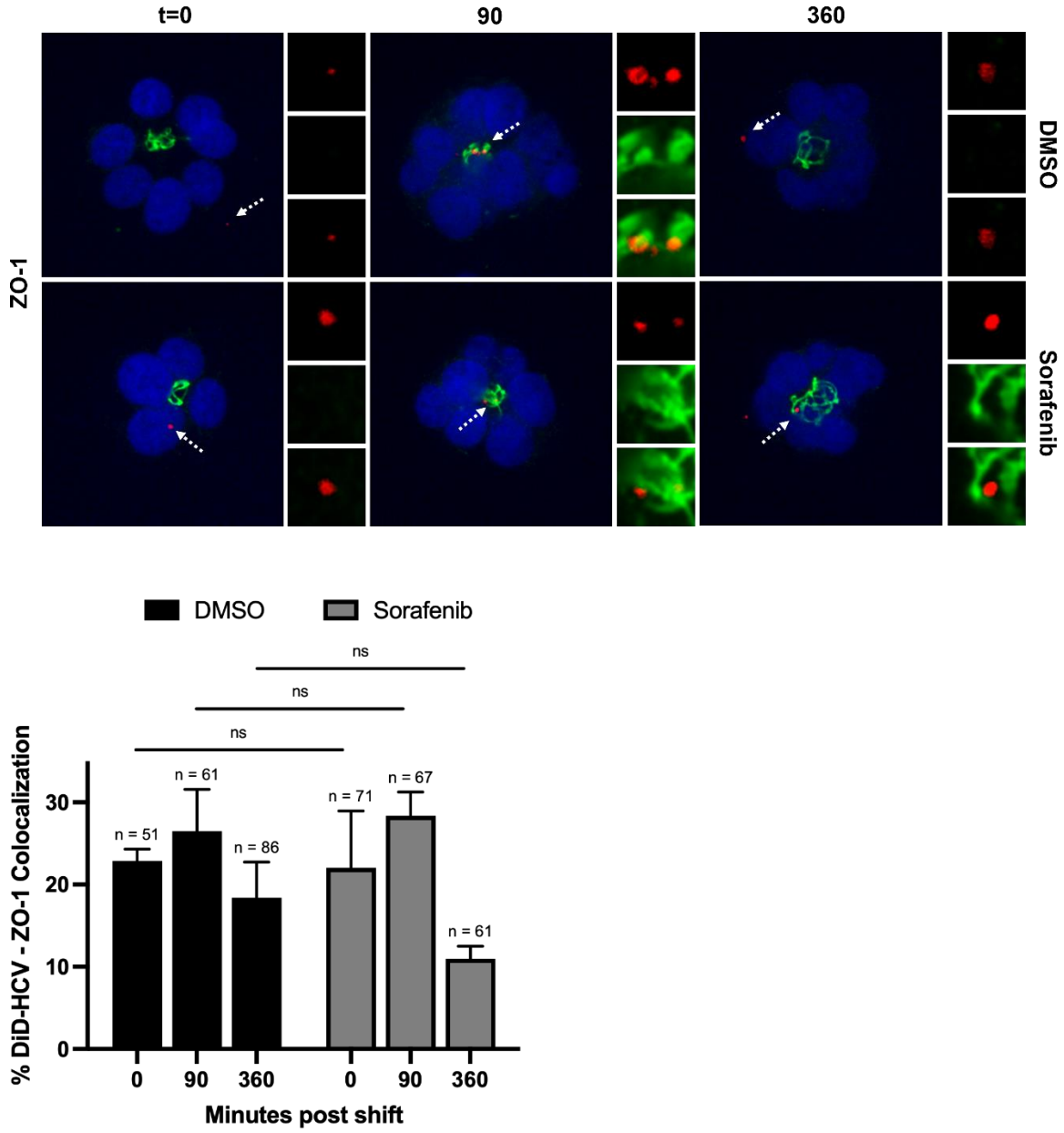

Figure 12. Sorafenib does not affect DiD-HCV trafficking to the tight junction or internalization. Huh-7.5 organoids were incubated with DMSO or 5 μM sorafenib for 2h, infected with DiD-HCV (red) with DMSO or sorafenib for 1h at 4°C, shifted to 37°C for the indicated times, fixed, and probed for ZO-1 (green) (A) or CLDN1 (B). n=total DiD signal. Mean +/- SEM.

B

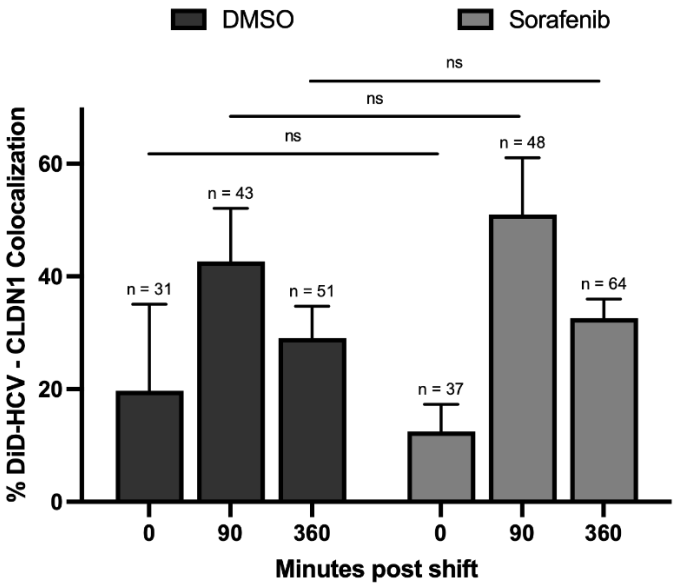

Figure 12, continued.

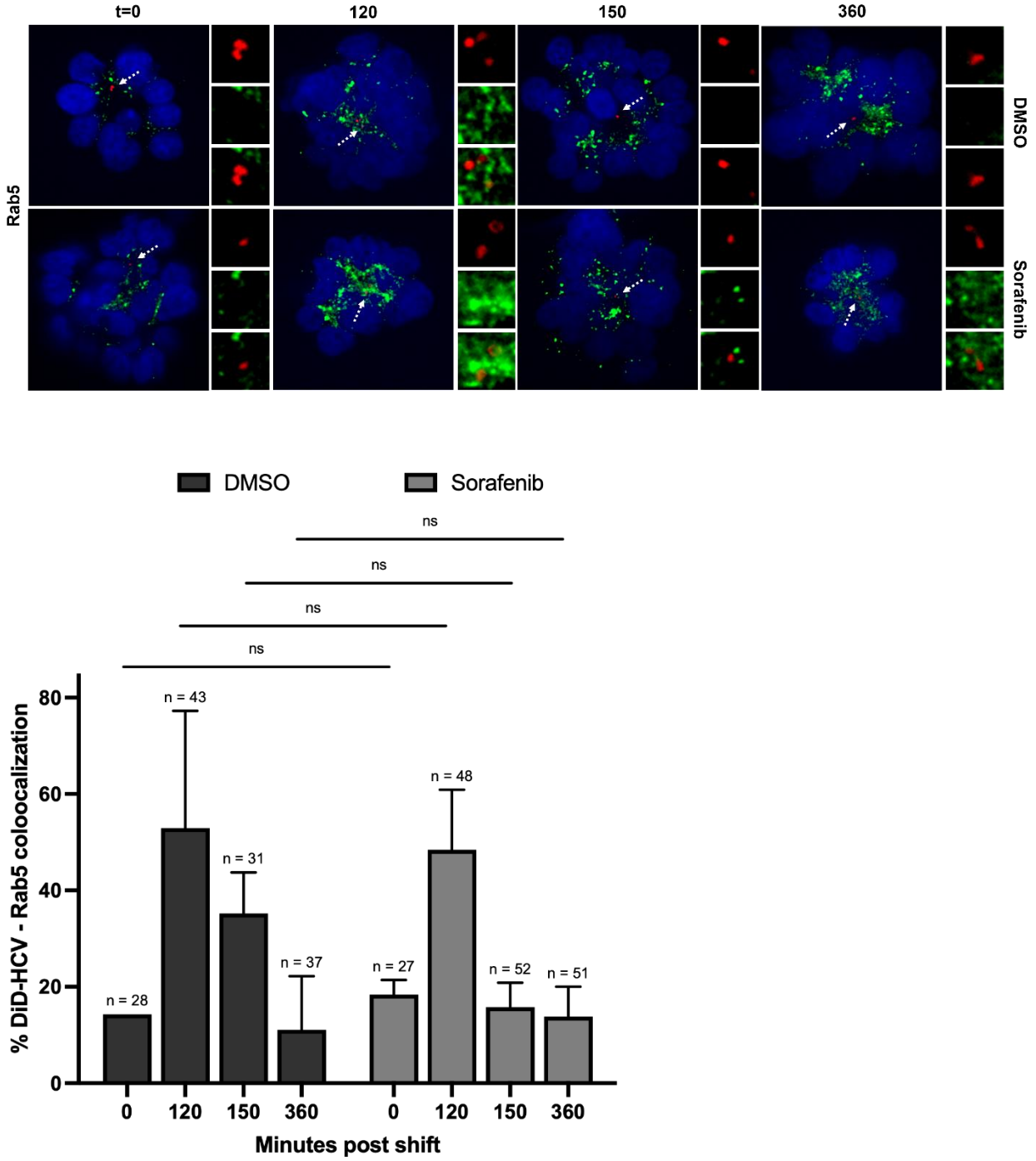

Figure 13. Sorafenib does not affect DiD-HCV colocalization with Rab5. Huh-7.5 organoids were incubated with DMSO or 5 μM sorafenib for 2h, infected with DiD-HCV (red) with DMSO or sorafenib for 1h at 4°C, shifted to 37°C for the indicated times, fixed, and probed for Rab5 (green). n=total DiD signal. Mean +/- SEM.

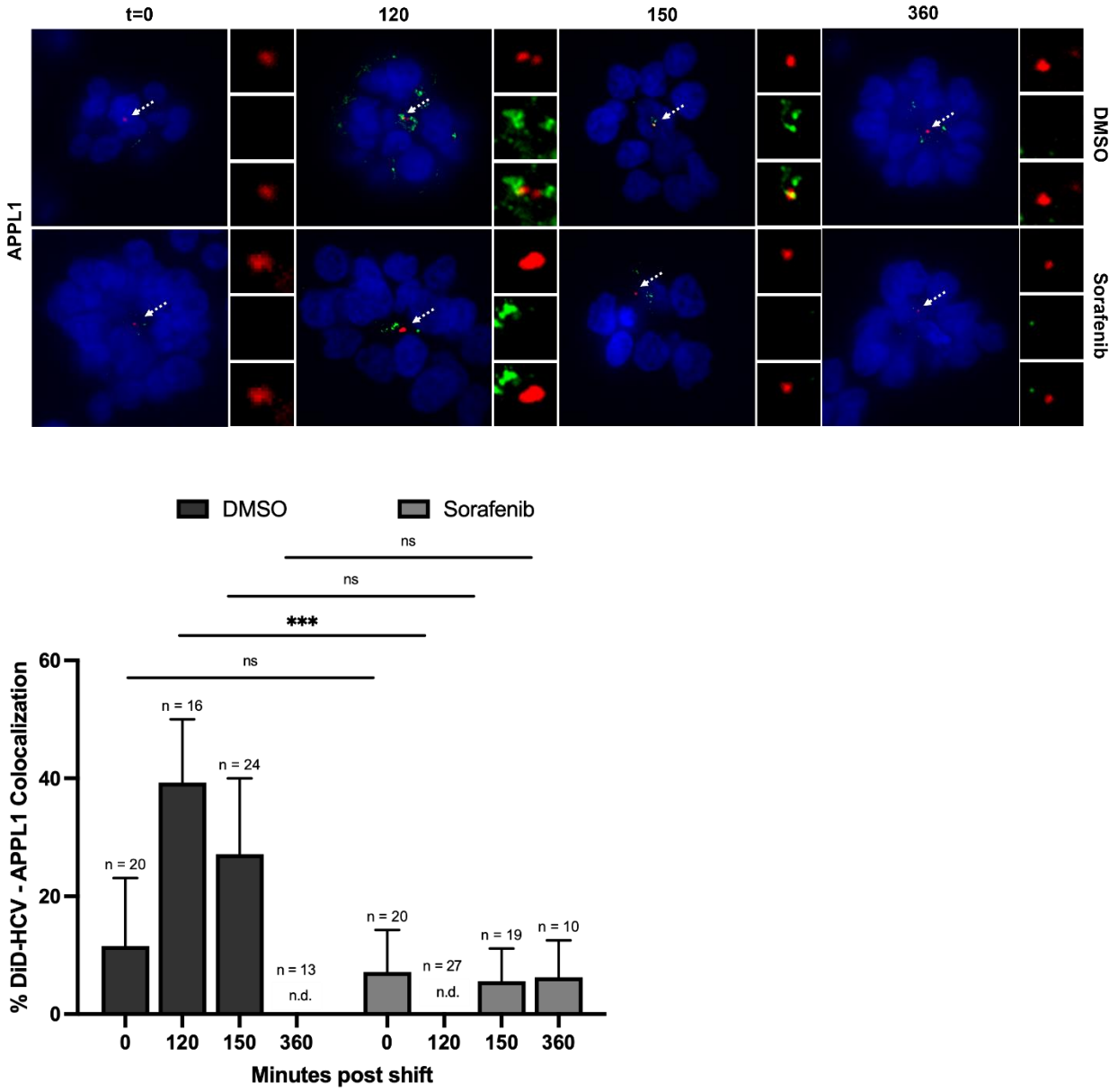

Figure 14. Inhibition of the RAF-MEK-ERK pathway blocks recruitment of APPL1 to DiD-HCV. Huh-7.5 organoids were incubated with DMSO or 5 μM sorafenib for 2h, infected with DiD-HCV (red) with DMSO or sorafenib for 1h at 4°C, shifted to 37°C for the indicated times, fixed, and probed for APPL1 (green). n=total DiD signal. Mean +/- SEM. ***p < 0.001.

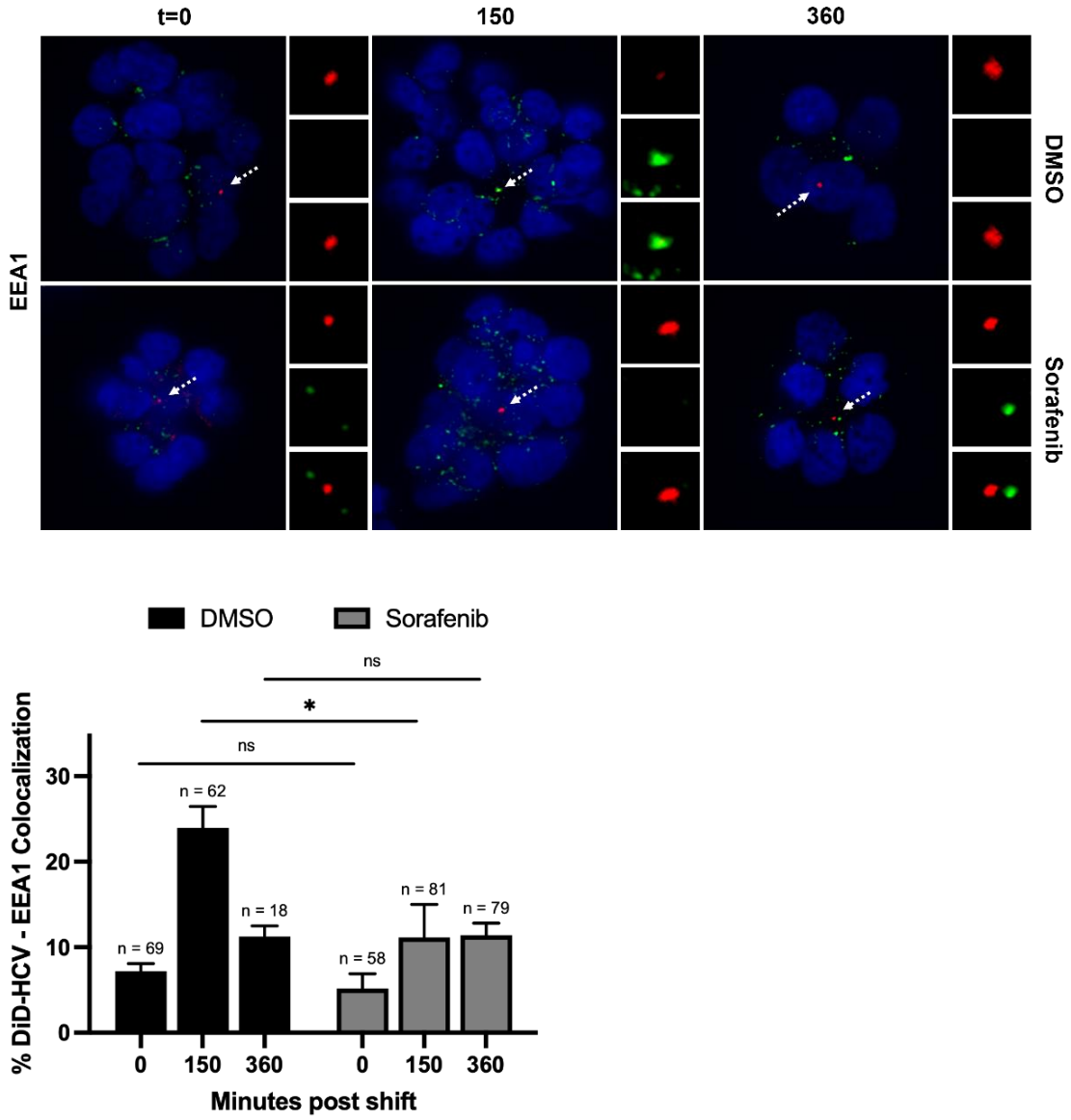

Figure 15. Inhibition of the RAF-MEK-ERK pathway blocks recruitment of EEA1 to DiD-HCV. Huh-7.5 organoids were incubated with DMSO or 5 μM sorafenib for 2h, infected with DiD-HCV (red) with DMSO or sorafenib for 1h at 4°C, shifted to 37°C for the indicated times, fixed, and probed for EEA1 (green). n=total DiD signal. Mean +/- SEM. *$p < 0.05$.

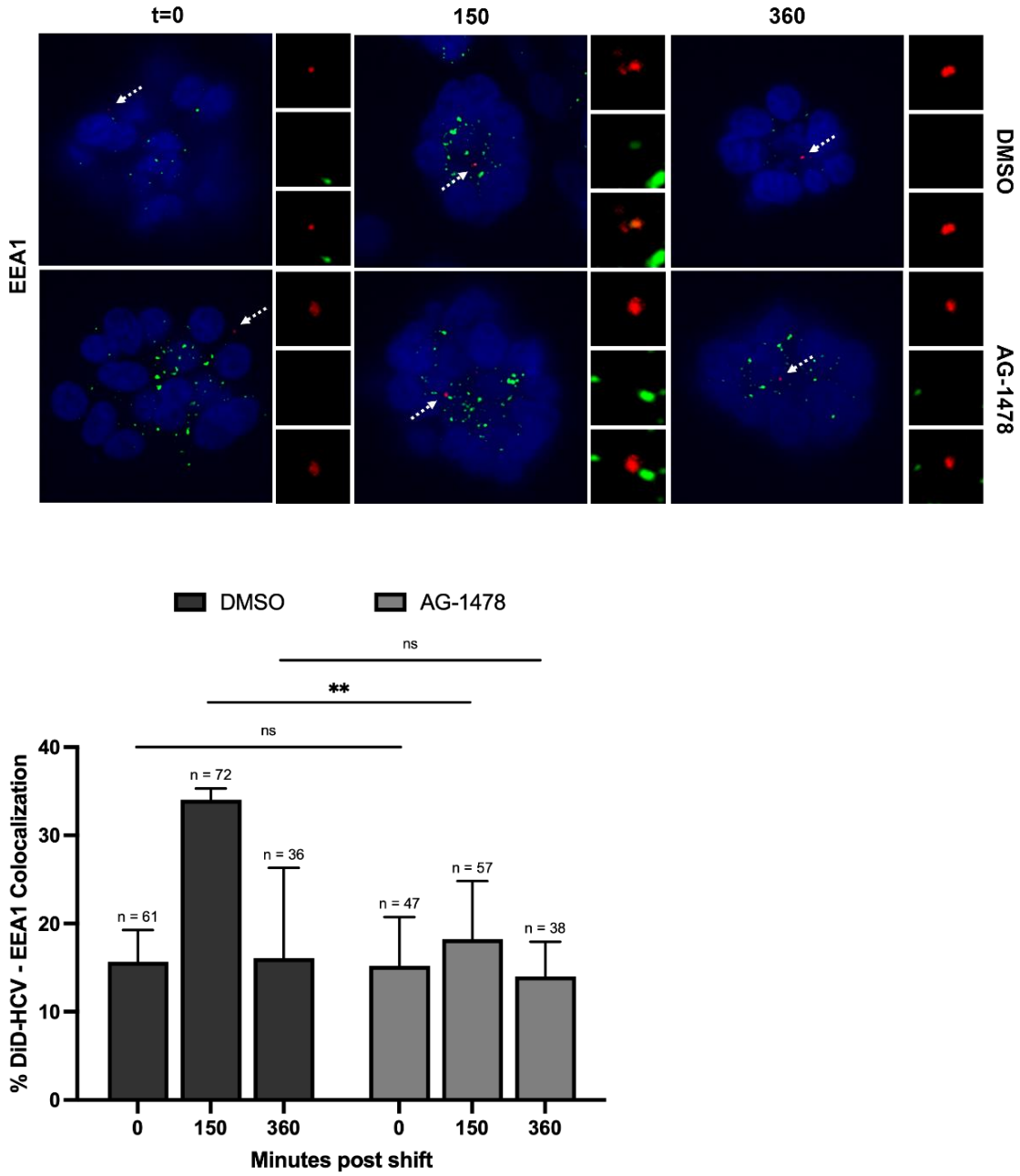

Figure 16. Inhibition of EGFR phosphorylation blocks DiD-HCV trafficking to the early endosomes. Huh-7.5 organoids were incubated with DMSO or 5 μM AG-1478 for 2h, infected with DiD-HCV (red) with DMSO or AG-1478 for 1h at 4°C, shifted to 37°C for the indicated times, fixed, and probed for EEA1 (green). n=total DiD signal. Mean +/- SEM. **p < 0.01.

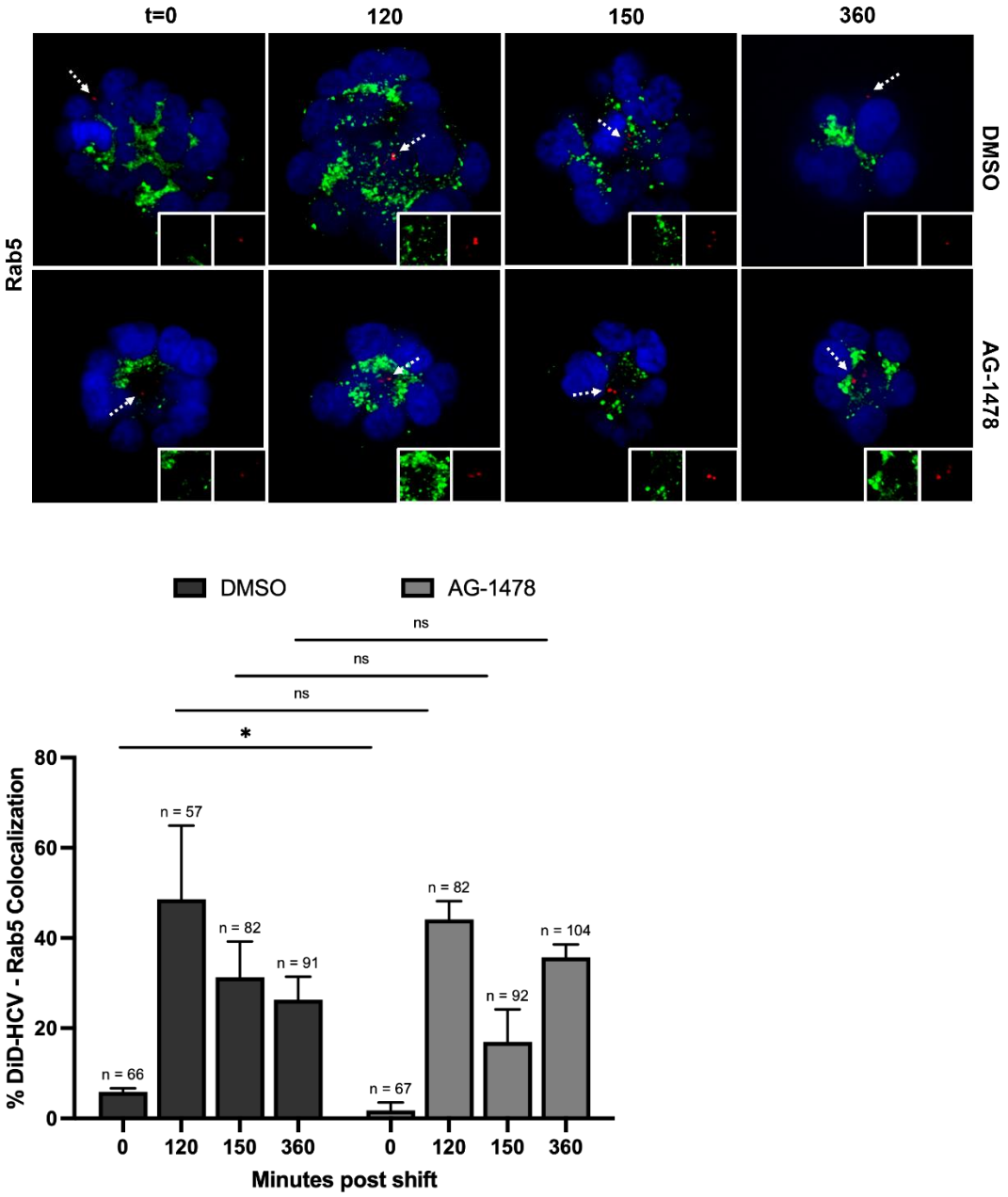

Figure 17. AG-1478 does not affect DiD-HCV colocalization with Rab5. Huh-7.5 organoids were incubated with DMSO or 5 μM AG-1478 for 2h, infected with DiD-HCV (red) with DMSO or AG-1478 for 1h at 4°C, shifted to 37°C for the indicated times, fixed, and probed for Rab5 (green). n=total DiD signal. Mean +/- SEM. *$p < 0.05$.

A

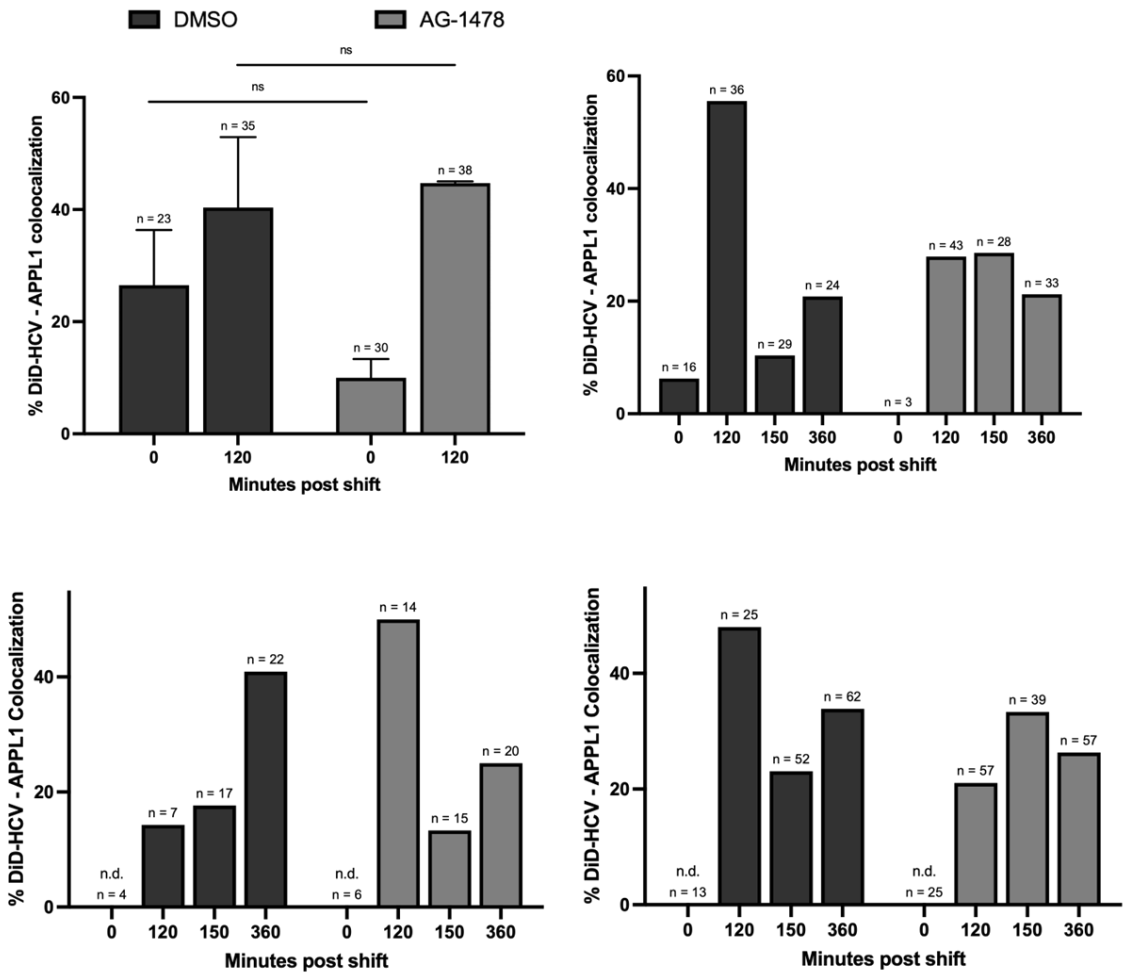

B

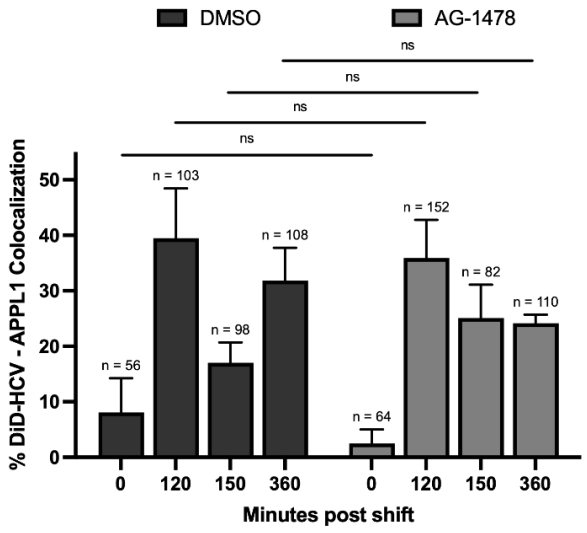

Figure 18. Effect of AG-1478 on DiD-HCV colocalization with APPL1. Huh-7.5 organoids

Figure 18, continued. were incubated with DMSO or 5 μM AG-1478 for 2h, infected with DiD-HCV with DMSO or AG-1478 for 1h at 4°C, shifted to 37°C for the indicated times, fixed, and probed for APPL1. n=total DiD signal. Mean +/- SEM. **(A)** Four separate trials. **(B)** Combined data of **(A)**.

A

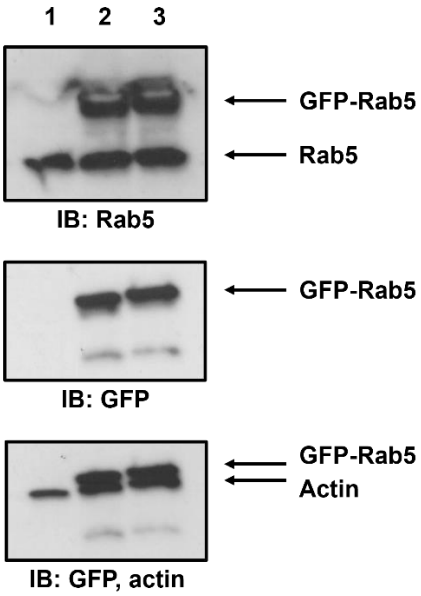

B

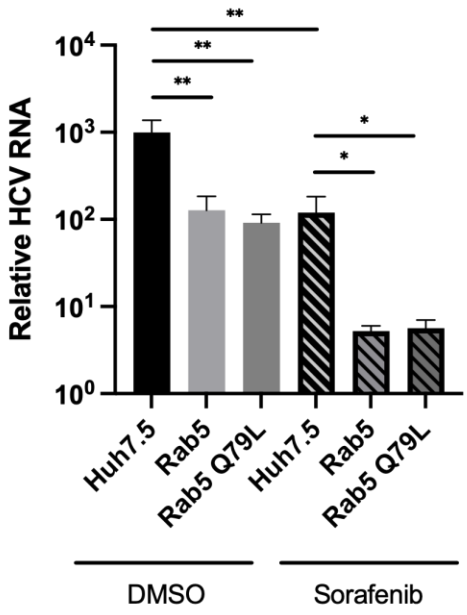

Figure 19. Expressing GFP-Rab5 inhibits HCV infection. (A) Western blot of Huh-7.5 cells (1) or Huh-7.5 cells expressing GFP-Rab5 (2) or GFP-Rab5 Q79L (3). **(B)** Huh-7.5 cells or Huh-7.5 cells expressing GFP-Rab5 or GFP-Rab5 Q79L were seeded onto 96-well plates, incubated with DMSO or 5 μM sorafenib for 2h, infected with HCV with DMSO or 5 μM sorafenib for 22hr, and then analyzed for relative HCV RNA levels. Mean +/- SD. *$p < 0.05$, **$p < 0.01$.

A

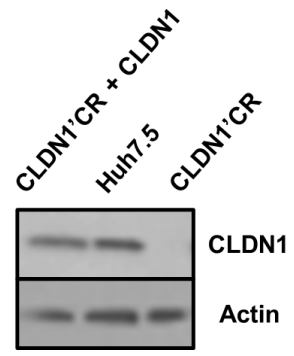

B

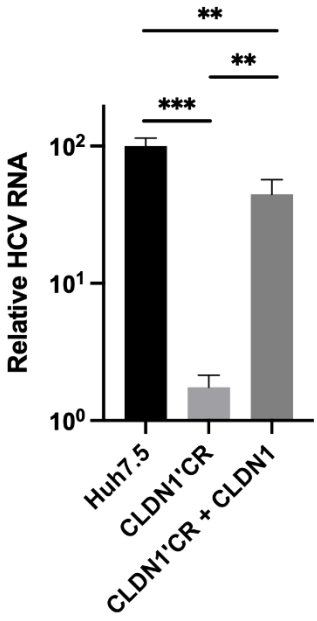

Figure 20. CLDN1 is required for HCV infection. (A) Western blot of Huh-7.5 wildtype, CLDN1 CRISPR'ed, and complemented cells. **(B)** Huh-7.5 wildtype, CLDN1 CRISPR'ed, or complemented cells were seeded onto 96-well plates, infected with HCV for 48hr, and then analyzed for relative HCV RNA levels. Mean +/- SD. **p < 0.01, ***p < 0.001.

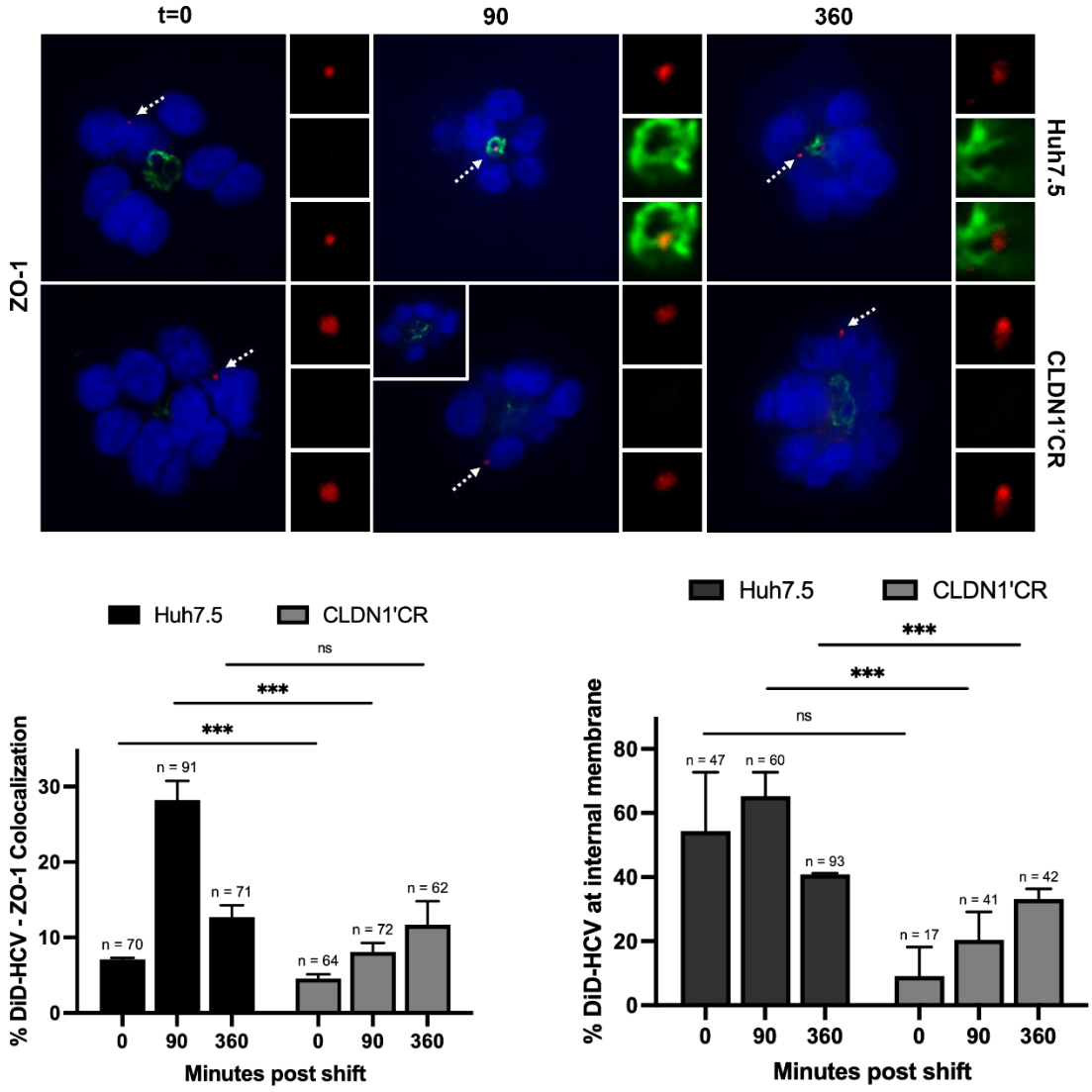

Figure 21. CLDN1 is required for DiD-HCV accumulation at the tight junction. Organoids of Huh-7.5 wildtype, CLDN1 CRISPR'ed, or complemented cells were infected with DiD-HCV (red) for 1h at 4°C, shifted to 37°C for the indicated times, fixed, and probed for ZO-1 (green). n=total DiD signal. Mean +/- SEM. ***p < 0.001.

A

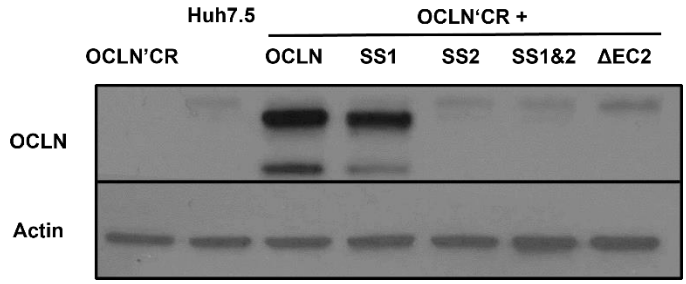

B

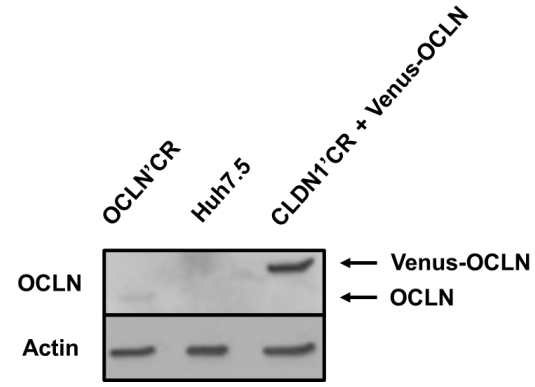

C

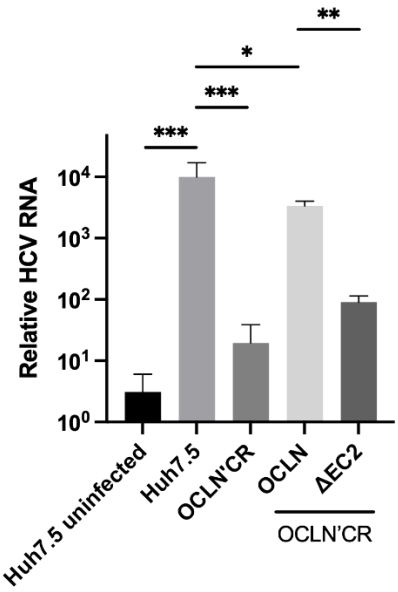

Figure 22. The second extracellular loop of OCLN is required for HCV infection. (A, B) Western blot of Huh-7.5 wildtype, OCLN CRISPR'ed, and complemented cells. **(C, D)** Huh-7.5 wildtype, OCLN CRISPR'ed, or complemented cells were seeded onto 96-well plates, infected

D

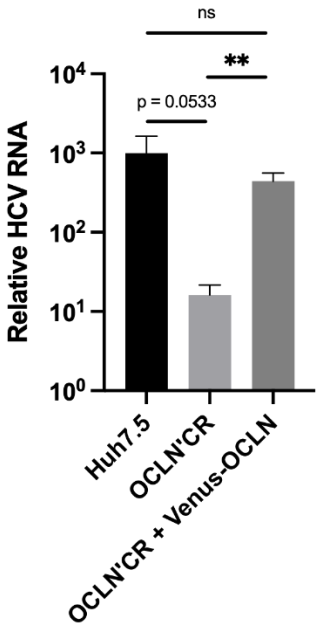

Figure 22, continued. with HCV for 48hr, and then analyzed for relative HCV RNA levels. Mean +/- SD. *p < 0.05, **p < 0.01, ***p < 0.001.

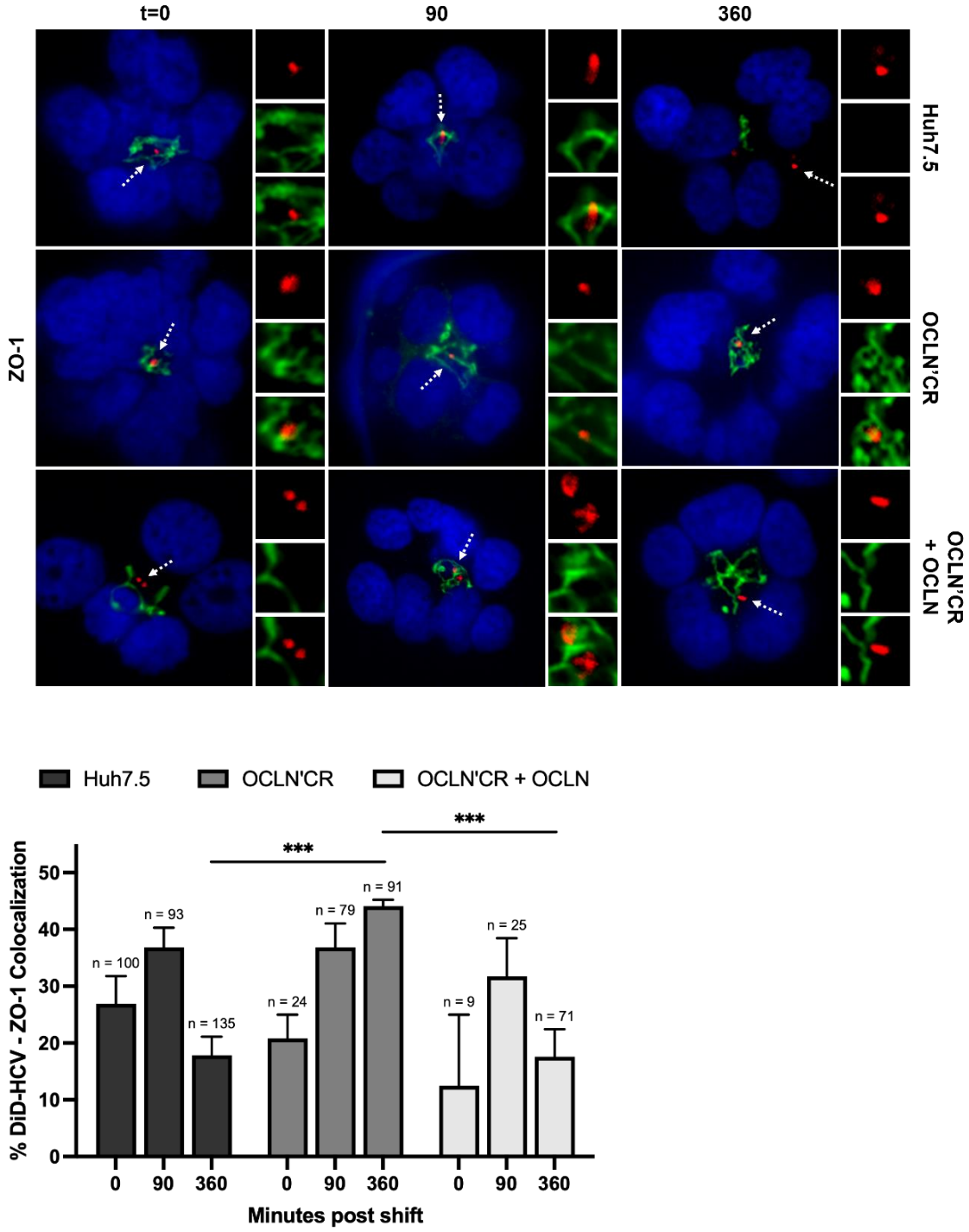

Figure 23. OCLN regulates DiD-HCV internalization. Organoids of Huh-7.5 wildtype, OCLN CRISPR'ed, or complemented cells were infected with DiD-HCV (red) for 1h at 4°C, shifted to 37°C for the indicated times, fixed, and probed for ZO-1 (B). n=total DiD signal. Mean +/- SEM. ***p < 0.001.

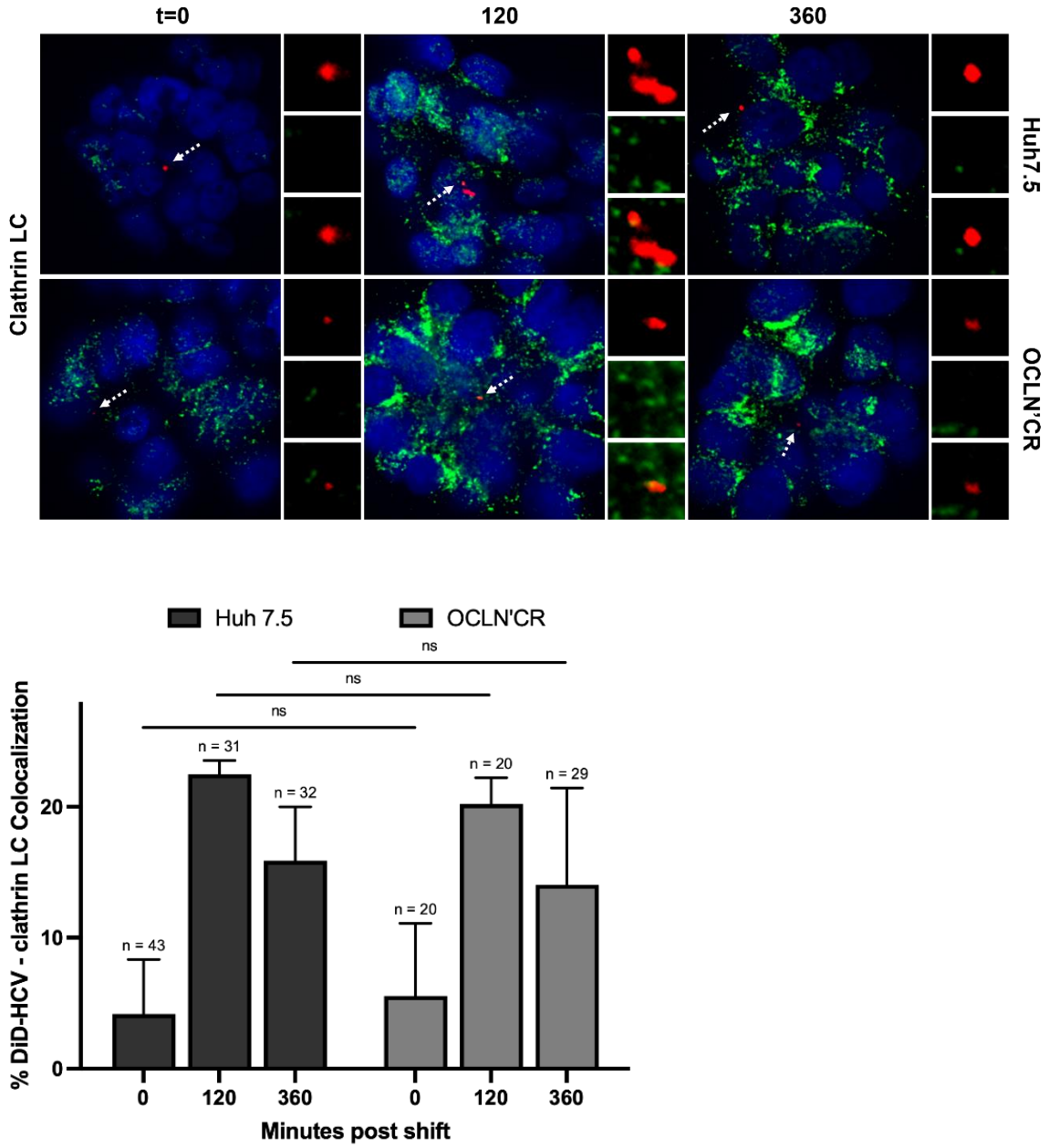

Figure 24. OCLN is not required for DiD-HCV recruitment of clathrin light chain. Organoids of Huh-7.5 wildtype or OCLN CRISPR'ed cells were infected with DiD-HCV (red) for 1h at 4°C, shifted to 37°C for the indicated times, fixed, and probed for clathrin light chain (clathrin LC) (green). n=total DiD signal. Mean +/- SEM.

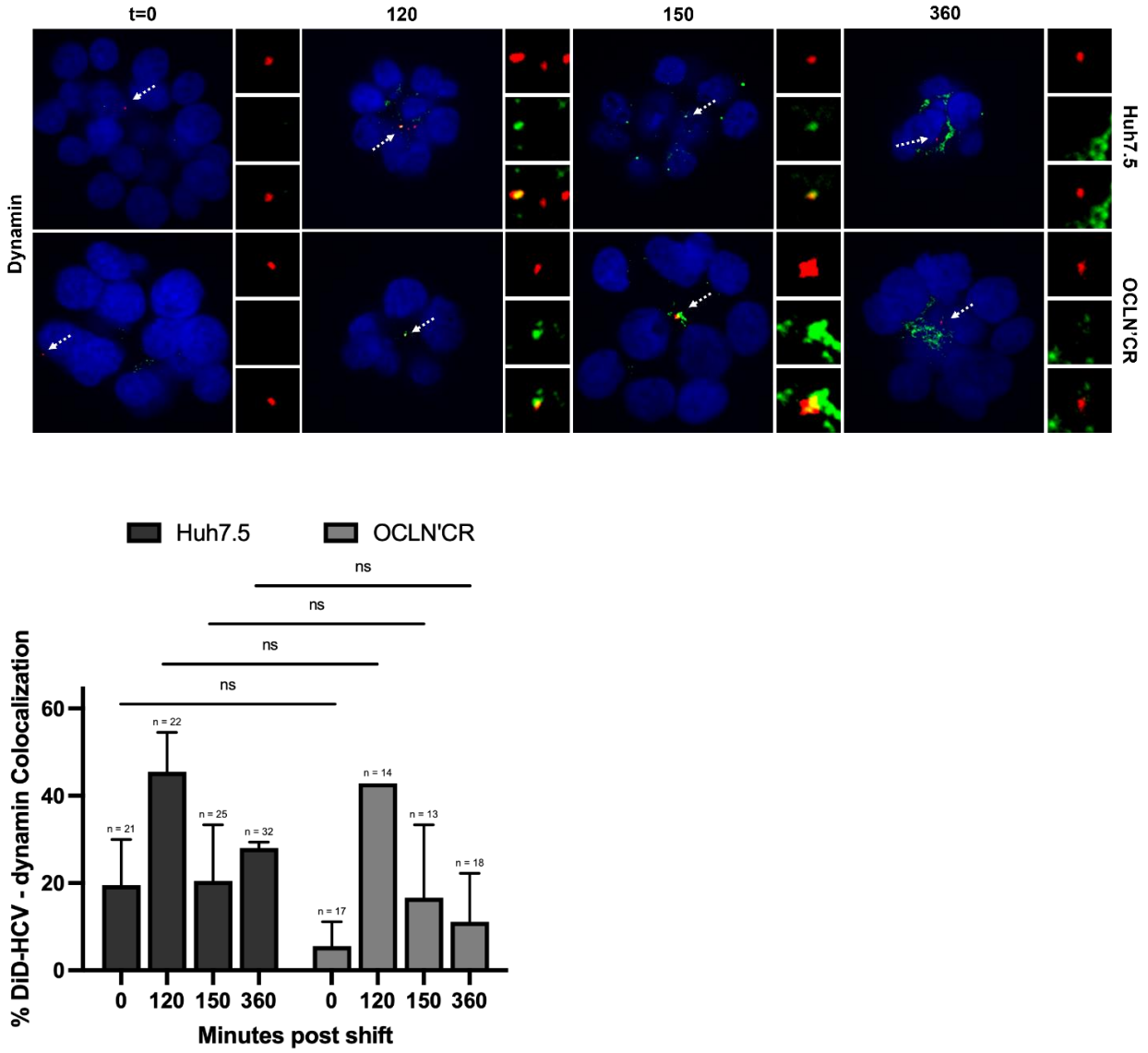

Figure 25. OCLN is not required for DiD-HCV recruitment of dynamin. Organoids of Huh-7.5 wildtype or OCLN CRISPR'ed cells were infected with DiD-HCV (red) for 1h at 4°C, shifted to 37°C for the indicated times, fixed, and probed for dynamin (green). n=total DiD signal. Mean +/- SEM.

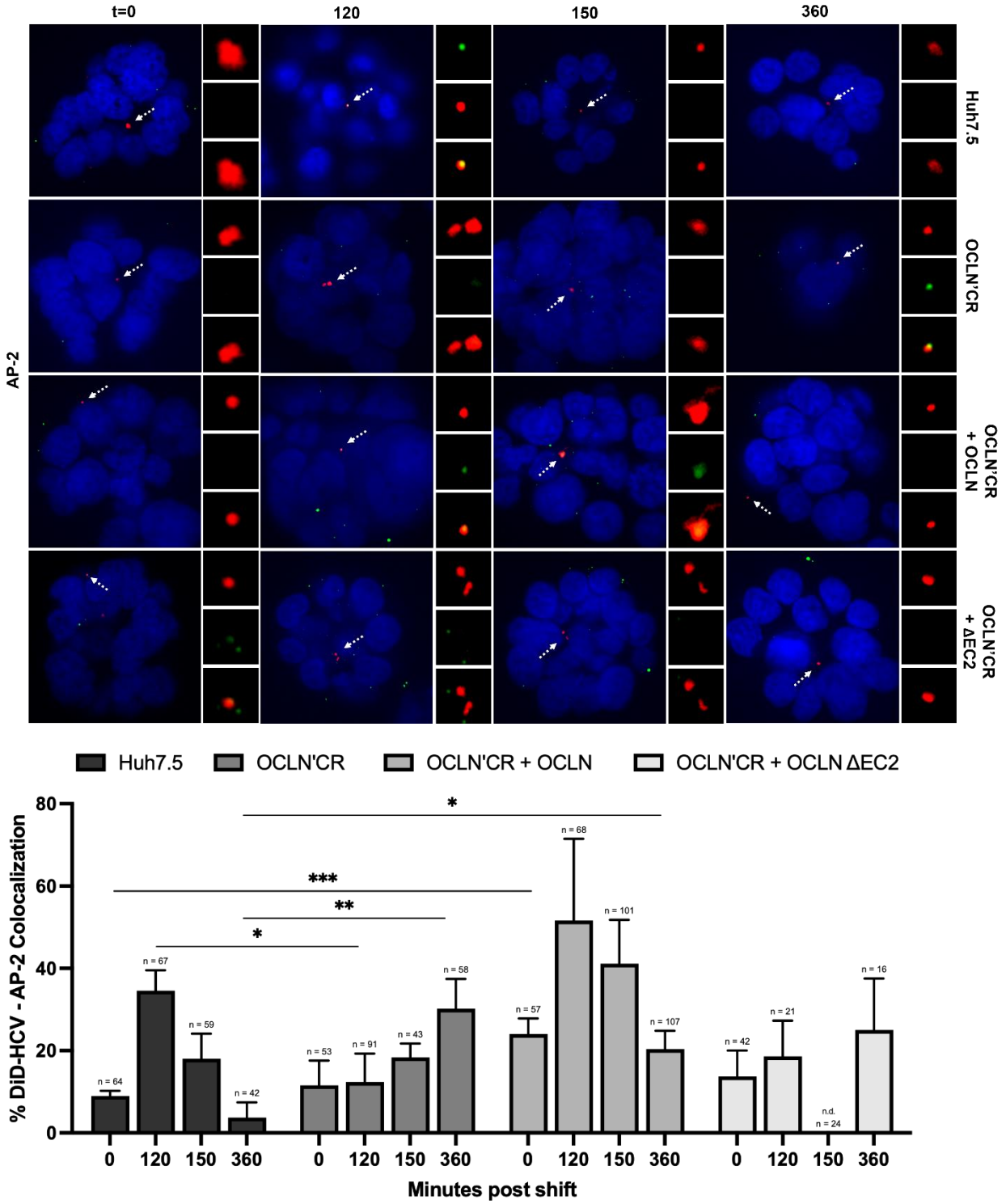

Figure 26. OCLN is not required for DiD-HCV recruitment of AP-2. Organoids of Huh-7.5 wildtype, OCLN CRISPR'ed, or complemented cells were infected with DiD-HCV (red) for 1h at 4°C, shifted to 37°C for the indicated times, fixed, and probed for AP-2µ1 (green). n=total DiD signal. Mean +/- SEM. *p < 0.05, **p < 0.01, ***p < 0.001.

A

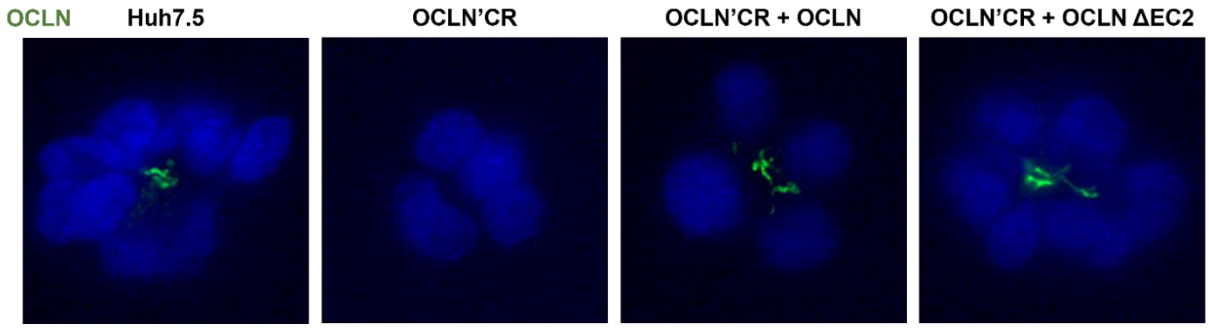

B

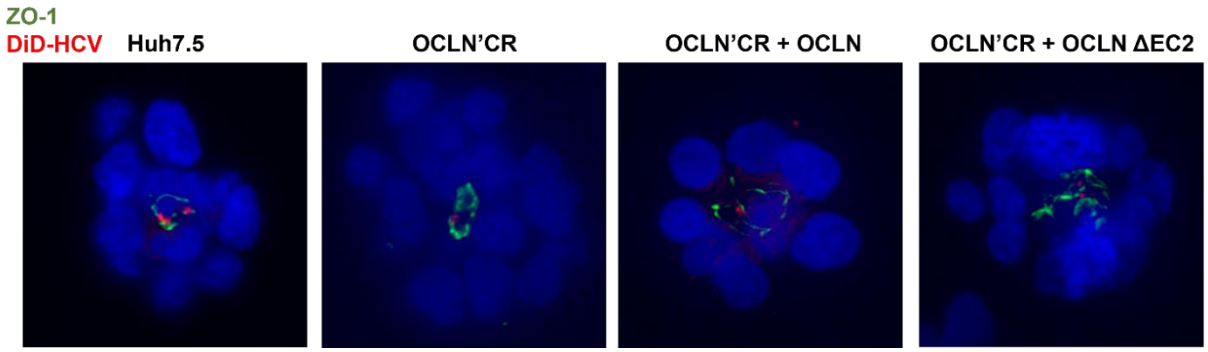

Figure 27. Deleting the second extracellular loop of OCLN does not affect its tight junction localization or ZO-1 localization. Organoids of Huh-7.5 wildtype, OCLN CRISPR'ed, or complemented cells were fixed and probed for **(A)** OCLN or **(B)** ZO-1 (green).

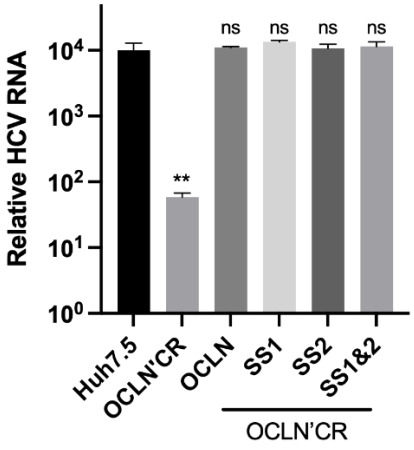

Figure 28. The two speculated YXXΦ sorting signal motifs of OCLN are not required for HCV infection. Huh-7.5 wildtype, OCLN CRISPR'ed, or complemented cells were seeded onto 96-well plates, infected with HCV for 48hr, and then analyzed for relative HCV RNA levels. Mean +/- SD. **$p < 0.01$.

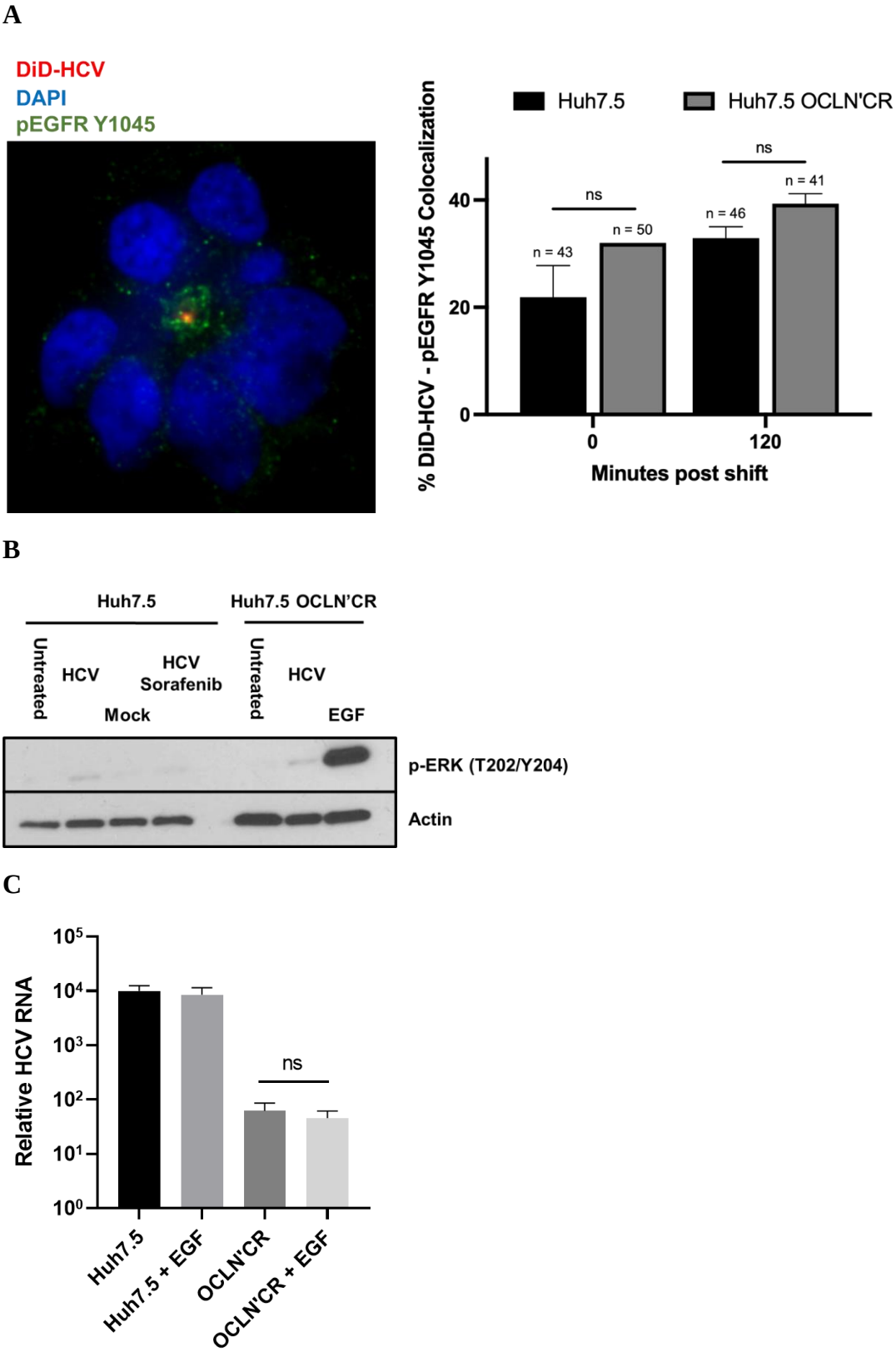

Figure 29. OCLN is not required for HCV-induced ERK activation. (A) Organoids of Huh-

Figure 29, continued. 7.5 wildtype or OCLN CRISPR'ed cells were serum starved, infected with DiD-HCV (red) for 1h at 4°C, shifted to 37°C for the indicated times, fixed, and probed for phospho-EGFR Y1045 (green). n=total DiD signal. Mean +/- SEM. **(B)** Organoids of Huh-7.5 wildtype or OCLN CRISPR'ed cells were serum starved, infected with concentrated HCV (if indicated) for 1h at 4°C, shifted to 37°C, processed with Matrigel cell recovery solution, and lysed at 120 min post temperature shift. For EGF-treated sample, organoids of Huh-7.5 wildtype cells were serum starved, stimulated with 40 ng/mL EGF, processed with Matrigel cell recovery solution, and lysed at 60 min post EGF stimulation. Lysate samples were immunoblotted for the indicated proteins. **(C)** Huh-7.5 wildtype or OCLN CRISPR'ed cells were seeded onto 96-well plates, stimulated with 40 ng/mL EGF and infected with HCV. After 48hr, cells were analyzed for relative HCV RNA levels. Mean +/- SD.

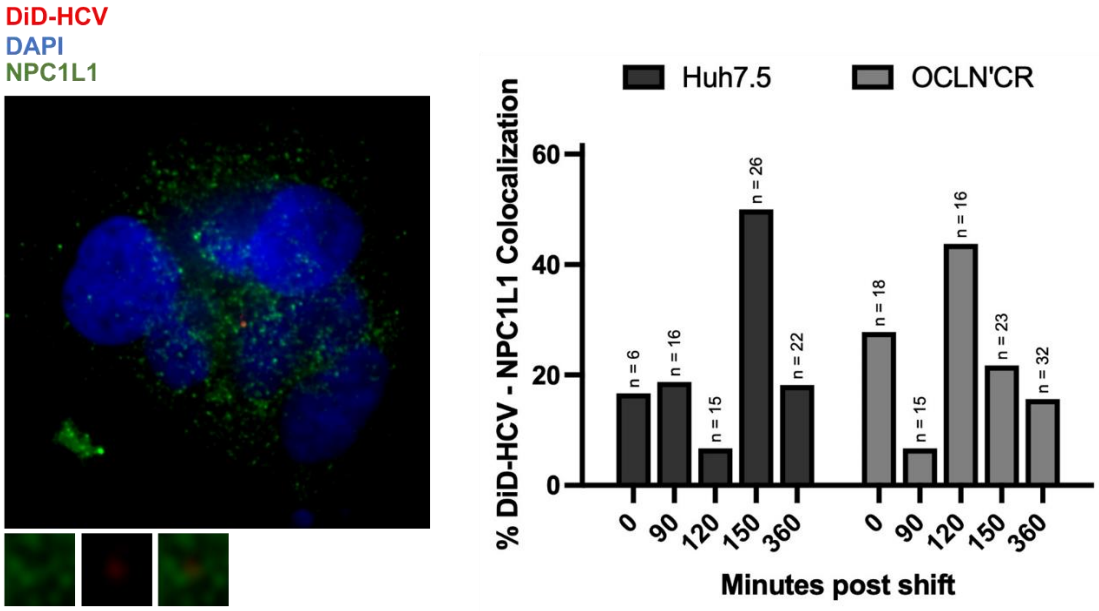

Figure 30. OCLN is not required for DiD-HCV colocalization with NPC1L1. Organoids of Huh-7.5 wildtype or OCLN CRISPR'ed cells were infected with DiD-HCV (red) for 1h at 4°C, shifted to 37°C for the indicated times, fixed, and probed for NPC1L1 (green). n=total DiD signal.

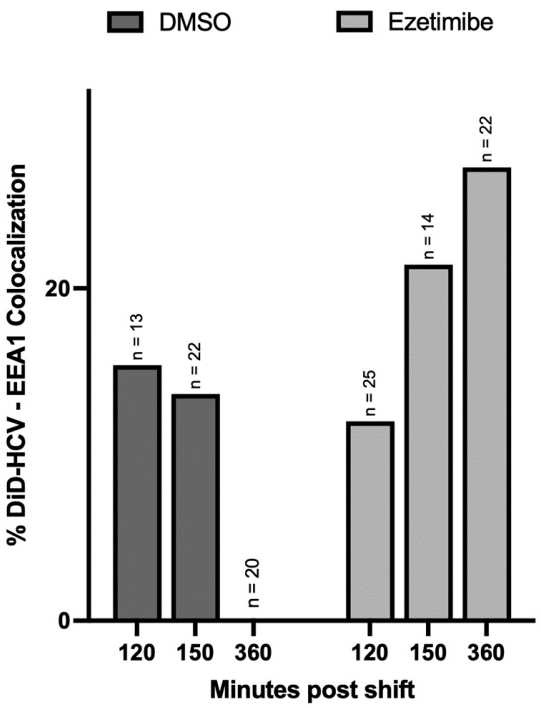

Figure 31. Inhibition of NPC1L1 blocks DiD-HCV dissociation from the early endosomes. Huh-7.5 organoids were incubated with DMSO or 30 μM ezetimibe for 2h, infected with DiD-HCV with DMSO or ezetimibe for 1h at 4°C, shifted to 37°C for the indicated times, fixed, and probed for EEA1. n=total DiD signal.

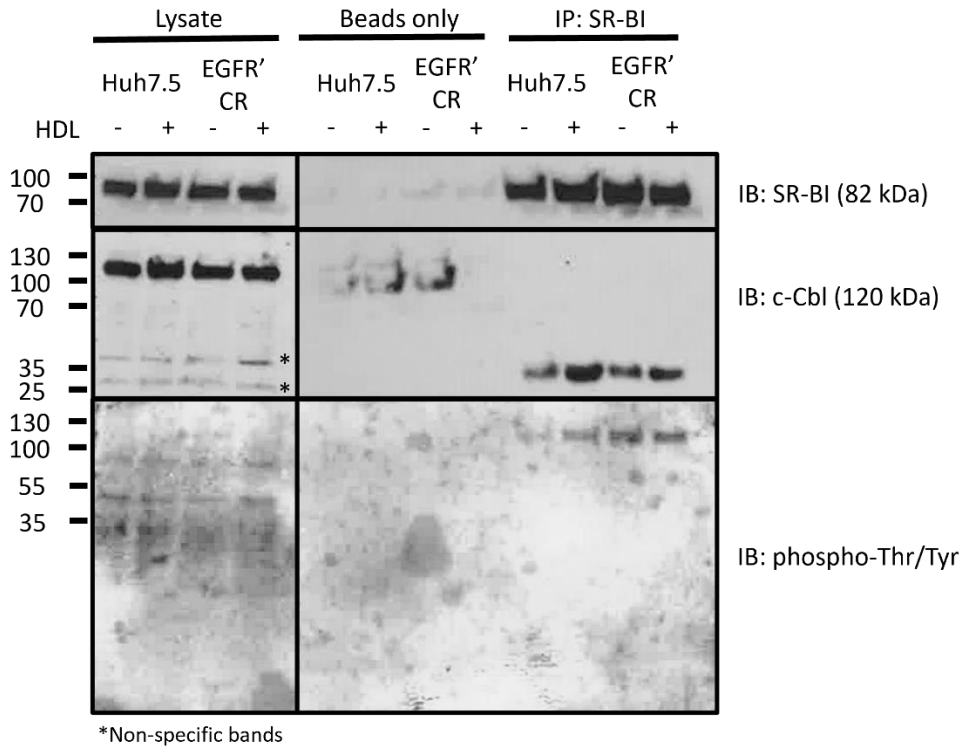

Figure 32. Immunoprecipitation of SR-BI. Huh-7.5 wildtype or EGFR CRISPR'ed cells were serum starved, treated with 20 μg/mL high density lipoprotein, incubated on ice for 1 hr, then incubated at 37°C for 10 min before lysis. SR-BI was immunoprecipitated from the lysate samples and immunoblotted for the indicated proteins.

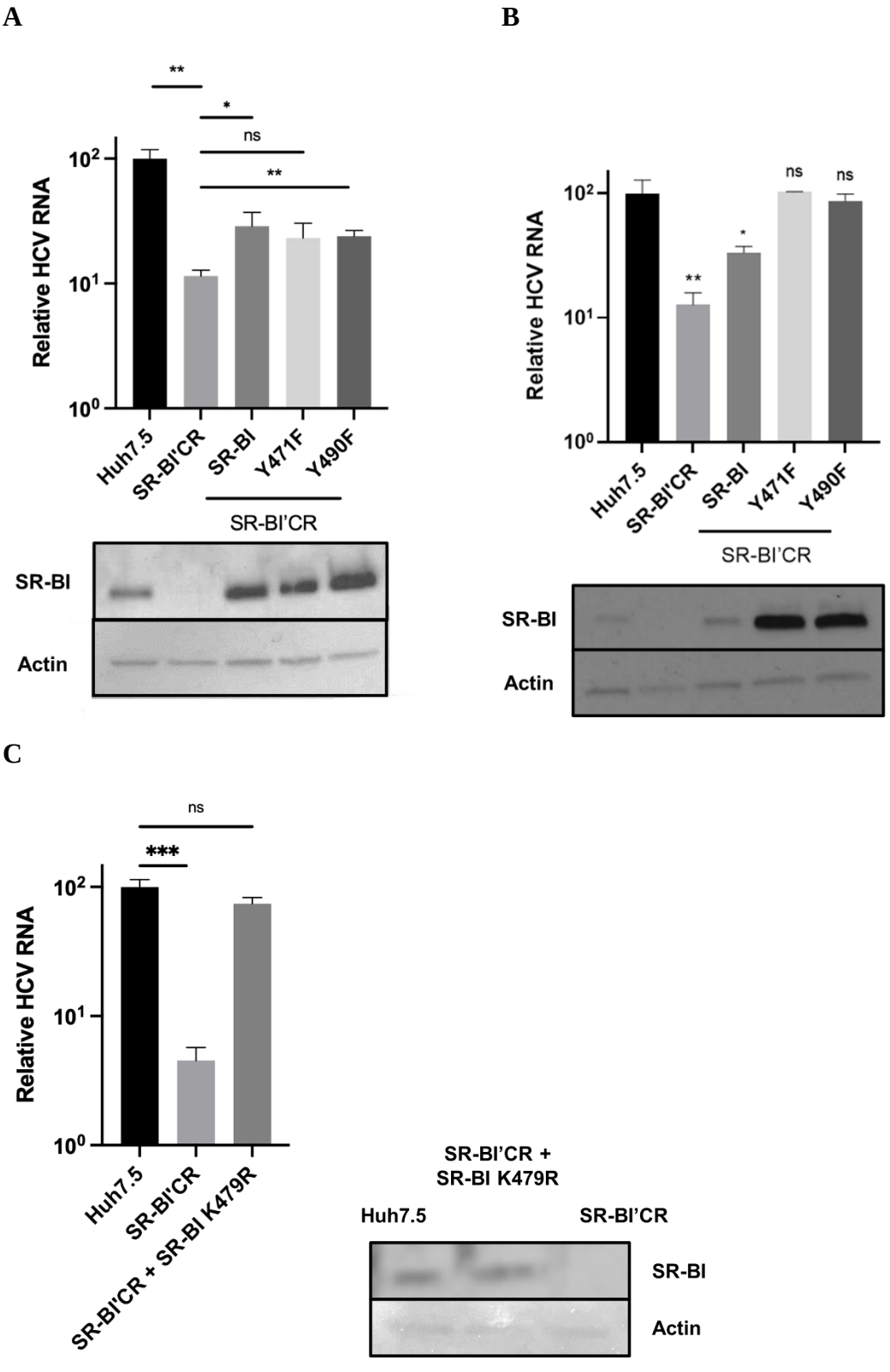

Figure 33. SR-BI Y471, Y490, and K479 are not required for HCV infection. Huh-7.5

D

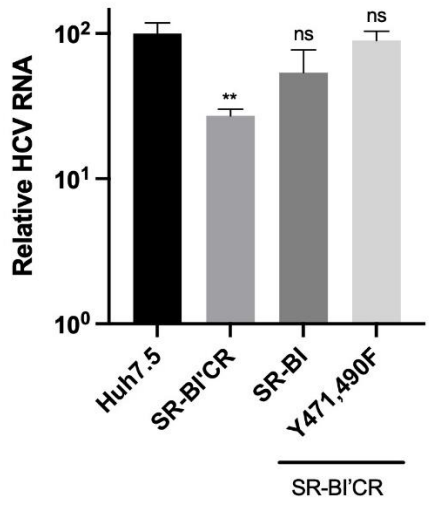

Figure 33, continued. wildtype, SR-BI CRISPR'ed, or complemented cells were seeded onto 96-well plates, infected with HCV for 48hr, and then analyzed for relative HCV RNA levels. Mean +/- SD. *$p < 0.05$, **$p < 0.01$, ***$p < 0.001$.

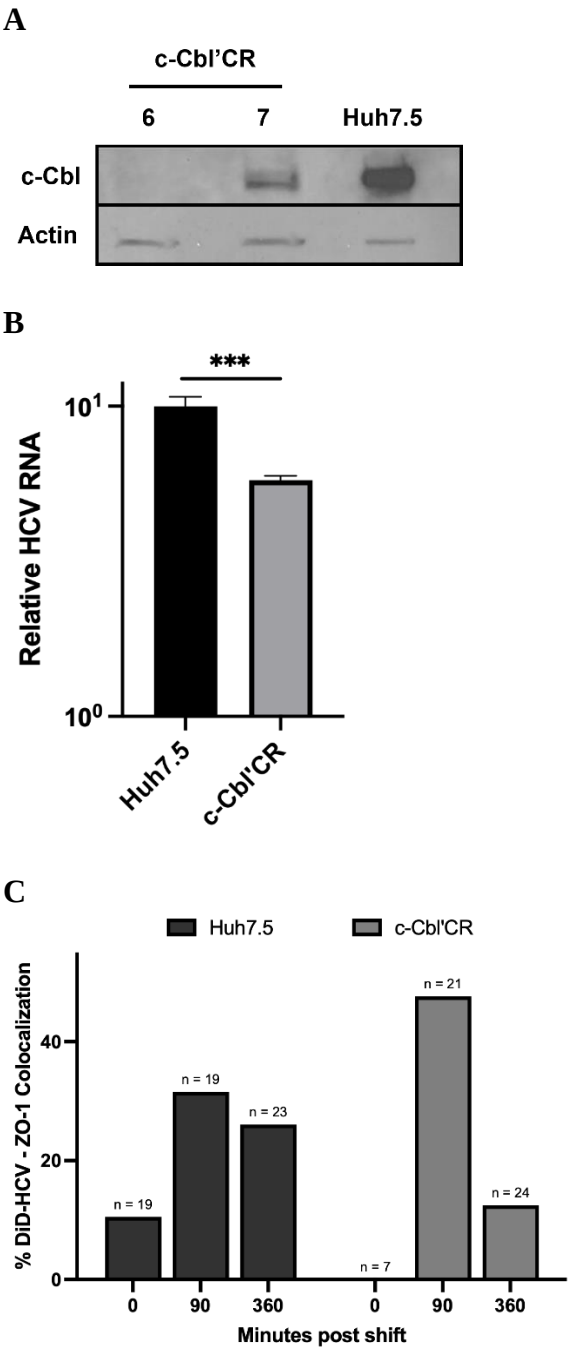

Figure 34. c-Cbl is not required for DiD-HCV migration to the tight junction. (A) Western blot of Huh-7.5 wildtype and c-Cbl CRISPR'ed cells. **(B)** Huh-7.5 wildtype or c-Cbl CRISPR'ed cells were seeded onto 96-well plates, infected with HCV for 48hr, and then analyzed for relative HCV RNA levels. Mean +/- SD. ***p < 0.001. **(C)** Organoids of Huh-7.5 wildtype or c-Cbl CRISPR'ed cells were infected with DiD-HCV for 1h at 4°C, shifted to 37°C for the indicated times, fixed, and probed for ZO-1. n=total DiD signal.

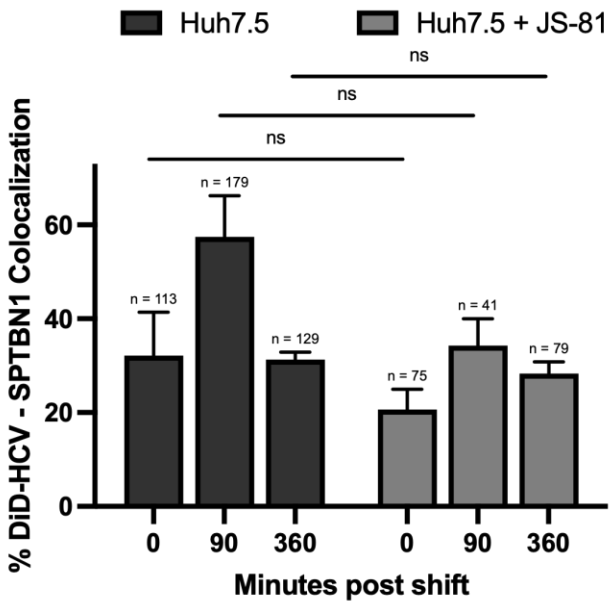

Figure 35. CD81 blocking antibody does not affect DiD-HCV colocalization with SPTBN1. Huh-7.5 organoids were pretreated with 10 μg/mL CD81 blocking antibody JS-81 for 1 hr (if indicated), infected with DiD-HCV for 1h at 4°C, shifted to 37°C for the indicated times, fixed, and probed for SPTBN1. n=total DiD signal.

A

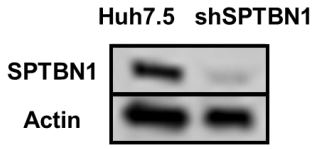

B

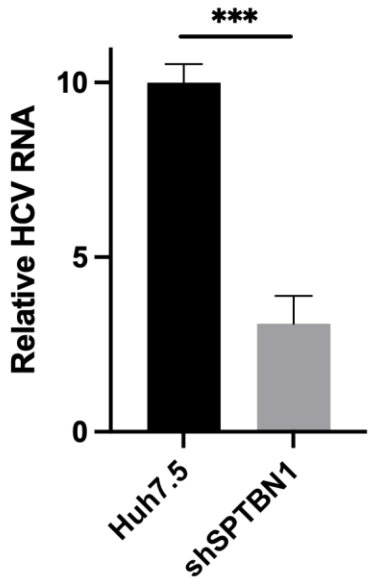

Figure 36. SPTBN1 is required for HCV infection. (A) Western blot of Huh-7.5 wildtype and shSPTBN1 cells. **(B)** Huh-7.5 wildtype or shSPTBN1 cells were seeded onto 96-well plates, infected with HCV for 48hr, and then analyzed for relative HCV RNA levels. Mean +/- SD. ***p < 0.001.

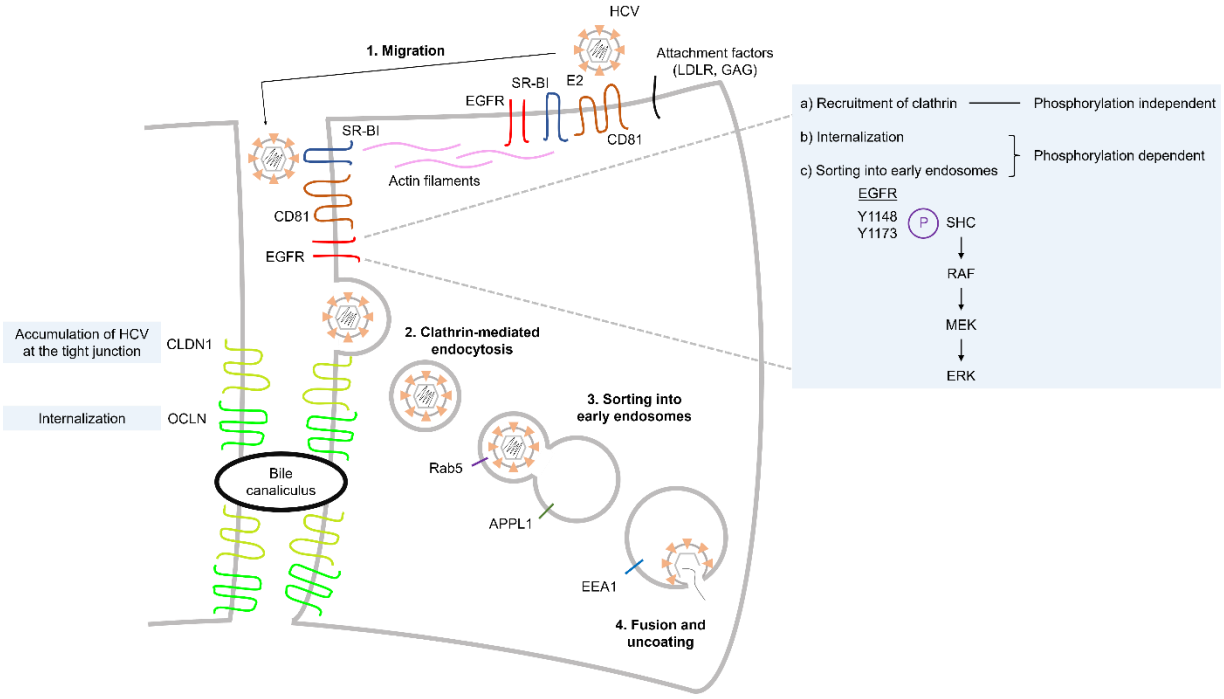

Figure 37. Model of HCV entry into polarized hepatoma organoids.

BIBLIOGRAPHY

Adnane L, Trail PA, Taylor I, Wilhelm SM. Sorafenib (BAY 43-9006, Nexavar), a dual-action inhibitor that targets RAF/MEK/ERK pathway in tumor cells and tyrosine kinases VEGFR/PDGFR in tumor vasculature. Methods Enzymol. 2006;407:597-612. PMID: 16757355.

Aizaki H, Nagamori S, Matsuda M, Kawakami H, Hashimoto O, Ishiko H, et al. Production and release of infectious hepatitis C virus from human liver cell cultures in the three-dimensional radial-flow bioreactor. Virology. 2003 Sep 15;314(1):16-25. PMID: 14517056.

Altmann SW, Davis HR Jr, Zhu LJ, Yao X, Hoos LM, Tetzloff G, et al. Niemann-Pick C1 Like 1 protein is critical for intestinal cholesterol absorption. Science. 2004 Feb 20;303(5661):1201-4. PMID: 14976318.

Aly HH, Shimotohno K, Hijikata M. 3D cultured immortalized human hepatocytes useful to develop drugs for blood-borne HCV. Biochem Biophys Res Commun. 2009 Feb 6;379(2):330-4. Dec 25. PMID: 19103167.

Amador-Cañizares Y, Bernier A, Wilson JA, Sagan SM. miR-122 does not impact recognition of the HCV genome by innate sensors of RNA but rather protects the 5' end from the cellular pyrophosphatases, DOM3Z and DUSP11. Nucleic Acids Res. 2018 Jun 1;46(10):5139-5158. PMID: 29672716.

André P, Komurian-Pradel F, Deforges S, Perret M, Berland JL, Sodoyer M, et al. Characterization of low- and very-low-density hepatitis C virus RNA-containing particles. J Virol. 2002 Jul;76(14):6919-28. PMID: 12072493.

Arteaga CL, Ramsey TT, Shawver LK, Guyer CA. Unliganded epidermal growth factor receptor dimerization induced by direct interaction of quinazolines with the ATP binding site. J Biol Chem. 1997 Sep 12;272(37):23247-54. PMID: 9287333.

Baines AJ. Evolution of spectrin function in cytoskeletal and membrane networks. Biochem Soc Trans. 2009 Aug;37(Pt 4):796-803. PMID: 19614597.

Baktash Y, Madhav A, Coller KE, Randall G. Single Particle Imaging of Polarized Hepatoma Organoids upon Hepatitis C Virus Infection Reveals an Ordered and Sequential Entry Process. Cell Host Microbe. 2018 Mar 14;23(3):382-394.e5. PMID: 29544098.

Balaji K, Mooser C, Janson CM, Bliss JM, Hojjat H, Colicelli J. RIN1 orchestrates the activation of RAB5 GTPases and ABL tyrosine kinases to determine the fate of EGFR. J Cell Sci. 2012 Dec 1;125(Pt 23):5887-96. PMID: 22976291.

Barbieri MA, Kong C, Chen PI, Horazdovsky BF, Stahl PD. The SRC homology 2 domain of Rin1 mediates its binding to the epidermal growth factor receptor and regulates receptor endocytosis. J Biol Chem. 2003 Aug 22;278(34):32027-36. PMID: 12783862.

Bartenschlager R, Baumert TF, Bukh J, Houghton M, Lemon SM, Lindenbach BD, et al. Critical challenges and emerging opportunities in hepatitis C virus research in an era of potent antiviral therapy: Considerations for scientists and funding agencies. Virus Res. 2018 Mar 15;248:53-62. PMID: 29477639.

Bartosch B, Vitelli A, Granier C, Goujon C, Dubuisson J, Pascale S, et al. Cell entry of hepatitis C virus requires a set of co-receptors that include the CD81 tetraspanin and the SR-B1 scavenger receptor. J Biol Chem. 2003 Oct 24;278(43):41624-30. PMID: 12913001.

Batzer AG, Rotin D, Ureña JM, Skolnik EY, Schlessinger J. Hierarchy of binding sites for Grb2 and Shc on the epidermal growth factor receptor. Mol Cell Biol. 1994 Aug;14(8):5192-201. PMID: 7518560.

Benedicto I, Gondar V, Molina-Jiménez F, García-Buey L, López-Cabrera M, Gastaminza P, et al. Clathrin mediates infectious hepatitis C virus particle egress. J Virol. 2015 Apr;89(8):4180-90. PMID: 25631092.

Betters JL, Yu L. Transporters as drug targets: discovery and development of NPC1L1 inhibitors. Clin Pharmacol Ther. 2010 Jan;87(1):117-21. PMID: 19907422.

Bignone PA, King MD, Pinder JC, Baines AJ. Phosphorylation of a threonine unique to the short C-terminal isoform of betaII-spectrin links regulation of alpha-beta spectrin interaction to neuritogenesis. J Biol Chem. 2007 Jan 12;282(2):888-96. PMID: 17088250.

Bilello JA, Bauer G, Dudley MN, Cole GA, Drusano GL. Effect of 2',3'-didehydro-3'-deoxythymidine in an in vitro hollow-fiber pharmacodynamic model system correlates with results of dose-ranging clinical studies. Antimicrob Agents Chemother. 1994 Jun;38(6):1386-91. PMID: 8092842.

Blanchard E, Belouzard S, Goueslain L, Wakita T, Dubuisson J, Wychowski C, et al. Hepatitis C virus entry depends on clathrin-mediated endocytosis. J Virol. 2006 Jul;80(14):6964-72. PMID: 16809302.

Blight KJ, McKeating JA, Rice CM. Highly permissive cell lines for subgenomic and genomic hepatitis C virus RNA replication. J Virol. 2002 Dec;76(24):13001-14. PMID: 12438626.

Brazzoli M, Bianchi A, Filippini S, Weiner A, Zhu Q, Pizza M, et al. CD81 is a central regulator of cellular events required for hepatitis C virus infection of human hepatocytes. J Virol. 2008 Sep;82(17):8316-29. PMID: 18579606.

Brown RJP, Tegtmeyer B, Sheldon J, Khera T, Anggakusuma, Todt D, et al. Liver-expressed Cd302 and Cr1l limit hepatitis C virus cross-species transmission to mice. Sci Adv. 2020 Nov 4;6(45):eabd3233. PMID: 33148654.

Bruening J, Lasswitz L, Banse P, Kahl S, Marinach C, Vondran FW, et al. Hepatitis C virus enters liver cells using the CD81 receptor complex proteins calpain-5 and CBLB. PLoS Pathog. 2018 Jul 19;14(7):e1007111. PMID: 30024968.

Bruewer M, Utech M, Ivanov AI, Hopkins AM, Parkos CA, Nusrat A. Interferon-gamma induces internalization of epithelial tight junction proteins via a macropinocytosis-like process. FASEB J. 2005 Jun;19(8):923-33. PMID: 15923402.

Bucci C, Parton RG, Mather IH, Stunnenberg H, Simons K, Hoflack B, et al. The small GTPase rab5 functions as a regulatory factor in the early endocytic pathway. Cell. 1992 Sep 4;70(5):715-28. PMID: 1516130.

Calvo D, Vega MA. Identification, primary structure, and distribution of CLA-1, a novel member of the CD36/LIMPII gene family. J Biol Chem. 1993 Sep 5;268(25):18929-35. PMID: 7689561.

Capuani F, Conte A, Argenzio E, Marchetti L, Priami C, Polo S, et al. Quantitative analysis reveals how EGFR activation and downregulation are coupled in normal but not in cancer cells. Nat Commun. 2015 Aug 12;6:7999. PMID: 26264748.

Cargnello M, Roux PP. Activation and function of the MAPKs and their substrates, the MAPK-activated protein kinases. Microbiol Mol Biol Rev. 2011 Mar;75(1):50-83. Erratum in: Microbiol Mol Biol Rev. 2012 Jun;76(2):496. PMID: 21372320.

Catanese MT, Uryu K, Kopp M, Edwards TJ, Andrus L, Rice WJ, et al. Ultrastructural analysis of hepatitis C virus particles. Proc Natl Acad Sci U S A. 2013 Jun 4;110(23):9505-10. PMID: 23690609.

Chang CP, Lazar CS, Walsh BJ, Komuro M, Collawn JF, Kuhn LA, et al. Ligand-induced internalization of the epidermal growth factor receptor is mediated by multiple endocytic codes analogous to the tyrosine motif found in constitutively internalized receptors. J Biol Chem. 1993 Sep 15;268(26):19312-20. PMID: 8396132.

Chavrier P, Parton RG, Hauri HP, Simons K, Zerial M. Localization of low molecular weight GTP binding proteins to exocytic and endocytic compartments. Cell. 1990 Jul 27;62(2):317-29. PMID: 2115402.

Coller KE, Berger KL, Heaton NS, Cooper JD, Yoon R, Randall G. RNA interference and single particle tracking analysis of hepatitis C virus endocytosis. PLoS Pathog. 2009 Dec;5(12):e1000702. PMID: 20041214.

Coyne CB, Shen L, Turner JR, Bergelson JM. Coxsackievirus entry across epithelial tight junctions requires occludin and the small GTPases Rab34 and Rab5. Cell Host Microbe. 2007 Sep 13;2(3):181-92. PMID: 18005733.

Cukierman L, Meertens L, Bertaux C, Kajumo F, Dragic T. Residues in a highly conserved claudin-1 motif are required for hepatitis C virus entry and mediate the formation of cell-cell contacts. J Virol. 2009 Jun;83(11):5477-84. PMID: 19297469.

Davis C, Harris HJ, Hu K, Drummer HE, McKeating JA, Mullins JG, et al. In silico directed mutagenesis identifies the CD81/claudin-1 hepatitis C virus receptor interface. Cell Microbiol. 2012 Dec;14(12):1892-903. PMID: 22897233.

Decaens C, Durand M, Grosse B, Cassio D. Which in vitro models could be best used to study hepatocyte polarity? Biol Cell. 2008 Jul;100(7):387-98. PMID: 18549352.

Diao J, Pantua H, Ngu H, Komuves L, Diehl L, Schaefer G, et al. Hepatitis C virus induces epidermal growth factor receptor activation via CD81 binding for viral internalization and entry. J Virol. 2012 Oct;86(20):10935-49. doi: 10.1128/JVI.00750-12. PMID: 22855500.

Ding Q, von Schaewen M, Hrebikova G, Heller B, Sandmann L, Plaas M, et al. Mice expressing minimally humanized CD81 and occludin genes support hepatitis C virus uptake in vivo. J Virol. 2017 Jan 31;91(4):e01799-16. PMID: 27928007.

Dinneen JL, Ceresa BP. Continual expression of Rab5(Q79L) causes a ligand-independent EGFR internalization and diminishes EGFR activity. Traffic. 2004 Aug;5(8):606-15. PMID: 15260830.

Dorobantu CM, Harak C, Klein R, van der Linden L, Strating JR, van der Schaar HM, et al. Tyrphostin AG1478 inhibits encephalomyocarditis virus and hepatitis C virus by targeting phosphatidylinositol 4-Kinase IIIα. Antimicrob Agents Chemother. 2016 Sep 23;60(10):6402-6. PMID: 27480860.

Douam F, Dao Thi VL, Maurin G, Fresquet J, Mompelat D, Zeisel MB, et al. Critical interaction between E1 and E2 glycoproteins determines binding and fusion properties of hepatitis C virus during cell entry. Hepatology. 2014 Mar;59(3):776-88. PMID: 24038151.

Dreux M, Pietschmann T, Granier C, Voisset C, Ricard-Blum S, Mangeot PE, et al. High density lipoprotein inhibits hepatitis C virus-neutralizing antibodies by stimulating cell entry via activation of the scavenger receptor BI. J Biol Chem. 2006 Jul 7;281(27):18285-95. PMID: 16675450.

Drusano GL, Bilello PA, Symonds WT, Stein DS, McDowell J, Bye A, et al. Pharmacodynamics of abacavir in an in vitro hollow-fiber model system. Antimicrob Agents Chemother. 2002 Feb;46(2):464-70. PMID: 11796359.

Eguchi S, Numaguchi K, Iwasaki H, Matsumoto T, Yamakawa T, Utsunomiya H, et al. Calcium-dependent epidermal growth factor receptor transactivation mediates the angiotensin II-induced mitogen-activated protein kinase activation in vascular smooth muscle cells. J Biol Chem. 1998 Apr 10;273(15):8890-6. PMID: 9535870.

Ehrlich M, Boll W, Van Oijen A, Hariharan R, Chandran K, Nibert ML, et al. Endocytosis by random initiation and stabilization of clathrin-coated pits. Cell. 2004 Sep 3;118(5):591-605. PMID: 15339664.

Evans MJ, von Hahn T, Tscherne DM, Syder AJ, Panis M, Wölk B, et al. Claudin-1 is a hepatitis C virus co-receptor required for a late step in entry. Nature. 2007 Apr 12;446(7137):801-5. PMID: 17325668.

Eyre NS, Drummer HE, Beard MR. The SR-BI partner PDZK1 facilitates hepatitis C virus entry. PLoS Pathog. 2010 Oct 7;6(10):e1001130. PMID: 20949066.

Farquhar MJ, Hu K, Harris HJ, Davis C, Brimacombe CL, Fletcher SJ, et al. Hepatitis C virus induces CD81 and claudin-1 endocytosis. J Virol. 2012 Apr;86(8):4305-16. PMID: 22318146.

Felder S, Miller K, Moehren G, Ullrich A, Schlessinger J, Hopkins CR. Kinase activity controls the sorting of the epidermal growth factor receptor within the multivesicular body. Cell. 1990 May 18;61(4):623-34. PMID: 2344614.

Feracci H, Connolly TP, Margolis RN, Hubbard AL. The establishment of hepatocyte cell surface polarity during fetal liver development. Dev Biol. 1987 Sep;123(1):73-84. PMID: 3305113.

Fletcher SJ, Rappoport JZ. Tight junction regulation through vesicle trafficking: bringing cells together. Biochem Soc Trans. 2014 Feb;42(1):195-200. PMID: 24450651.

Fortian A, Dionne LK, Hong SH, Kim W, Gygi SP, Watkins SC, et al. Endocytosis of ubiquitylation-deficient egfr mutants via clathrin-coated pits is mediated by ubiquitylation. Traffic. 2015 Nov;16(11):1137-54. PMID: 26251007.

Fredriksson K, Van Itallie CM, Aponte A, Gucek M, Tietgens AJ, Anderson JM. Proteomic analysis of proteins surrounding occludin and claudin-4 reveals their proximity to signaling and trafficking networks. PLoS One. 2015 Mar 19;10(3):e0117074. PMID: 25789658.

Gardner JK, Herbst-Kralovetz MM. Three-Dimensional Rotating Wall Vessel-Derived Cell Culture Models for Studying Virus-Host Interactions. Viruses. 2016 Nov 9;8(11):304. PMID: 27834891.

Ge L, Wang J, Qi W, Miao HH, Cao J, Qu YX, et al. The cholesterol absorption inhibitor ezetimibe acts by blocking the sterol-induced internalization of NPC1L1. Cell Metab. 2008 Jun;7(6):508-19. PMID: 18522832.

Gerold G, Meissner F, Bruening J, Welsch K, Perin PM, Baumert TF, et al. Quantitative proteomics identifies serum response factor binding protein 1 as a host factor for hepatitis c virus entry. Cell Rep. 2015 Aug 4;12(5):864-78. PMID: 26212323.

Goh LK, Huang F, Kim W, Gygi S, Sorkin A. Multiple mechanisms collectively regulate clathrin-mediated endocytosis of the epidermal growth factor receptor. J Cell Biol. 2010 May 31;189(5):871-83. PMID: 20513767.

Gotoh N, Tojo A, Muroya K, Hashimoto Y, Hattori S, Nakamura S, et al. Epidermal growth factor-receptor mutant lacking the autophosphorylation sites induces phosphorylation of Shc protein and Shc-Grb2/ASH association and retains mitogenic activity. Proc Natl Acad Sci U S A. 1994 Jan 4;91(1):167-71. PMID: 7506413.

Haas AK, Fuchs E, Kopajtich R, Barr FA. A GTPase-activating protein controls Rab5 function in endocytic trafficking. Nat Cell Biol. 2005 Sep;7(9):887-93. PMID: 16086013.

Haid S, Grethe C, Dill MT, Heim M, Kaderali L, Pietschmann T. Isolate-dependent use of claudins for cell entry by hepatitis C virus. Hepatology. 2014 Jan;59(1):24-34. PMID: 23775920.

Han L, Wong D, Dhaka A, Afar D, White M, Xie W, et al. Protein binding and signaling properties of RIN1 suggest a unique effector function. Proc Natl Acad Sci U S A. 1997 May 13;94(10):4954-9. PMID: 9144171.

Han Y, Caday CG, Nanda A, Cavenee WK, Huang HJ. Tyrphostin AG 1478 preferentially inhibits human glioma cells expressing truncated rather than wild-type epidermal growth factor receptors. Cancer Res. 1996 Sep 1;56(17):3859-61. PMID: 8752145.

Harris HJ, Davis C, Mullins JG, Hu K, Goodall M, Farquhar MJ, et al. Claudin association with CD81 defines hepatitis C virus entry. J Biol Chem. 2010 Jul 2;285(27):21092-102. PMID: 20375010.

Heukers R, Vermeulen JF, Fereidouni F, Bader AN, Voortman J, Roovers RC, et al. Endocytosis of EGFR requires its kinase activity and N-terminal transmembrane dimerization motif. J Cell Sci. 2013 Nov 1;126(Pt 21):4900-12. PMID: 23943881.

Honegger AM, Dull TJ, Felder S, Van Obberghen E, Bellot F, Szapary D, et al. Point mutation at the ATP binding site of EGF receptor abolishes protein-tyrosine kinase activity and alters cellular routing. Cell. 1987 Oct 23;51(2):199-209. PMID: 3499230.

Hopkins AM, Walsh SV, Verkade P, Boquet P, Nusrat A. Constitutive activation of Rho proteins by CNF-1 influences tight junction structure and epithelial barrier function. J Cell Sci. 2003 Feb 15;116(Pt 4):725-42. PMID: 12538773.

Huang F, Goh LK, Sorkin A. EGF receptor ubiquitination is not necessary for its internalization. Proc Natl Acad Sci U S A. 2007 Oct 23;104(43):16904-9. Erratum in: Proc Natl Acad Sci U S A. 2009 Aug 18;106(33):14180. PMID: 17940017.

Huch M, Gehart H, van Boxtel R, Hamer K, Blokzijl F, Verstegen MM, et al. Long-term culture of genome-stable bipotent stem cells from adult human liver. Cell. 2015 Jan 15;160(1-2):299-312. PMID: 25533785.

Jiang J, Cun W, Wu X, Shi Q, Tang H, Luo G. Hepatitis C virus attachment mediated by apolipoprotein E binding to cell surface heparan sulfate. J Virol. 2012 Jul;86(13):7256-67. PMID: 22532692.

Jozic I, Saliba SC, Barbieri MA. Effect of EGF-receptor tyrosine kinase inhibitor on Rab5 function during endocytosis. Arch Biochem Biophys. 2012 Sep 1;525(1):16-24. PMID: 22683472.

Kawada M, Nagamori S, Aizaki H, Fukaya K, Niiya M, Matsuura T, et al. Massive culture of human liver cancer cells in a newly developed radial flow bioreactor system: ultrafine structure of functionally enhanced hepatocarcinoma cell lines. In Vitro Cell Dev Biol Anim. 1998 Feb;34(2):109-15. PMID: 9542647.

Kim DS, Ryu JW, Son MY, Oh JH, Chung KS, Lee S, et al. A liver-specific gene expression panel predicts the differentiation status of in vitro hepatocyte models. Hepatology. 2017 Nov;66(5):1662-1674. PMID: 28640507.

Kleinman HK, McGarvey ML, Hassell JR, Star VL, Cannon FB, Laurie GW, et al. Basement membrane complexes with biological activity. Biochemistry. 1986 Jan 28;25(2):312-8. PMID: 2937447.

Knazek RA, Gullino PM, Kohler PO, Dedrick RL. Cell culture on artificial capillaries: an approach to tissue growth in vitro. Science. 1972 Oct 6;178(4056):65-6. PMID: 4560879.

Knudsen SL, Mac AS, Henriksen L, van Deurs B, Grøvdal LM. EGFR signaling patterns are regulated by its different ligands. Growth Factors. 2014 Oct;32(5):155-63. PMID: 25257250.

Kovackova S, Chang L, Bekerman E, Neveu G, Barouch-Bentov R, Chaikuad A, et al. Selective Inhibitors of Cyclin G Associated Kinase (GAK) as Anti-Hepatitis C Agents. J Med Chem. 2015 Apr 23;58(8):3393-410. PMID: 25822739.

Kovacs E, Zorn JA, Huang Y, Barros T, Kuriyan J. A structural perspective on the regulation of the epidermal growth factor receptor. Annu Rev Biochem. 2015;84:739-64. PMID: 25621509.

Krieger SE, Zeisel MB, Davis C, Thumann C, Harris HJ, Schnober EK, et al. Inhibition of hepatitis C virus infection by anti-claudin-1 antibodies is mediated by neutralization of E2-CD81-claudin-1 associations. Hepatology. 2010 Apr;51(4):1144-57. PMID: 20069648.

Kubota Y, Kleinman HK, Martin GR, Lawley TJ. Role of laminin and basement membrane in the morphological differentiation of human endothelial cells into capillary-like structures. J Cell Biol. 1988 Oct;107(4):1589-98. PMID: 3049626.

Lavoie H, Therrien M. Regulation of RAF protein kinases in ERK signalling. Nat Rev Mol Cell Biol. 2015 May;16(5):281-98. PMID: 25907612.

Lee JY, Han HJ, Lee SJ, Cho EH, Lee HB, Seok JH, et al. Use of 3D human liver organoids to predict drug-Induced phospholipidosis. Int J Mol Sci. 2020 Apr 23;21(8):2982. PMID: 32340283.

Levkowitz G, Waterman H, Ettenberg SA, Katz M, Tsygankov AY, Alroy I, et al. Ubiquitin ligase activity and tyrosine phosphorylation underlie suppression of growth factor signaling by c-Cbl/Sli-1. Mol Cell. 1999 Dec;4(6):1029-40. PMID: 10635327.

Li DK, Chung RT. Overview of direct-acting antiviral drugs and drug resistance of hepatitis C virus. Methods Mol Biol. 2019;1911:3-32. PMID: 30593615.

Li Q, Sodroski C, Lowey B, Schweitzer CJ, Cha H, Zhang F, et al. Hepatitis C virus depends on E-cadherin as an entry factor and regulates its expression in epithelial-to-mesenchymal transition. Proc Natl Acad Sci U S A. 2016 Jul 5;113(27):7620-5. PMID: 27298373.

Lindenbach BD, Evans MJ, Syder AJ, Wölk B, Tellinghuisen TL, Liu CC, et al. Complete replication of hepatitis C virus in cell culture. Science. 2005 Jul 22;309(5734):623-6. PMID: 15947137.

Liu S, Chen R, Hagedorn CH. Direct visualization of hepatitis C virus-infected Huh7.5 cells with a high titre of infectious chimeric JFH1-EGFP reporter virus in three-dimensional Matrigel cell cultures. J Gen Virol. 2014 Feb;95(Pt 2):423-433. PMID: 24243732.

Liu S, Yang W, Shen L, Turner JR, Coyne CB, Wang T. Tight junction proteins claudin-1 and occludin control hepatitis C virus entry and are downregulated during infection to prevent superinfection. J Virol. 2009 Feb;83(4):2011-4. PMID: 19052094.

Liu Z, Tian Y, Machida K, Lai MM, Luo G, Foung SK, et al. Transient activation of the PI3K-AKT pathway by hepatitis C virus to enhance viral entry. J Biol Chem. 2012 Dec 7;287(50):41922-30. PMID: 23095753.

Luo H, Yanagawa B, Zhang J, Luo Z, Zhang M, Esfandiarei M, et al. Coxsackievirus B3 replication is reduced by inhibition of the extracellular signal-regulated kinase (ERK) signaling pathway. J Virol. 2002 Apr;76(7):3365-73. PMID: 11884562.

Lupberger J, Zeisel MB, Xiao F, Thumann C, Fofana I, Zona L, et al. EGFR and EphA2 are host factors for hepatitis C virus entry and possible targets for antiviral therapy. Nat Med. 2011 May;17(5):589-95. PMID: 21516087.

Luzzatto AC. Hepatocyte differentiation during early fetal development in the rat. Cell Tissue Res. 1981;215(1):133-42. PMID: 7226191.

Machnicka B, Czogalla A, Hryniewicz-Jankowska A, Bogusławska DM, Grochowalska R, Heger E, et al. Spectrins: a structural platform for stabilization and activation of membrane channels, receptors and transporters. Biochim Biophys Acta. 2014 Feb;1838(2):620-34. PMID: 23673272.

Mailly L, Xiao F, Lupberger J, Wilson GK, Aubert P, Duong FHT, et al. Clearance of persistent hepatitis C virus infection in humanized mice using a claudin-1-targeting monoclonal antibody. Nat Biotechnol. 2015 May;33(5):549-554. PMID: 25798937.

Malarkey DE, Johnson K, Ryan L, Boorman G, Maronpot RR. New insights into functional aspects of liver morphology. Toxicol Pathol. 2005;33(1):27-34. PMID: 15805053.

Matallanas D, Birtwistle M, Romano D, Zebisch A, Rauch J, von Kriegsheim A, et al. Raf family kinases: old dogs have learned new tricks. Genes Cancer. 2011 Mar;2(3):232-60. PMID: 21779496; PMCID: PMC3128629.

Mateu G, Donis RO, Wakita T, Bukh J, Grakoui A. Intragenotypic JFH1 based recombinant hepatitis C virus produces high levels of infectious particles but causes increased cell death. Virology. 2008 Jul 5;376(2):397-407. PMID: 18455749.

Matter K, Balda MS. Biogenesis of tight junctions: the C-terminal domain of occludin mediates basolateral targeting. J Cell Sci. 1998 Feb;111 (Pt 4):511-9. PMID: 9443899.

McSharry JJ, Drusano GL. Antiviral pharmacodynamics in hollow fibre bioreactors. Antivir Chem Chemother. 2011 May 12;21(5):183-92. PMID: 21566264.

McSharry JJ, Weng Q, Brown A, Kulawy R, Drusano GL. Prediction of the pharmacodynamically linked variable of oseltamivir carboxylate for influenza A virus using an in vitro hollow-fiber infection model system. Antimicrob Agents Chemother. 2009 Jun;53(6):2375-81. PMID: 19364864.

Mee CJ, Harris HJ, Farquhar MJ, Wilson G, Reynolds G, Davis C, et al. Polarization restricts hepatitis C virus entry into HepG2 hepatoma cells. J Virol. 2009 Jun;83(12):6211-21. PMID: 19357163.

Meertens L, Bertaux C, Dragic T. Hepatitis C virus entry requires a critical postinternalization step and delivery to early endosomes via clathrin-coated vesicles. J Virol. 2006 Dec;80(23):11571-8. PMID: 17005647.

Meertens L, Bertaux C, Cukierman L, Cormier E, Lavillette D, Cosset FL, et al. The tight junction proteins claudin-1, -6, and -9 are entry cofactors for hepatitis C virus. J Virol. 2008 Apr;82(7):3555-60. PMID: 18234789.

Meng Q. Three-dimensional culture of hepatocytes for prediction of drug-induced hepatotoxicity. Expert Opin Drug Metab Toxicol. 2010 Jun;6(6):733-46. PMID: 20380484.

Merz A, Long G, Hiet MS, Brügger B, Chlanda P, Andre P, et al. Biochemical and morphological properties of hepatitis C virus particles and determination of their lipidome. J Biol Chem. 2011 Jan 28;286(4):3018-32. PMID: 21056986.

Meyer K, Kwon YC, Liu S, Hagedorn CH, Ray RB, Ray R. Interferon-α inducible protein 6 impairs EGFR activation by CD81 and inhibits hepatitis C virus infection. Sci Rep. 2015 Mar 11;5:9012. PMID: 25757571.

Miaczynska M, Christoforidis S, Giner A, Shevchenko A, Uttenweiler-Joseph S, Habermann B, et al. APPL proteins link Rab5 to nuclear signal transduction via an endosomal compartment. Cell. 2004 Feb 6;116(3):445-56. PMID: 15016378.

Miao Z, Xie Z, Miao J, Ran J, Feng Y, Xia X. Regulated entry of hepatitis c virus into hepatocytes. Viruses. 2017 May 9;9(5):100. PMID: 28486435.

Michta ML, Hopcraft SE, Narbus CM, Kratovac Z, Israelow B, Sourisseau M, et al. Species-specific regions of occludin required by hepatitis C virus for cell entry. J Virol. 2010 Nov;84(22):11696-708. PMID: 20844048.

Mohapatra B, Ahmad G, Nadeau S, Zutshi N, An W, Scheffe S, et al. Protein tyrosine kinase regulation by ubiquitination: critical roles of Cbl-family ubiquitin ligases. Biochim Biophys Acta. 2013 Jan;1833(1):122-39. PMID: 23085373.

Molina JR, Adjei AA. The Ras/Raf/MAPK pathway. J Thorac Oncol. 2006 Jan;1(1):7-9. PMID: 17409820.

Molina-Jimenez F, Benedicto I, Dao Thi VL, Gondar V, Lavillette D, Marin JJ, et al. Matrigel-embedded 3D culture of Huh-7 cells as a hepatocyte-like polarized system to study hepatitis C virus cycle. Virology. 2012 Mar 30;425(1):31-9. PMID: 22280897.

Morrison P, Chung KC, Rosner MR. Mutation of Di-leucine residues in the juxtamembrane region alters EGF receptor expression. Biochemistry. 1996 Nov 19;35(46):14618-24. PMID: 8931560.

Mosesson Y, Shtiegman K, Katz M, Zwang Y, Vereb G, Szollosi J, et al. Endocytosis of receptor tyrosine kinases is driven by monoubiquitylation, not polyubiquitylation. J Biol Chem. 2003 Jun 13;278(24):21323-6. Apr 28. PMID: 12719435.

Mu FT, Callaghan JM, Steele-Mortimer O, Stenmark H, Parton RG, Campbell PL, et al. EEA1, an early endosome-associated protein. EEA1 is a conserved alpha-helical peripheral membrane protein flanked by cysteine "fingers" and contains a calmodulin-binding IQ motif. J Biol Chem. 1995 Jun 2;270(22):13503-11. PMID: 7768953.

Murakami K, Inoue Y, Hmwe SS, Omata K, Hongo T, Ishii K, et al. Dynamic behavior of hepatitis C virus quasispecies in a long-term culture of the three-dimensional radial-flow bioreactor system. J Virol Methods. 2008 Mar;148(1-2):174-81. PMID: 18164425.

Narbus CM, Israelow B, Sourisseau M, Michta ML, Hopcraft SE, Zeiner GM, et al. HepG2 cells expressing microRNA miR-122 support the entire hepatitis C virus life cycle. J Virol. 2011 Nov;85(22):12087-92. PMID: 21917968.

Neveu G, Barouch-Bentov R, Ziv-Av A, Gerber D, Jacob Y, Einav S. Identification and targeting of an interaction between a tyrosine motif within hepatitis C virus core protein and AP2M1 essential for viral assembly. PLoS Pathog. 2012;8(8):e1002845. PMID: 22916011.

Neveu G, Ziv-Av A, Barouch-Bentov R, Berkerman E, Mulholland J, Einav S. AP-2-associated protein kinase 1 and cyclin G-associated kinase regulate hepatitis C virus entry and are potential drug targets. J Virol. 2015 Apr;89(8):4387-404. PMID: 25653444.

Ng SS, Saeb-Parsy K, Blackford SJI, Segal JM, Serra MP, Horcas-Lopez M, et al. Human iPS derived progenitors bioengineered into liver organoids using an inverted colloidal crystal poly (ethylene glycol) scaffold. Biomaterials. 2018 Nov;182:299-311. PMID: 30149262.

Ohno H, Stewart J, Fournier MC, Bosshart H, Rhee I, Miyatake S, et al. Interaction of tyrosine-based sorting signals with clathrin-associated proteins. Science. 1995 Sep 29;269(5232):1872-5. PMID: 7569928.

Okabayashi Y, Kido Y, Okutani T, Sugimoto Y, Sakaguchi K, Kasuga M. Tyrosines 1148 and 1173 of activated human epidermal growth factor receptors are binding sites of Shc in intact cells. J Biol Chem. 1994 Jul 15;269(28):18674-8. PMID: 8034616.

Olusanya O, Andrews PD, Swedlow JR, Smythe E. Phosphorylation of threonine 156 of the mu2 subunit of the AP2 complex is essential for endocytosis in vitro and in vivo. Curr Biol. 2001 Jun 5;11(11):896-900. PMID: 11516654.

Owen DM, Huang H, Ye J, Gale M Jr. Apolipoprotein E on hepatitis C virion facilitates infection through interaction with low-density lipoprotein receptor. Virology. 2009 Nov 10;394(1):99-108. PMID: 19751943.

Park SY, Yoon SJ, Freire-de-Lima L, Kim JH, Hakomori SI. Control of cell motility by interaction of gangliosides, tetraspanins, and epidermal growth factor receptor in A431 versus KB epidermoid tumor cells. Carbohydr Res. 2009 Aug 17;344(12):1479-86. PMID: 19559406.

Pelicci G, Lanfrancone L, Grignani F, McGlade J, Cavallo F, Forni G, et al. A novel transforming protein (SHC) with an SH2 domain is implicated in mitogenic signal transduction. Cell. 1992 Jul 10;70(1):93-104. PMID: 1623525.

Pennock S, Wang Z. A tale of two Cbls: interplay of c-Cbl and Cbl-b in epidermal growth factor receptor downregulation. Mol Cell Biol. 2008 May;28(9):3020-37. PMID: 18316398.

Pihl AF, Offersgaard AF, Mathiesen CK, Prentoe J, Fahnøe U, Krarup H, et al. High density Huh7.5 cell hollow fiber bioreactor culture for high-yield production of hepatitis C virus and studies of antivirals. Sci Rep. 2018 Nov 30;8(1):17505. PMID: 30504788.

Pileri P, Uematsu Y, Campagnoli S, Galli G, Falugi F, Petracca R, et al. Binding of hepatitis C virus to CD81. Science. 1998 Oct 30;282(5390):938-41. PMID: 9794763.

Pleschka S, Wolff T, Ehrhardt C, Hobom G, Planz O, Rapp UR, et al. Influenza virus propagation is impaired by inhibition of the Raf/MEK/ERK signalling cascade. Nat Cell Biol. 2001 Mar;3(3):301-5. PMID: 11231581.

Ploss A, Evans MJ, Gaysinskaya VA, Panis M, You H, de Jong YP, et al. Human occludin is a hepatitis C virus entry factor required for infection of mouse cells. Nature. 2009 Feb 12;457(7231):882-6. PMID: 19182773.

Ploss A, Evans MJ. Hepatitis C virus host cell entry. Curr Opin Virol. 2012 Feb;2(1):14-9. PMID: 22440961.

Poulikakos PI, Zhang C, Bollag G, Shokat KM, Rosen N. RAF inhibitors transactivate RAF dimers and ERK signalling in cells with wild-type BRAF. Nature. 2010 Mar 18;464(7287):427-30. PMID: 20179705.

Rajalakshmy AR, Malathi J, Madhavan HN, Samuel JK. Mebiolgel, a thermoreversible polymer as a scaffold for three dimensional culture of Huh7 cell line with improved hepatocyte differentiation marker expression and HCV replication. Indian J Med Microbiol. 2015 Oct-Dec;33(4):554-9. PMID: 26470963.

Randall G, Chen L, Panis M, Fischer AK, Lindenbach BD, Sun J, et al. Silencing of USP18 potentiates the antiviral activity of interferon against hepatitis C virus infection. Gastroenterology. 2006 Nov;131(5):1584-91. PMID: 17101330.

Randall G, Panis M, Cooper JD, Tellinghuisen TL, Sukhodolets KE, Pfeffer S, et al. Cellular cofactors affecting hepatitis C virus infection and replication. Proc Natl Acad Sci U S A. 2007 Jul 31;104(31):12884-9. PMID: 17616579.

Reynolds GM, Harris HJ, Jennings A, Hu K, Grove J, Lalor PF, et al. Hepatitis C virus receptor expression in normal and diseased liver tissue. Hepatology. 2008 Feb;47(2):418-27. PMID: 18085708.

Ricotta D, Conner SD, Schmid SL, von Figura K, Honing S. Phosphorylation of the AP2 mu subunit by AAK1 mediates high affinity binding to membrane protein sorting signals. J Cell Biol. 2002 Mar 4;156(5):791-5. PMID: 11877457.

Rigotti A, Miettinen HE, Krieger M. The role of the high-density lipoprotein receptor SR-BI in the lipid metabolism of endocrine and other tissues. Endocr Rev. 2003 Jun;24(3):357-87. PMID: 12788804.

Roepstorff K, Grandal MV, Henriksen L, Knudsen SL, Lerdrup M, Grøvdal L, et al. Differential effects of EGFR ligands on endocytic sorting of the receptor. Traffic. 2009 Aug;10(8):1115-27. PMID: 19531065.

Rubino M, Miaczynska M, Lippé R, Zerial M. Selective membrane recruitment of EEA1 suggests a role in directional transport of clathrin-coated vesicles to early endosomes. J Biol Chem. 2000 Feb 11;275(6):3745-8. PMID: 10660521.

Sainz B Jr, Barretto N, Martin DN, Hiraga N, Imamura M, Hussain S, et al. Identification of the Niemann-Pick C1-like 1 cholesterol absorption receptor as a new hepatitis C virus entry factor. Nat Med. 2012 Jan 8;18(2):281-5. PMID: 22231557.

Sainz B Jr, TenCate V, Uprichard SL. Three-dimensional Huh7 cell culture system for the study of Hepatitis C virus infection. Virol J. 2009 Jul 15;6:103. PMID: 19604376.

Salcini AE, McGlade J, Pelicci G, Nicoletti I, Pawson T, Pelicci PG. Formation of Shc-Grb2 complexes is necessary to induce neoplastic transformation by overexpression of Shc proteins. Oncogene. 1994 Oct;9(10):2827-36. PMID: 8084588.

Scarselli E, Ansuini H, Cerino R, Roccasecca RM, Acali S, Filocamo G, et al. The human scavenger receptor class B type I is a novel candidate receptor for the hepatitis C virus. EMBO J. 2002 Oct 1;21(19):5017-25. PMID: 12356718.

Sekhar V, Pollicino T, Diaz G, Engle RE, Alayli F, Melis M, et al. Infection with hepatitis C virus depends on TACSTD2, a regulator of claudin-1 and occludin highly downregulated in hepatocellular carcinoma. PLoS Pathog. 2018 Mar 14;14(3):e1006916. PMID: 29538454.

Shimizu Y, Shirasago Y, Kondoh M, Suzuki T, Wakita T, Hanada K, et al. Monoclonal Antibodies against Occludin Completely Prevented Hepatitis C Virus Infection in a Mouse Model. J Virol. 2018 Mar 28;92(8):e02258-17. PMID: 29437969.

Shulla A, Randall G. Hepatitis C virus-host interactions, replication, and viral assembly. Curr Opin Virol. 2012 Dec;2(6):725-32. PMID: 23083892.

Sigismund S, Argenzio E, Tosoni D, Cavallaro E, Polo S, Di Fiore PP. Clathrin-mediated internalization is essential for sustained EGFR signaling but dispensable for degradation. Dev Cell. 2008 Aug;15(2):209-19. PMID: 18694561.

Simonsen A, Lippé R, Christoforidis S, Gaullier JM, Brech A, Callaghan J, et al. EEA1 links PI(3)K function to Rab5 regulation of endosome fusion. Nature. 1998 Jul 30;394(6692):494-8. PMID: 9697774.

Snooks MJ, Bhat P, Mackenzie J, Counihan NA, Vaughan N, Anderson DA. Vectorial entry and release of hepatitis A virus in polarized human hepatocytes. J Virol. 2008 Sep;82(17):8733-42. PMID: 18579610.

So CW, Randall G. Three-Dimensional Cell Culture Systems for Studying Hepatitis C Virus. Viruses. 2021 Jan 30;13(2):211. doi: 10.3390/v13020211. PMID: 33573191.

Sorkin A, Mazzotti M, Sorkina T, Scotto L, Beguinot L. Epidermal growth factor receptor interaction with clathrin adaptors is mediated by the Tyr974-containing internalization motif. J Biol Chem. 1996 Jun 7;271(23):13377-84. PMID: 8662849.

Sourisseau M, Michta ML, Zony C, Israelow B, Hopcraft SE, Narbus CM, et al. Temporal analysis of hepatitis C virus cell entry with occludin directed blocking antibodies. PLoS Pathog. 2013 Mar;9(3):e1003244. PMID: 23555257.

Stamatovic SM, Johnson AM, Sladojevic N, Keep RF, Andjelkovic AV. Endocytosis of tight junction proteins and the regulation of degradation and recycling. Ann N Y Acad Sci. 2017 Jun;1397(1):54-65. PMID: 28415156.

Stamatovic SM, Sladojevic N, Keep RF, Andjelkovic AV. Relocalization of junctional adhesion molecule A during inflammatory stimulation of brain endothelial cells. Mol Cell Biol. 2012 Sep;32(17):3414-27. PMID: 22733993.

Stenmark H, Parton RG, Steele-Mortimer O, Lütcke A, Gruenberg J, Zerial M. Inhibition of rab5 GTPase activity stimulates membrane fusion in endocytosis. EMBO J. 1994;13(6):1287-96. PMID: 8137813.

Suh Y, Yoon CH, Kim RK, Lim EJ, Oh YS, Hwang SG, et al. Claudin-1 induces epithelial-mesenchymal transition through activation of the c-Abl-ERK signaling pathway in human liver cells. Oncogene. 2013 Oct 10;32(41):4873-82. Erratum in: Oncogene. 2017 Feb 23;36(8):1167-1168. PMID: 23160379.

Takebe T, Sekine K, Enomura M, Koike H, Kimura M, Ogaeri T, et al. Vascularized and functional human liver from an iPSC-derived organ bud transplant. Nature. 2013 Jul 25;499(7459):481-4. PMID: 23823721.

Tall GG, Barbieri MA, Stahl PD, Horazdovsky BF. Ras-activated endocytosis is mediated by the Rab5 guanine nucleotide exchange activity of RIN1. Dev Cell. 2001 Jul;1(1):73-82. PMID: 11703925.

Treyer A, Müsch A. Hepatocyte polarity. Compr Physiol. 2013 Jan;3(1):243-87. PMID: 23720287.

Utech M, Mennigen R, Bruewer M. Endocytosis and recycling of tight junction proteins in inflammation. J Biomed Biotechnol. 2010;2010:484987. PMID: 20011071.

van der Beek J, de Heus C, Liv N, Klumperman J. Quantitative correlative microscopy reveals the ultrastructural distribution of endogenous endosomal proteins. J Cell Biol. 2022 Jan 3;221(1):e202106044. PMID: 34817533.

van der Geer P, Wiley S, Lai VK, Olivier JP, Gish GD, Stephens R, et al. A conserved amino-terminal Shc domain binds to phosphotyrosine motifs in activated receptors and phosphopeptides. Curr Biol. 1995 Apr 1;5(4):404-12. PMID: 7542991.

Voisset C, Callens N, Blanchard E, Op De Beeck A, Dubuisson J, Vu-Dac N. High density lipoproteins facilitate hepatitis C virus entry through the scavenger receptor class B type I. J Biol Chem. 2005 Mar 4;280(9):7793-9. PMID: 15632171.

Wakita T, Pietschmann T, Kato T, Date T, Miyamoto M, Zhao Z, et al. Production of infectious hepatitis C virus in tissue culture from a cloned viral genome. Nat Med. 2005 Jul;11(7):791-6. Erratum in: Nat Med. 2005 Aug;11(8):905. PMID: 15951748.

Wan PT, Garnett MJ, Roe SM, Lee S, Niculescu-Duvaz D, Good VM, et al. Mechanism of activation of the RAF-ERK signaling pathway by oncogenic mutations of B-RAF. Cell. 2004 Mar 19;116(6):855-67. PMID: 15035987.

Wang Q, Villeneuve G, Wang Z. Control of epidermal growth factor receptor endocytosis by receptor dimerization, rather than receptor kinase activation. EMBO Rep. 2005 Oct;6(10):942-8. PMID: 16113650.

Wang Y, Pennock S, Chen X, Wang Z. Endosomal signaling of epidermal growth factor receptor stimulates signal transduction pathways leading to cell survival. Mol Cell Biol. 2002 Oct;22(20):7279-90. PMID: 12242303.

Wang Y, Waldron RT, Dhaka A, Patel A, Riley MM, Rozengurt E, et al. The RAS effector RIN1 directly competes with RAF and is regulated by 14-3-3 proteins. Mol Cell Biol. 2002b Feb;22(3):916-26. PMID: 11784866.

Waterman H, Katz M, Rubin C, Shtiegman K, Lavi S, Elson A, et al. A mutant EGF-receptor defective in ubiquitylation and endocytosis unveils a role for Grb2 in negative signaling. EMBO J. 2002 Feb 1;21(3):303-13. PMID: 11823423.

Wee P, Wang Z. Epidermal Growth Factor Receptor Cell Proliferation Signaling Pathways. Cancers (Basel). 2017 May 17;9(5):52. PMID: 28513565.

WHO. Global Hepatitis Report. World Health Organization: Geneva, Switzerland. 2017.

World Health Organization (WHO, 2023). Accessed in February 2023. https://www.who.int/news-room/fact-sheets/detail/hepatitis-c

Wilhelm SM, Carter C, Tang L, Wilkie D, McNabola A, Rong H, et al. BAY 43-9006 exhibits broad spectrum oral antitumor activity and targets the RAF/MEK/ERK pathway and receptor tyrosine kinases involved in tumor progression and angiogenesis. Cancer Res. 2004 Oct 1;64(19):7099-109. PMID: 15466206.

Wilkins C, Woodward J, Lau DT, Barnes A, Joyce M, McFarlane N, et al. IFITM1 is a tight junction protein that inhibits hepatitis C virus entry. Hepatology. 2013 Feb;57(2):461-9. PMID: 22996292.

Yamamoto S, Fukuhara T, Ono C, Uemura K, Kawachi Y, Shiokawa M, et al. Lipoprotein Receptors Redundantly Participate in Entry of Hepatitis C Virus. PLoS Pathog. 2016 May 6;12(5):e1005610. PMID: 27152966.

Yamazaki T, Nicolaes GA, Sørensen KW, Dahlbäck B. Molecular basis of quantitative factor V deficiency associated with factor V R2 haplotype. Blood. 2002 Oct 1;100(7):2515-21. PMID: 12239164.

Yang W, Qiu C, Biswas N, Jin J, Watkins SC, Montelaro RC, et al. Correlation of the tight junction-like distribution of Claudin-1 to the cellular tropism of hepatitis C virus. J Biol Chem. 2008 Mar 28;283(13):8643-53. PMID: 18211898.

Yu D, Turner JR. Stimulus-induced reorganization of tight junction structure: the role of membrane traffic. Biochim Biophys Acta. 2008 Mar;1778(3):709-16. PMID: 17915190.

Zeisel MB, Koutsoudakis G, Schnober EK, Haberstroh A, Blum HE, Cosset FL, et al. Scavenger receptor class B type I is a key host factor for hepatitis C virus infection required for an entry step closely linked to CD81. Hepatology. 2007 Dec;46(6):1722-31. PMID: 18000990.

Zheng A, Yuan F, Li Y, Zhu F, Hou P, Li J, et al. Claudin-6 and claudin-9 function as additional coreceptors for hepatitis C virus. J Virol. 2007 Nov;81(22):12465-71. doi: 10.1128/JVI.01457-07. PMID: 17804490.

Zhong J, Gastaminza P, Cheng G, Kapadia S, Kato T, Burton DR, et al. Robust hepatitis C virus infection in vitro. Proc Natl Acad Sci U S A. 2005 Jun 28;102(26):9294-9. PMID: 15939869.

Zhu G, Chen J, Liu J, Brunzelle JS, Huang B, Wakeham N, et al. Structure of the APPL1 BAR-PH domain and characterization of its interaction with Rab5. EMBO J. 2007 Jul 25;26(14):3484-93. PMID: 17581628.

Zona L, Lupberger J, Sidahmed-Adrar N, Thumann C, Harris HJ, Barnes A, et al. HRas signal transduction promotes hepatitis C virus cell entry by triggering assembly of the host tetraspanin receptor complex. Cell Host Microbe. 2013 Mar 13;13(3):302-13. PMID: 23498955.

Zoncu R, Perera RM, Balkin DM, Pirruccello M, Toomre D, De Camilli P. A phosphoinositide switch controls the maturation and signaling properties of APPL endosomes. Cell. 2009 Mar 20;136(6):1110-21. PMID: 19303853.